The Weldability of Stainless Steel with Solid State Laser

by

BAHADIR GÜNGÖR

Diploma work No. 119/2013
at Department of Materials and Manufacturing Technology
CHALMERS UNIVERSITY OF TECHNOLOGY
Gothenburg, Sweden

Diploma work in the Master programme Materials Engineering

Performed at: Trumpf Maskin AB
                          SE-441 17 Alingsås
                          Sweden

Supervisors: Hubert Wilbs and Joakim Kilén

Examiner: Docent Johan Ahlström
                      Department of Materials and Manufacturing Technology
                      Chalmers University of Technology, SE-412 96 Gothenburg

The Weldability of Stainless Steel with Solid State Laser
BAHADIR GÜNGÖR

The Weldability of Stainless Steel with Solid State Laser
BAHADIR GÜNGÖR
Department of Materials and Manufacturing Technology
Chalmers University of Technology

Abstract

Laser welding can offer many advantages over conventional welding when used in the right applications. Some of these advantages include smaller heat affected zone (HAZ) and lower thermal stresses, narrow weld seams with smooth surfaces reducing or even eliminating additional steps of refining work, high strength coupled with low weld volume, high welding speeds relative to conventional welding and easy integration potential to name a few. Laser welding even with its obvious benefits faces a lot of skepticism among manufacturers; especially sub suppliers who could benefit the most from committing to laser welding. Conventional welding have established and proven guidelines and standards within the manufacturing industry, techniques quantifying for example the throat measure. Laser welding lacks universal measures or guidelines aside from data and documentation provided by the producer of laser welding systems.

The weldability of the stainless steel EN 1.4301 (AISI 304) sheets of 1.5 mm thickness has been investigated. The goal has been to achieve a method that can be applied also in future investigations of other alloys.

Iteration of welding parameters has been made in order to find optimized welding parameters. Butt joint welded test specimens with geometrical tolerance deviations were manufactured to investigate the process sensitivity against tolerance deviation. To characterize the influence on the mechanical properties a series of ASTM standardized mechanical tests were performed. Tests include tensile testing, bend testing and hardness testing on metallographically prepared cross-sections. Computer simulations of the heat-affected zone were made using the numerical computing environment MATLAB.

Results show a local increase in peak hardness of approximately 28-43%. Bend testing results show that even with this local increase of the peak hardness, ductility is not critically affected. Bend testing was performed without fracture or presence of surface irregularities but for one sheet. In this case the specimens had the most extreme tolerance deviation in the specimen series, giving rise to incomplete welding and severe stress concentration. Tensile tests results show no significant effect on tensile strength and elongation at break for specimens with tolerance deviations up to 150 μm. Larger tolerance deviations showed an abrupt drop in both tensile strength and elongation at break.

Preface

This master thesis was carried out during the spring and summer of 2013 by a student with a background in mechanical and materials engineering. The project was carried out at Trumpf Maskin AB in collaboration with Alingsås Tunnplåtcenter (ATC). The thesis project is the final part of the master program Materials Engineering at Chalmers University of Technology. The experience from the project was very educational, as it covered a topic that wasn't addressed earlier in the master program. It enabled me to apply and broaden theory from earlier studies as well as gaining new knowledge in the field of materials and production engineering.

I would like to thank my supervisors Hubert Wilbs and Joakim Kilén at Trumpf Maskin AB for all their support and commitment towards the project, Steeltech AB for their help with manufacturing test specimens, especially Jimmy Johansson whom has been of great help and shown great interest in the project, Anders Dahllöf at Volvo Cars who helped me perform tensile tests, my examiner Johan Ahlström from the Department of Materials and Manufacturing Technology, for all his support, expertise and guidance throughout the project.

I would also like to thank all employees at Trumpf Maskin AB for all the help I have received throughout the project, but also for making me feel at home at their company,

Gothenburg, August 2013

Bahadır Güngör

Table of Contents

1. Introduction

1.1 Background

Laser has come a long way since its discovery in the 1960's. Today, lasers have many different applications and fields of use. One field were a lot of progress has been made and is continued to be made is within materials processing technology; laser welding being one of these applications and topic of the project.

Despite its maturity and obvious advantages in many applications, laser welding faces a lot of skepticism within the manufacturing industry. Unlike conventional welding, where guidelines, measures and data have been established and standardized, i.e. effective throat measure, there are no such standards, universal measures or guidelines for laser welding, aside from data and documentation provided by producers of laser welding systems.

This leads to confusion and skepticism among manufacturers who could benefit from committing to implementation of laser welding. This is especially true for sub suppliers, who tend to work with a lot of different materials and products.

This skepticism could be exemplified with an example. Traditional design conventions would require a specific effective throat. Since laser welding doesn't produce a weld throat, many producers and sub suppliers tend to feel disbelief towards laser welding. All of a sudden, old conventional ways of designing and methods of measuring the quality of the weld are not applicable or valid.

Laser welding is employed in various applications and industries today. It holds many advantages over conventional welding when used for the right applications. Some of the advantages are:

- Selective energy application within small volumes, resulting in low thermal stresses and small heat affected zone (HAZ) as well as extremely low distortion.

- Laser welding achieves narrow seams and smooth surfaces, reducing or even eliminating additional steps of refining work.

- High strength coupled with low weld volume. Work pieces can be shaped after welding by mechanical forming or hydro-forming.

- Easy integration potential. Laser welding can easily be combined with other production operations such as alignment and bending, making it suitable for automation.

- Only one side of the joint needs to be accessible in order to make a weld.

- Machine and sensor systems can be used to monitor the process, ensuring good process control.

- The weld is created without physical contact or applying force except for fixtures.

- Very high welding speeds relative to conventional welding.

From the above-mentioned advantages, it is easy to affirm advantages that laser welding offers in comparison to conventional welding, for certain applications.

1.2 Problem Description

In order for laser welding to establish universal standards and measures, the process window needs to be investigated and characterized. Process parameters, susceptibility to tolerance deviation and mechanical properties of the weld are all topics of interest for producers and designers.

Welds are often subjected to post-weld mechanical forming as well as the final product being subjected to mechanical loading. It is therefore desirable to have standardized methods to evaluate the mechanical properties of the weld. Since there is no addition of material with laser welding, narrow geometrical tolerances are required in order to achieve good results. Knowledge about the tolerance range helps simplify the design requirements for welding fixtures.

There are plenty of variations of geometrical tolerances that need to be taken into account in order to optimize the process. The weld joint can have geometrical offset horizontally, vertically or by angle. Irregularities can be present on the surface and as a result from cutting not being perpendicular. Weld joints come in many forms: butt joint, flange joint, fillet weld, corner weld, lap joint, circular weld and pipe circumference weld. All joints hold their own strengths and weaknesses but also have their own geometrical tolerance requirements.

This project will investigate the process window for 1.5mm thick Cr-Ni stainless steel sheets. Horizontal (X) and vertical (Y) offset in joint will be investigated for butt joint welding. Geometry, mechanical properties and aesthetics will be evaluated.
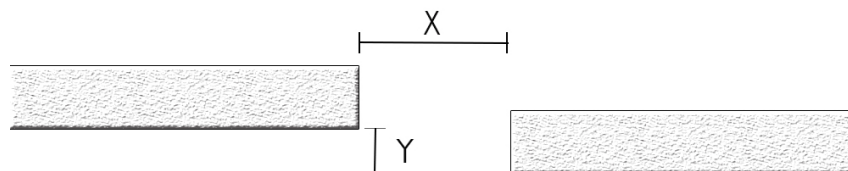

Figure 1: Illustration of offset values X and Y

1.3 Methodology

1.3.1 Literature Study

The project was started with a literature study in order to gain knowledge and get familiar with laser welding, as well as to review and increase knowledge in the area of material science (metallurgy, welding, mechanical properties, mechanical testing). Databases, books and expertise accessible through Chalmers and Trumpf Maskin AB were used as resources during the literature study. Relevant theory is presented in the report and serves as the backbone in understanding the work.

1.3.2 Courses, Training and Study Visit

In order to get practical experience and gain a deeper understanding for laser welding, a six-day course in operating and programming the TruLaser 5020 laser system was taken at Alingsås Tunnplåtscenter (ATC). The training enabled for independent welding without assistance from a second party.

A workshop was attended on the subject of "Designing for Laser Welding" at ATC. The workshop gave design ideas as well as valuable knowledge in fixture design in order to design around common pitfalls when designing for laser welding.

Study visits were taken to KBW GmbH and Ha-Be GmbH, in Germany. The study visits gave a chance to see laser welding implemented in actual production chains, and thus observe industrial application.

1.3.3 Welding

All welding was performed by solid-state laser using the Trumpf TruLaser 5020 system. The beam source used was a Trumpf TruDisc 2002, disc laser.

1.3.4 Mechanical Testing

A series of mechanical tests were performed in order to investigate the influence on the mechanical properties and the effect of tolerance deviation.

The test methods used include tensile testing, bend testing and Vickers hardness test. Standards and methods found in literature were used and adapted to the equipment available at Chalmers, ATC, SteelTech AB and Volvo Cars. Before any actual tests were made, a detailed plan was carefully compiled in order to overview the different types of properties that were of interest to evaluate, as well as which test methods were to be used. Both testing and test specimens were performed and manufactured in accordance with ASTM standards.

1.3.5 Computer Simulations

In order to predict the temperature distribution in the welding process, simulations were made with the help of MATLAB. Predictions of the thermal cycle help understanding phenomena as width and penetration depth as the function of a given heat input, microstructural changes in the HAZ and residual stresses.

1.4 Delimitations

- The project will only consider the austenitic stainless steel EN 1.4301 (AISI 304) produced and delivered from Outokumpu. Specimens for mechanical testing will only be manufactured from the same sheet to avoid spread in material properties between different batches. Only laser cut and non-surface treated sheets of thickness 1.5 mm will be tested.

- Welding geometry to be welded is butt joint.

- Variation in gap width will be varied up to 15% of sheet thickness. Variation in vertical offset at gap will be varied up to 10%.

- Welding mode will be restricted to deep penetration welding

- Continuous welds will be made with a continuous wave laser with Argon used as shielding gas.

- Welding will only be made with the Trumpf TruLaser5020 system.

- Beam source will be a Trumpf TruDisc2002 (Nd:YAG Disc) with a power of 2000 W, beam quality of $8\mu m$.

- Net length of project is 21 weeks

2. Theory

2.1 Laser Welding

Metal welding is a joining technique in which two or more pieces of metal are joined into a single piece. The bond is metallurgical and achieved by melting or diffusion. Created joints are permanent as opposed to other methods of joining and don't run the risk for accidental disassembly or loosening. Processes are amenable to both manual and automated operation, enabling flexibility in production.

Fundamentally laser welding is achieved with a beam source and optics – shaping, guiding and finally focusing the laser light into a tiny focal spot. The optics consisting of mirrors and lenses reflect and refract the beam to its focus. At the focus, the power density is several orders of magnitude higher than the raw beam.

The two most basic components of a beam source are the active medium and the resonator. The active medium is the material that emits the laser light and is also the medium in which light is amplified. In its simplest form the resonator consist of two mirrors that reflect light repeatedly back into the active medium.

Before any laser light can be emitted, the active medium has to be excited by feeding energy into it. This is referred to as "laser pumping". All beam sources require a pump source that energizes the active medium with optical, electrical or chemical energy. The majority of the excitation energy is lost to heat rather than converted into laser light. The heat is dissipated to ensure that excessive heating of the resonator does not occur.

Principally there are several materials that can be used as gain medium for laser. These materials consist of gases, liquids and solids. The requirement is that the material must be able to emit electromagnetic radiation of a certain wavelength. This is achieved exciting electrons to a higher energy state upon pumping. When an electron drops from its excited stage to a lower energy stage, light is emitted.

2.1.1 Solid State Lasers

Laser light in solids is created by fluorescing foreign ions, which are introduced in small amounts into a glass or crystalline host material. The process of introducing these elements is called doping. Neodymium (Nd) and Ytterbium (Yb) are the primary dopants used in the beam sources for industrial material processing. For example, Nd:YAG (neodymium doped ytterbium aluminum garnet), which produces a light with wavelength 1060 nanometer.

Together with power, the time-related behavior is an as important characteristic in material processing. Lasers either operate in short bursts or continuously. In order to achieve deep penetration welding (also referred to as keyhole welding), continuous laser light is required.
In continuous wave mode welding, the active medium is continuously excited and emits a continuous laser beam. For pulsed mode, the active medium is excited to generate short laser pulses, often used in laser spot welding. The power, duration and frequency of the laser pulses determine the mean power of the laser beam, which is always less than the power of each laser pulse.

One of many advantages offered by solid-state lasers is that they can be led into fiber optic laser cables. Fiber optics enables transportation of the laser light without any appreciable loss of quality or power. An advantage of such cables is that the laser source and workstation are separate and can be located in different places.

2.1.2 Heat Conduction welding

Heat conduction laser welding is used for joining thin walled parts. The laser beam melts mating parts along a common joint. Molten material flows together and solidifies, forming the weld. Common applications include corner welds on visible surfaces of device housings. The produced weld seam is smooth and rounded, eliminating the need for grinding or finishing.

Welding energy is coupled into the material entirely through heat conduction. Heat conductivity is thus the limiting factor. If the heat isn't able to dissipate quickly enough, the process temperature reaches above the vaporization temperature. Metal vapor forms, the welding depth increases sharply and the process turns into deep penetration welding. Because of this reason, the weld depth ranges from only a few tenths of a millimeter to 1 millimeter. [6.]

2.1.3 Deep Penetration Welding

High power densities in the order of 1 megawatt per square centimeter are required for deep penetration welding. In deep penetration welding, the laser beam not only melts the metal but also produces vapor. The dissipating vapor exerts pressure on the molten metal and partially displaces it. Overflow and spatter can result from this displaced molten metal.

Meanwhile, as the material continues to melt, a deep narrow vapor-filled hole surrounded by molten metal is achieved. While the laser beam is moving onward along the weld joint, the keyhole moves with it through the work piece. As the laser beam moves, molten metal is flowing around the keyhole, solidifying in its trail. The results is a deep, narrow weld with a uniform internal structure, with a weld depth reaching up to ten times the width, up to a maximum of 25 millimeters. The molten material absorbs the laser beam almost completely, increasing the efficiency of the welding process.

2.2 Austenitic Stainless Steel 1.4301 (AISI 304)

Stainless steels are normally classified into three different types. Classification is based on the crystalline structure and the primary phases. Stainless steels are thus divided into austenitic, ferritic or martensitic stainless.

The austenitic steels are the most common and familiar type of stainless steels. They can easily be identified in practice by their non-magnetic properties. They have certain mechanical properties, they are soft enough to be easily formed with the same tools as carbon steels, but have the ability to be hardened by work hardening. Austenite has a face centered cubic (FCC) structure and is tough and ductile. It does not lose its strength at elevated temperatures as early as ferritic iron base alloys. Corrosion resistance stretches from normal day-to-day environments to more aggressive environments like boiling seawater. It provides very predictable levels of corrosion resistance and mechanical properties.

The prominent feature of the austenitic steels is that as chromium and molybdenum are raised to improve certain material properties, most often corrosion resistance, nickel and other austenite stabilizers are added in order for the austenitic structure to be preserved. As an example, if molybdenum, a chromium equivalent is added, corrosion resistance is enhanced but not the oxidation resistance. Nitrogen is an austenite stabilizer added to balance increased chromium or molybdenum. Silicon is used to as an alloy to promote oxidation resistance and resistance to corrosion by oxidizing acids. Low carbon levels prevent sensitization; stabilized grades may still be preferred in special applications.
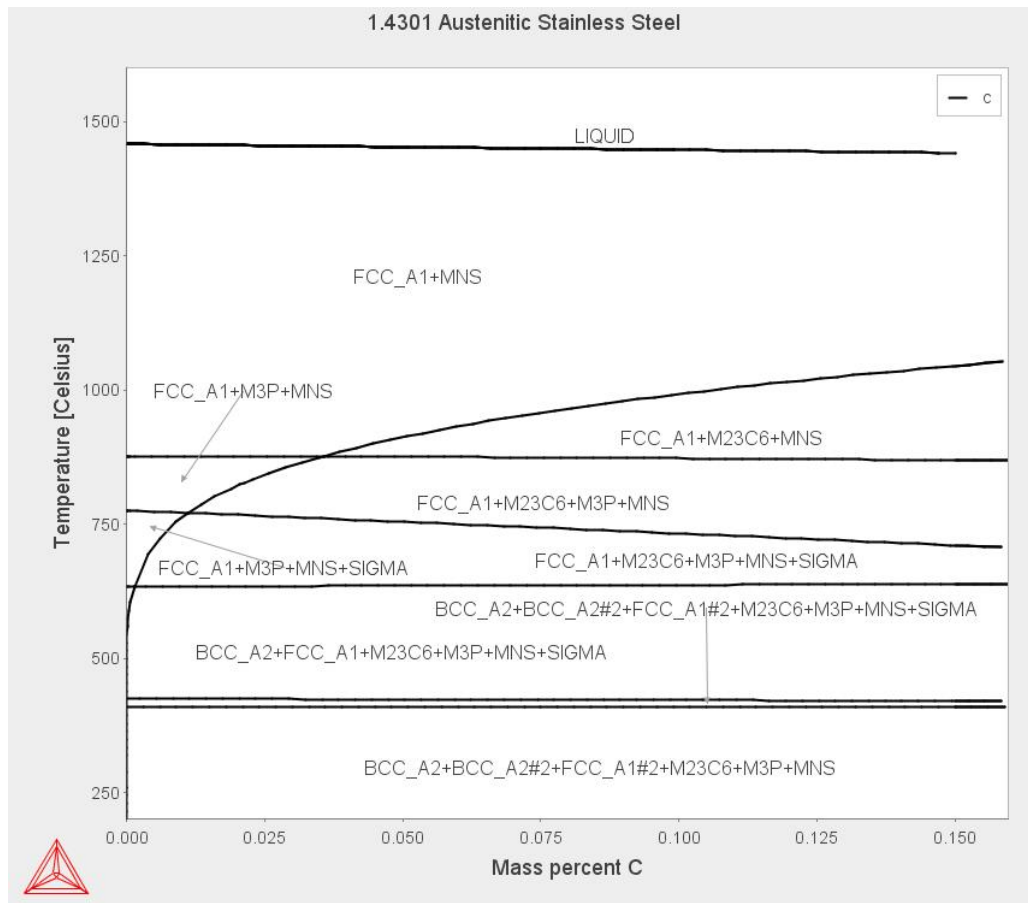
Figure 2: Phase diagram for 1.4301

Lean austenitic stainless steels are often called lean alloys. The lean alloys constitute the majority of all produced stainless steels. EN 1.4301 (AISI 304), the studied alloy in the project is a general-purpose alloy among the group. The two other lean alloys are EN 1.4372 (AISI 201) and EN 1.4310 (AISI 301). Alloys with less than 20% chromium and 14% nickel fall into this category. The lean alloys are very formable and weldable, thus making them very attractive alloys for many applications.[9]

The material composition for EN 1.4301 is given below according to the supplier Outokumpu.[10]

C	Mn	P	S	Si	Cr	Ni	Mo	Others
0.08	2.00	0.045	0.030	0.75	18.0–20.0	8.0–10.5	…	0.10N

Table 1: Material composition 1.4301

2.3 Tensile Testing

Tensile testing, also known as tension testing, is one of the most common mechanical stress-strain tests. Tensile testing is used to determine several mechanical properties. Test specimens are mounted by their ends to the holding grips/mounts of the tensile test apparatus. A gradually increasing tensile strain deforms a test specimen uniaxially at a constant rate along its long axis. The required load and elongation is recorded by the use of extensometers (elongation/strain) and load cell (force/stress).

For welds that only extend over part of the gage length, tensile tests can be performed very similar to those performed on regular base metals as well as deposited weld metals, on round and rectangular test specimens. Non-uniformities as stresses and deformations of the weld metal, HAZ and base metal limit obtainable information for tensile testing. Only overall data can be recorded. Data for the individual zones are not recorded due to the complexity in performing such readings. This is why commonly; only ultimate tensile strength and location of fracture are recorded from tensile tests for welds.[13] All tensile testing were performed in accordance to ASTM A370 [2] and E 8M [3] standard.

2.4 Bend Testing

Bend testing is used as a quick method of evaluating the ductility and strength of a weld, evidenced by its ability to resist cracking during bending. It offers low-cost evaluation on shop floor thanks to its simplicity and tooling requirements. Bend testing is intending to serve as a subjective material inspection (pass/fail) to whether or not cracking occurs. Workshops that have laser welding implemented into their production, most likely also have easy access to manual or automated bending machines. [11]

If material thickness, tool setup or mechanical properties hinders the specimen from being bent to the desired angle, force can be applied at the ends of the already bent test specimen.

Surface irregularities such as loss of coating adherence and other discontinuities as a result of the bend test are evaluated and documented. Cases where the weld haven't achieved full weld penetration are not be evaluated as a crack failure. If criterions are set for max allowable crack size, inspections are made in accordance to these. Fractured specimens count as failed tests. Corner cracks are ignored unless a criterion is set regarding max allowable size of corner cracks. Defects not normally detected by X-ray evaluation can be detected when exposed to excessive localized overstressing [5]

2.4.1 Guided Bend Testing

Bending is performed by supporting a flat test specimen on pins, rollers or radiused flats near the weld and applying force through a pin, mandrel or plunger between two supports onto the weld, situated midpoint. This test method is also referred to as 3-point bending

Tools have pre-determined radii and angle. No force is applied to the outer face of the bend specimen. The distance between supports (C) shall be three thicknesses plus twice the punch radius, with a tolerance of half a thickness of the specimen, $C = 2r + 3t \pm t/2$.[5]
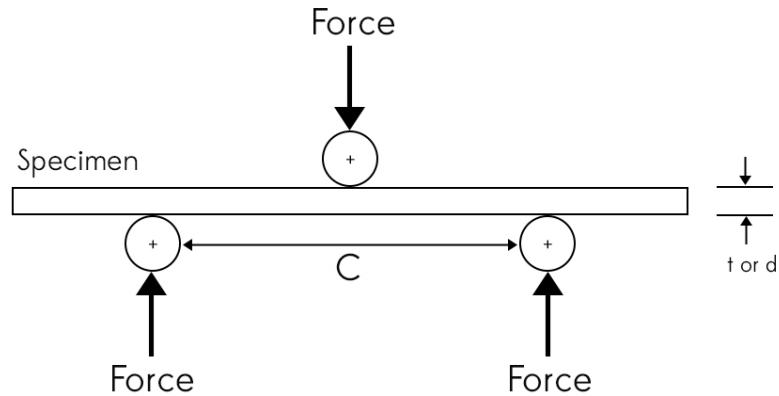
Figure 3: 3-point bending test

2.6 Heat affected Zone

In welding, following heating a very rapid cooling takes place that is controlled by factors like the material properties, the welding environment and joint geometry among other factors.

The thermal cycle of the welding results in a change of the microstructure close to the region of the weld as well as the material properties. This region or zone of the metal is called the heat affected zone (HAZ)

The HAZ is conveniently divided into sub-zones. The number of sub-zones depends on the material, present microstructure and phases. Every sub-zone corresponds to a different type of microstructure and, perhaps most crucial is the fact that each sub-zone posses different mechanical properties. Heat and mechanical treatment of the metal influence the outcome of the HAZ.

In order to obtain a sound understanding of the HAZ, it is necessary to study how the microstructure of the base metal reacts to the complete thermal cycle and its effect of e.g. phase transformation and precipitation reactions.

2.6.1 Heat Flow Equations

The Rosenthal equation solves the heat-flow equation of a moving heat-source. It is assumed that the energy of the heat source moves with a constant speed v, along the x-axis of a fixed rectangular co-ordinate system as in figure 4. Equation 1 describes the differential equation of the heat flow.

$$\frac{\partial^2 T}{\partial x^2} + \frac{\partial^2 T}{\partial y^2} + \frac{\partial^2 T}{\partial z^2} = \frac{1}{a}\frac{\partial T}{\partial t}, \ a = \frac{\lambda}{\rho C_p} \tag{1}$$

Assumption is made that thermal conductivity (λ) and the specific heat x density product (ρC_p) of the base metal are constants. Equation 2 describes the case of a stationary co-

ordinate system and can be modified for a moving co-ordinate system. This is achieved by replacing x with ξ, where ξ is the distance of the point heat source from some fixed position along the x-axis, with dependence on the velocity of the moving heat source.

$$\xi = x - vt \tag{2.}$$

Equation 1 with x substituted with ξ, gives equation 3.

$$\frac{\partial^2 T}{\partial \xi^2} + \frac{\partial^2 T}{\partial y^2} + \frac{\partial^2 T}{\partial z^2} = -\frac{v}{a}\frac{\partial T}{\partial \xi} + \frac{1}{a}\frac{\partial T}{\partial t} \tag{3.}$$

Assuming a quasi-stationary temperature distribution $(\frac{\partial T}{\partial t} \equiv 0)$, meaning the temperature distribution around a heat source of uniform velocity will settle down to a constant form, provided that the heat input is constant equation 3 can be simplified to equation 4.

$$\frac{\partial^2 T}{\partial \xi^2} + \frac{\partial^2 T}{\partial y^2} + \frac{\partial^2 T}{\partial z^2} = -\frac{v}{a}\frac{\partial T}{\partial \xi} \tag{4.}$$

Heat flow of course depends on the weld geometry and plate thickness. Since the project only investigates the case of butt joint welded thin sheets, the flow of heat will be two-dimensional. Heat losses through the surface are thus assumed to be negligible.

The solution to equation 4 for the two dimensional case is given below. [8.]

$$T - T_0 = \frac{\frac{q}{v}}{2\pi\lambda t} \exp\left(\frac{v\xi}{2a}\right) K_0\left(\frac{vr}{2a}\right) \tag{5.}$$

K_0, is a modified Bessel function of the second kind, zero order, $r = (\xi^2 + y^2)^{1/2}$.
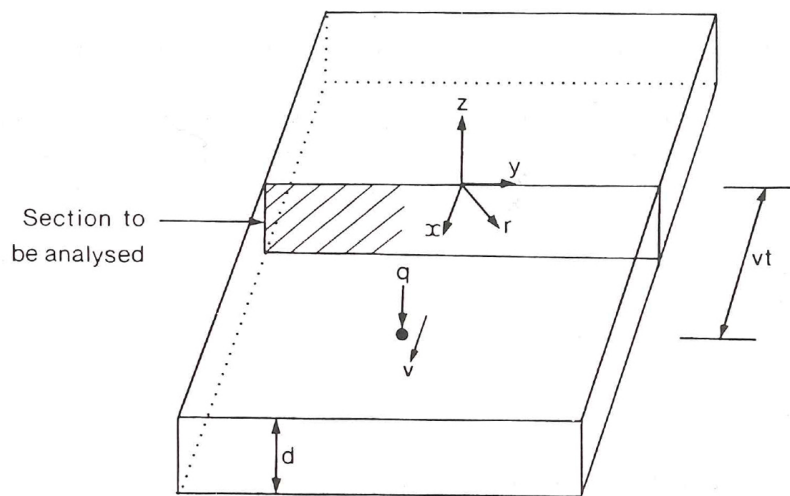
Figure 4: Welding configuration in terms of point heat source, q and a constant velocity, v

2.6 Hardness Testing

Hardness testing is performed in order to study the hardness in the weld metal and the HAZ. Hardness is a measure of the materials resistance to localized plastic deformation, i.e. small dents and scratches and correlates to material strength. With the Vickers technique, a very small diamond indenter with pyramidal geometry is forced into the surface of the test specimen with a specified load. Indentations are inspected under microscope and measured. Measurements are converted to hardness numbers. In order to ensure well-defined indentations, specimens are grinded and polished upon inspection under microscope.

3. Experimental Process

Properties of weldments vary throughout the weld metal, adjacent HAZ and the base metal. These variations in properties pose complexity in testing mechanical properties, strength and ductility.

In order to evaluate the effect of laser weldments, a series of mechanical tests and analyzes were made. This section presents all applied methods of mechanical testing and the tools that were used in the project.

3.1 Welding

All welding was carried out at ATC using the Trumpf TruLaser 5020 system with a Trumpf TruDisc 2002 as beam source. The TruDisc 2002 has a maximum power output of 2000 W.
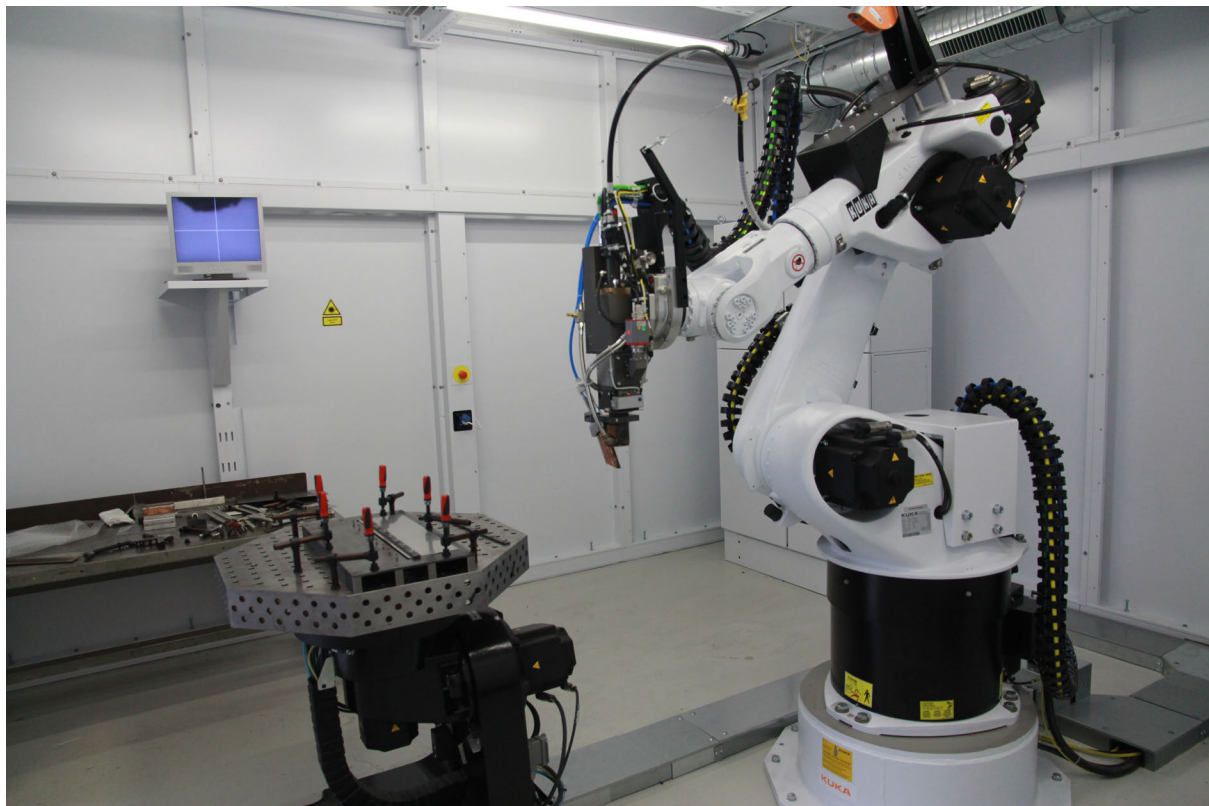
Figure 5: The Trumpf TruLaser 5020 system

In order to find appropriate welding parameters a series of trial and error welding was performed. The parameters used were documented and test specimens manufactured for inspection under stereo microscope and micro hardness testing. The starting point in iterating towards optimized welding parameters was Trumpf's own documentation. A set of different parameters was varied out of experimental purposes. This was done in order to evaluate their influence on weld penetration, spatter and micro hardness.

The following welding parameters were fixed throughout all experiments if nothing else is mentioned. Welding-in angle refers to the angle of the laser relative to the weld joint in the welding direction. A slight addition from 90° is often used in order to prevent reflections back into the optics, which can cause damage.

Power [W]:	2000
LLK ⌀ [µm]:	400
Focal length [mm]:	200
Collimation [mm]:	200
Welding-in angle:	96°
Gas quantity/flow [l/min]:	24
Inert gas	Argon
Focus point position:	Butt joint center line
Focus diameter [µm]:	200
Gas nozzle:	4-way copper nozzle

Table 2: Fixed welding parameters

The following parameters were used during the process of weld parameter iteration.

Specimen	Weld Speed [m/min]	Focus [mm]	Notes
1	1.25	6	
2	1.25	3	
3	1.75	6	
4	1.75	3	
5	2.25	6	
6	2.25	3	
7	3.25	-1	
8	3.75	-1	
9	4.25	-1	
10	4.5	-1	
11	5	-1	Bead on Plate
12	5	-1	Unwanted gap
13	5	-1	Power used: 1kW

Table 3: Welding Parameters

Bead on plate (BOP) refers to welds made directly on top of a sheet instead of in a joint. BOP is theoretically the best-case scenario in terms of tolerances, since no gap or offset exists.

All programming of the TruLaser 5020 robot was made with the internal software TeachLine. Writing programs with TeachLine works so that the operator stepwise positions the robot at the desired position in space. The robot is maneuvered with the control and programming pad. The pad is also the primary way of accessing the interface of the TruLaser 5020.

Figure 6: (left) Control pad for the TruLaser 5020 (Right) Lcd screen

For every point in space that is defined in TeachLine, it writes a piece of code based on the robots position in space. The more steps are used the more precise the operation will be. As an aid the operator has a camera with magnification connected parallel to the welding optics. Between these positional program lines, the operator manually adds code for when the laser is switched on, and set welding parameters. In order to achieve a good accuracy the cross hair function was enabled on the lcd-monitor. All programs programmed during the project were straight welds. Straight lines were achieved by tracing butt joints with the camera and adding several points with somewhat even spacing in space.

The TruLaser 5020 was calibrated before each session with the anodized aluminum piece method in order to find the focal plane. This calibration method is achieved by running a pre-installed program that comes delivered with the system. The optics is brought to a height of 200mm above the working table. A black anodized aluminum piece is placed on the table. When run, the program tells the system to mark a series of tiny spots with different focus settings on the aluminum piece. The program is run stepwise (one line of code at a time) a second time with beam source off-line. Spots are evaluated with the camera and lcd-screen. The machine focal plane is calibrated as the setting yielding the tiniest spot.

3.2 Welding Fixture

A welding fixture was designed and manufactured together with ATC in order to produce test specimens with well-defined gap and offset. The welding fixture was designed so that two sheets of stainless steel can be welded to form one sheet with a centered weld seam, from which several test specimens for mechanical testing can be cut out.

Figure 7: Welding fixture placed on working table

The welding fixture consists of a laser cut carbon steel plate attached to four supporting steel rulers. The rulers were manufactured at a third party workshop. The rulers were manufactured by milling in order to guarantee as flat as possible contact surface. The surface of the carbon plate is polished in order to avoid unevenness on the surface. Since the carbon plate was subjected to thermal deformations from the laser cutting and stud welding, the function of the rulers is to straighten out deformations, improve flatness and stiffness. Countersunk socket head screws mount the rulers to the upper carbon steel plate.

Eight weld studs were welded along each side of the slit of the carbon steel plate. The weld studs and nuts are used to guide and fixate the stainless steel sheets into place with the help of two steel strips. The nuts are hand tightened from the middle and out to the edges with a socket wrench.
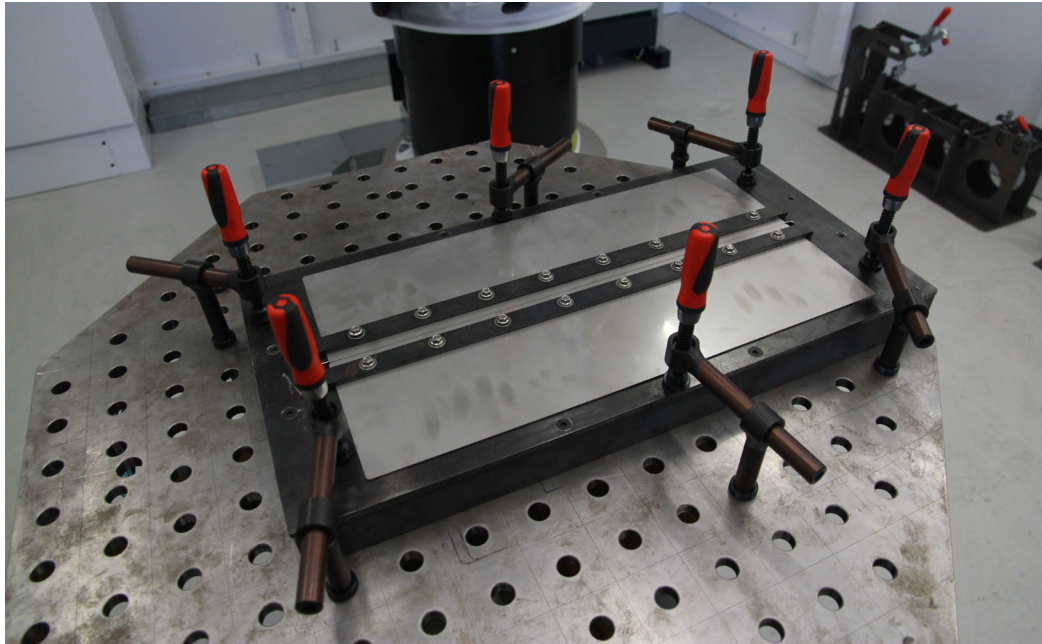
Figure 8: Fixture mounted on welding table with sheets fixated

The fixture was mounted to the Demmeler welding table with Demmeler fixation tools. It should be mentioned that the fixation tools are only compatible with Demmeler welding tables. The used Demmeler system was the D16 system (16 mm). [7.]

The sheets used with the fixture were laser cut with the dimension 480 x 130 mm. They all had eight 10 mm holes along one of its long sides for guidance and fixation on the fixture.
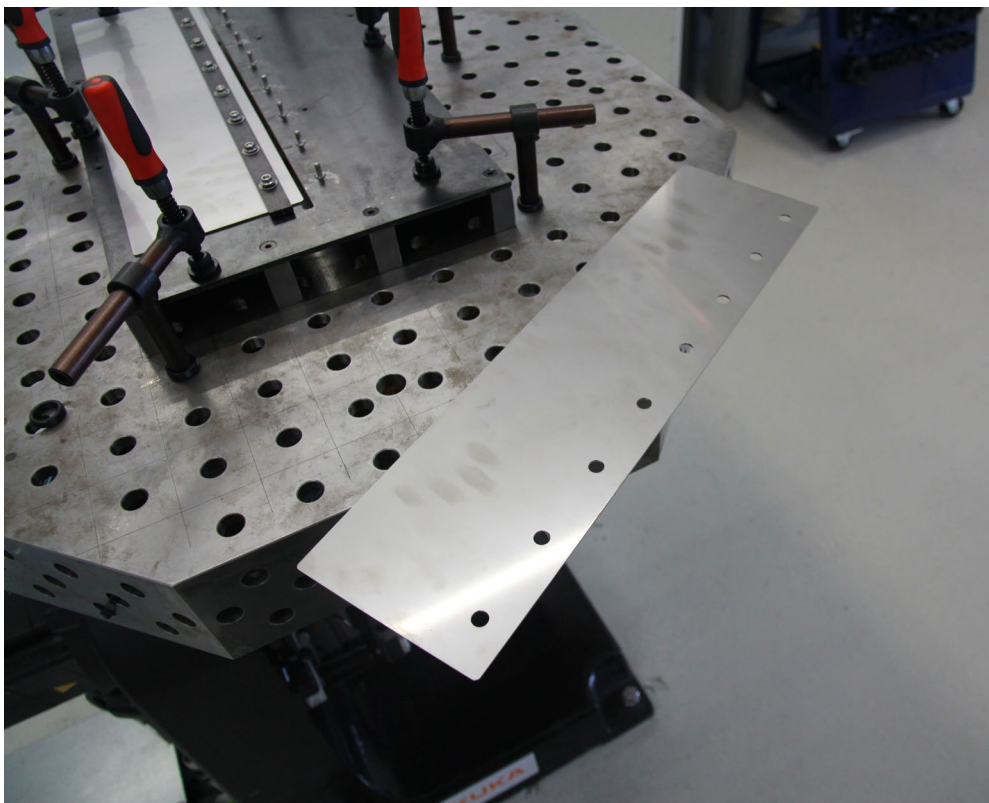
Figure 9: Laser cut stainless steel sheet with guiding holes.

The surfaces of the manufactured test specimens are to be smooth, without deep machining marks. Imperfections from welding and cutting present on the gage length should be avoided as these will act as stress-concentration zones/points. Before all weld experiments, sheets were cleaned in order to guarantee a surface free from oil or other pollutants.

All cutting of test specimens from the welded stainless steel sheets was made with CO_2-laser using the Trumpf TruLaser 3030 (L20) system and TruFlow 3200 (V1), beam source.

3.3 Manufacturing of Test Specimens for Tensile and Bend Testing

Test specimens for both tensile testing and bend testing were laser-cut from the same welded sheet. This was made in order to achieve repeatability in testing and data and avoid deviations and inaccuracies between different batches. Rolling direction of the sheet lies in the longitudinal direction of the test specimens. Sheets with combinations of different tolerance deviations were welded. This was achieved by offsetting the un-welded sheets before welding. This offset was achieved by using thin stainless steel shims. These offsets are illustrated below in figure 10. Shims were placed in between the unwelded butt joint to achieve a horizontal offset, the X-offset (figure 1). The shims were left sitting in-between until the sheets were fixated and removed afterwards. Y-offset was achieved by stacking shims between one sheet and the fixture. These shims had to be cut with scissors in order to fit around weld studs. These shims were left on the fixture during welding.
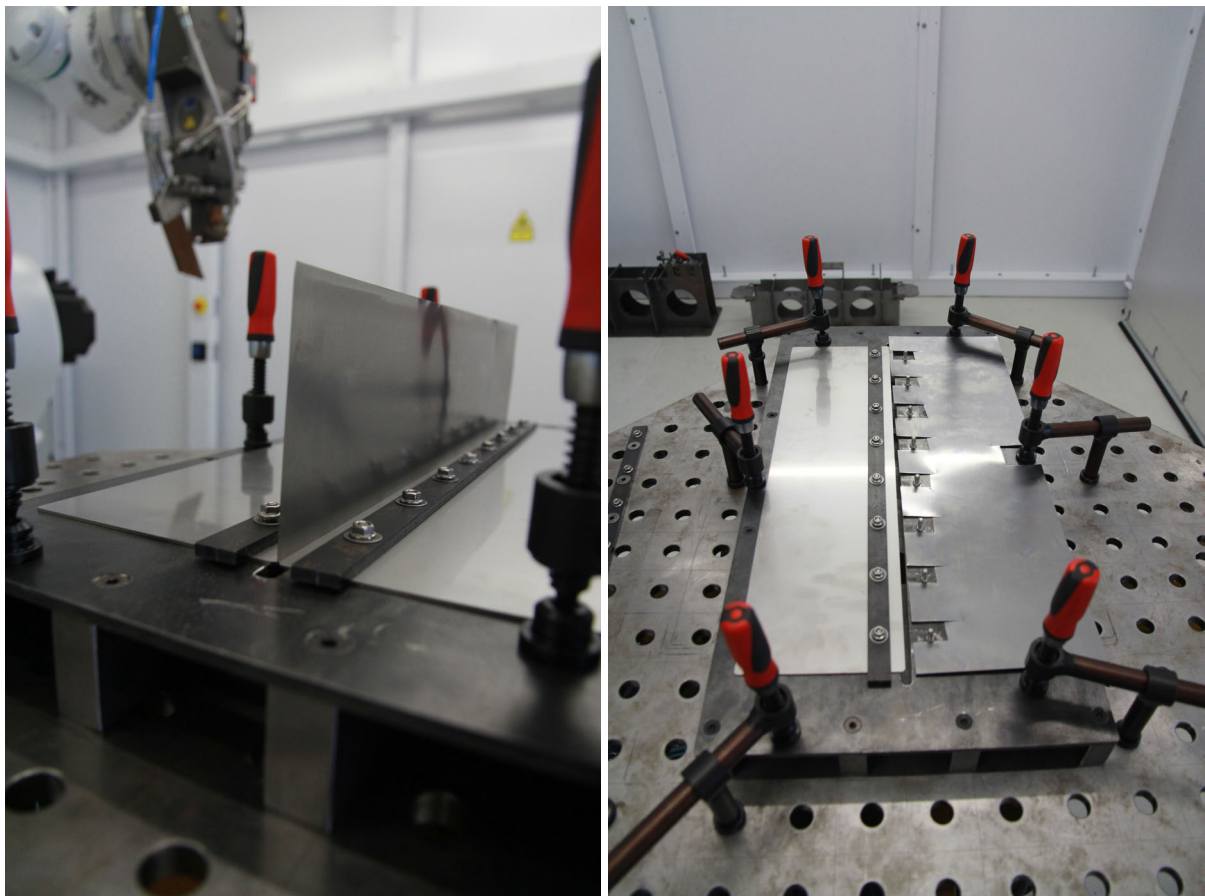
Figure 10: (Left) Shim between weld butt joint. (Right) Shim cut in order to fit fixture.

Sheets with the following variations of geometrical deviations were manufactured.

Sheet	X, Horizontal offset [mm]	Y, Vertical offset [mm]	Notes
A	0	0	
B	0.075	0	
C	0.150	0	
D	0.225	0	
E	0	0.075	
F	0.075	0.075	
G	0.150	0.075	
H	0.225	0.075	
I	0	0.150	
J	0.075	0.150	
K	0.150	0.150	
L	0.225	0.150	
BOP	0	0	Bead on plate
REFERENCE	0	0	No Weld

Table 4: Variations of welded Test specimens

Test specimens for tensile testing follow the ASTM A370-77 standard for mechanical testing of steel products. The picture below illustrates the dimensions of the test specimen.
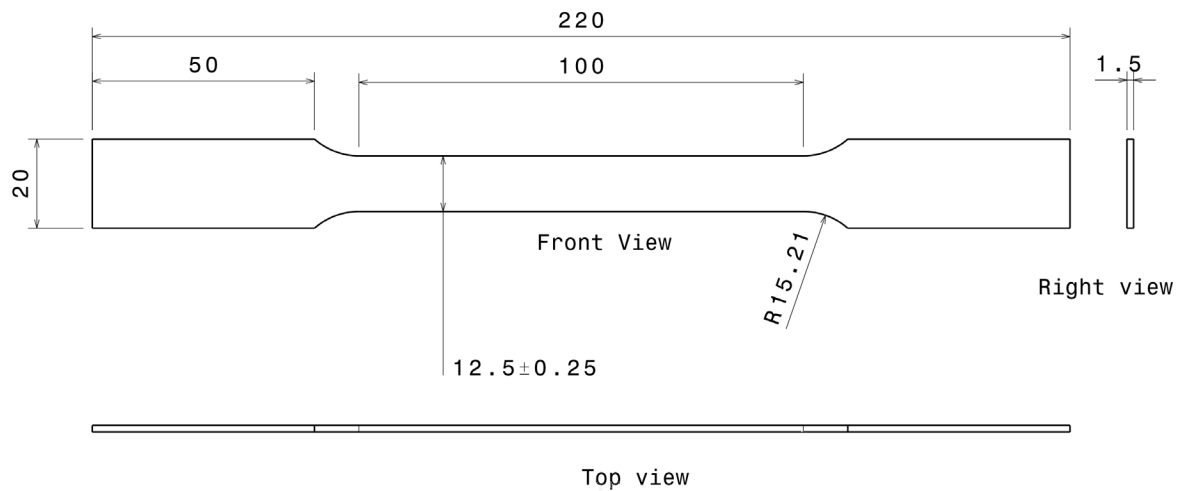
Figure 2: Drawing of tensile test specimen. Measures in millimeter (mm).

Test specimens for bend testing follow the ASTM standard E 190-92, Guided bend test for ductility of welds. Because of practicality the same design was used for the Vickers hardness test.
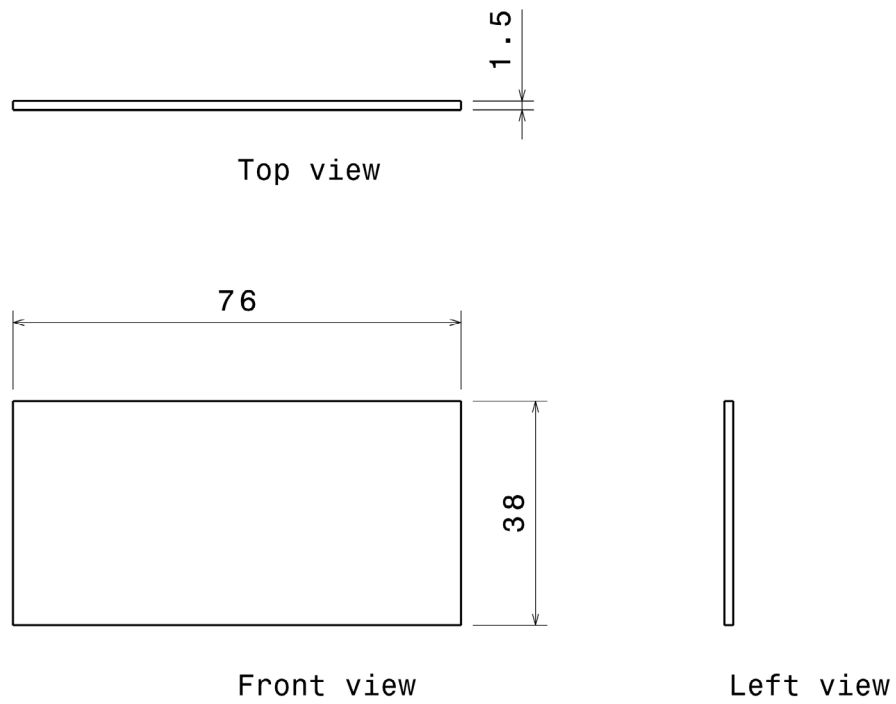
Figure 3: Drawing of bending test specimen. Measures in millimeter (mm)

All test specimens were laser cut according to their respective design.

3.3 Tensile Testing

All tensile tests were performed at Volvo, Gothenburg with a Zwick tensile tester. The used software to control the tensile test apparatus was testXpert V3.31 produced by Zwick/Roell. Detailed information about the tensile tester can be found in the table below
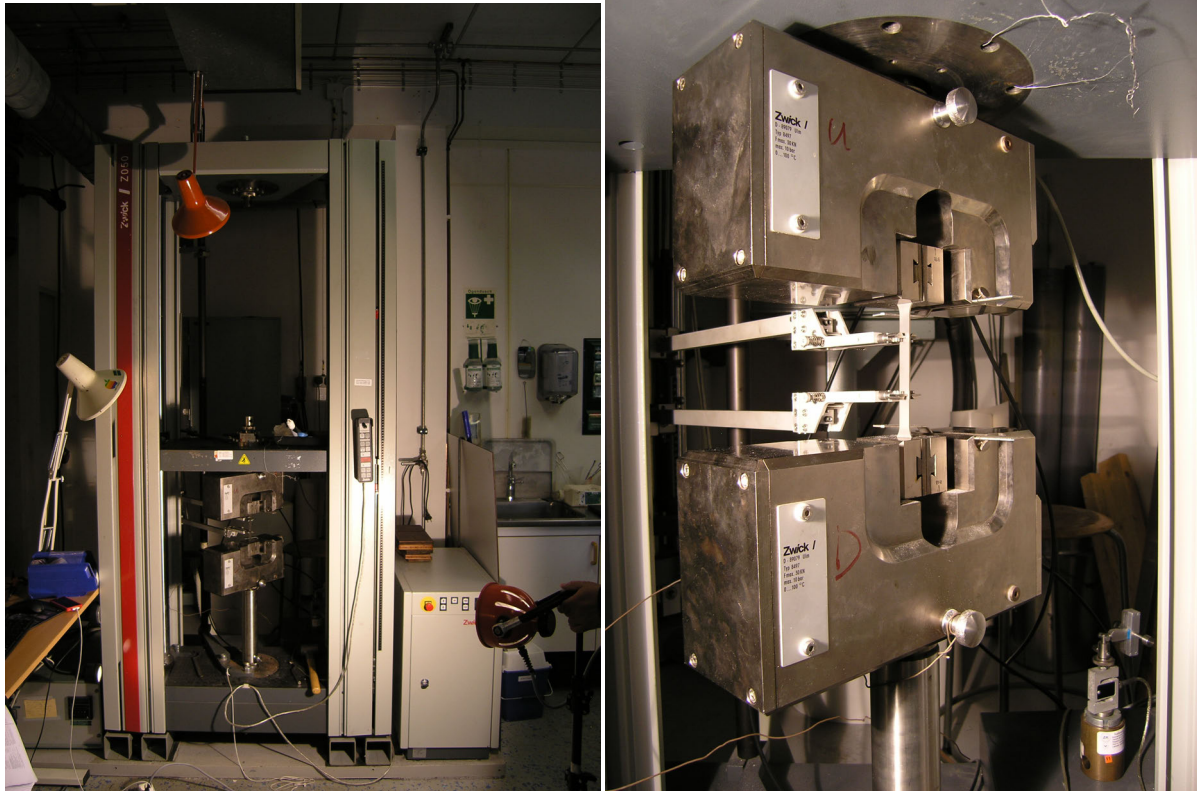
Figure 4: (Left) Overview tensile tester. (Right) Close up: loading cell, pneumatic grips & extensometer

Manufacturer:	Zwick	
Model name:	Z050/SN3A UR-1153	
Type:	Screw power tensile testing machine	
Extensometer:	Long-stroke. Deviation less than 1.0%	
Load cell:	30kN	
Mounts:	Pneumatic grips (compressed air at 9Bar)	
Calibration standard:	ISO 9513-1	
Calibration performance:	Load cell 50kN:	100-500N deviation less than 1%
		500N-50kN less than 0.5%

Table 5: Details about Zwick tensile tester

The strain rates for the tensile test was sought to mimic the standard that Outokumpu uses. Outokumpu performs their tensile tests at room temperature with a strain rate of 0.001/s up to 2% elongation and is then changed to 0.008/s. Due to limitations in the software; these parameters couldn't be entirely conformed to.

The software was set up to the strain rate 0.001/s while the E-modulus was calculated. The strain rate is then changed to 0.008/s. Since the elastic modulus is not sensitive to difference between weld metal, HAZ and base metal, except in rare cases of dissimilar joining, E-modulus was not of interest.

For each type of specimen a total of four specimens were tested in order to assure repeatability of the results without too much deviation. In the case of the reference specimen three samples were sufficient

Figure 5: Tensile test parameters. Print screened from testXpert interface.

3.4 Bend Testing

All bend testing was performed in accordance with ASTM standard E290-97a and E190-92.[6.]

Bend testing was performed at SteelTech with a Trumpf TrumaBend V130 bending machine. Bending is achieved by forcing a V-shaped punch into a V-shaped die, causing local overstressing, as the specimen wraps around the punch.

Figure 6: (Left) Overview, TrumaBend V130 (Right) Test specimen being bent between punch and die

Welds were transverse to the longitudinal axis of the specimen. Testing was performed for two cases, one where the weld-face becomes the convex surface and one where the weld-root is situated on the convex surface. Bending was performed step-wise to achieve 45°, 90° and 180° bends.

Due to the limitations of the set-up, the 180° bend was achieved by applying force on the ends of the specimen. This was done with a different tool set up; flat die and punch, pictured in figure 16.

Figure 7: Tool setup for completing 180° bending.

Between bending steps, the convex surface was visually inspected with the unaided eye for cracks, and open defects. For the 90° and 180° bends observation and photography was made under stereo microscope in order to observe the bends even closer, even if this is outside the ASTM standard. This was made in order to ensure that no cracks, surface irregularities or defects had occurred between subsequent bends.

3.5 Vickers Hardness Testing

Vickers hardness testing was performed at Chalmers University of Technology, Gothenburg.

Testing was performed on the cross section of the weld, using rectangular test specimens as mentioned above. Before indentations, specimens were wet ground with grit 240 and 320 SiC paper with a circular wet grinding machine. One sample from each test setup was investigated.

1 kilogram (kg) of load was used during the Vickers hardness testing. Indentations were made with 20 μm spacing. Normally spacing corresponding to two indentations is used. However, as the indentations didn't interfere with each other by plastic deformation and stress, the 20 μm spacing was used in order to get a more detailed picture of the local hardness around the weld.

The indentations were then later observed and photographed under stereo microscope. The vertical and horizontal was measured and the average calculated for each indent. These

calculations were then converted to HV1-scale that correlates the indentation to the hardness.

3.6 MATLAB Simulations of Heat Affected Zone

Simulations of the weld thermal cycle, based on the Rosenthal equation [8], were made using the numeric-computing environment MATLAB [12].

The used script (Appendix V) calculates and plots the three-dimensional temperature distribution, isotherms and time-temperature relationship. Calculations are based on the analytical solutions to the Rosenthal equation.

An efficiency factor of 65% was selected. This factor was chosen since it was mentioned for similar welding conditions but for CO_2 laser welding in a publication from the literature study. [1]

4. Results

4.1 Welding

The experimental welding showed that welding with a focus of -1mm and weld speed 5 m/min produced the best results among the tested parameters. These parameters performed best in terms of producing a narrow and even weld face and full penetration. These parameters also produced an insignificant amount of spatter. This spatter could easily be removed by polishing if design specification would require so.

The starting point of the iteration was based on the documentation provided by Trumpf. However the documentation provided by Trumpf did not have weld parameters for a beam source of 2000 W, but was specified for 3000 W. Adaptation and iteration was therefore made for the used beam source.
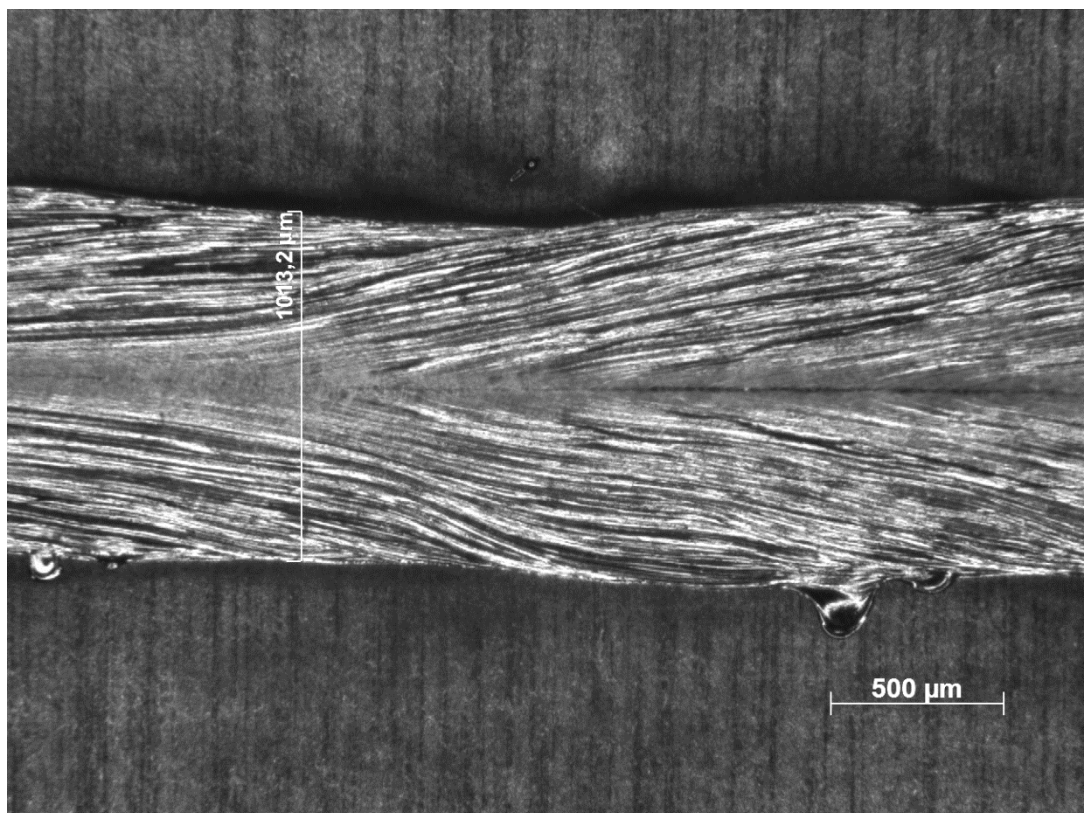
Figure 8: Weld face, specimen 11
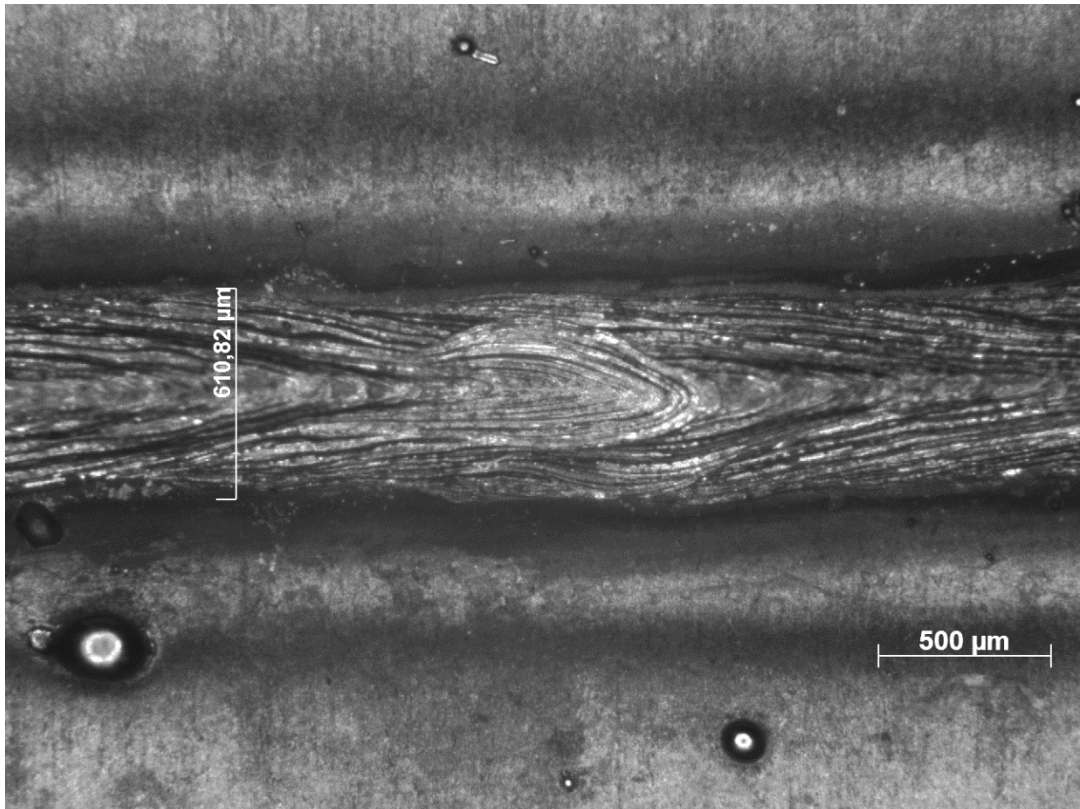
Figure 9: Weld root, specimen 11. Spatter visible on the sides

All test specimens were photographed with a Zeiss stereomicroscope using the software Zeiss AxioVision. The weld face and root topography were photographed for specimens 1-13. These images are all presented in the in Appendix I. The topography images show the solidified weld and its appearance, including spatter. Width of the weld face and root was marked in the images to enable easy analysis and comparison.

The original idea with testing two different elevated focus settings, 3 and 6 mm, was to investigate if a butt joint with a wider x-measure than 200 μm could be welded by adapting a lower welding speed. The lower weld speed would be compensating for the focus being elevated above the sheet, which results in a lower energy concentration. Full penetration was never achieved with neither 3 or 6 mm focus. For welding speeds from 2.25 m/min and below heavy oxidation started to occur. The weld flame would reach close to the optics and large amounts of soot were produced. Even though the system is equipped with a cross jet (compressed air) and shielding gas, it was considered not necessary to evaluate slower welding speeds. This decision was taken with respect to the equipment, not wanting to damage it. Welding speeds were also starting to reach speeds that could be matched with conventional fusion welding.

Throughout all welding performed in the project, it became very apparent that the laser itself is very stable. Instead importance was concentrated in making sure that the lasers cut steel sheets were free from spatter, and that they were thoroughly cleaned. The sheets were fixated with as little tolerance deviation as possible in order to achieve the best possible results. Some welded sheets were noted to get some mild oxidation on a small fraction of the weld seem. One possibility why this occurred could be local impurities in the material, spatter or dirt on the surface.

28

Test specimens from sheets A-L used for tensile and bend testing were observed under stereo microscope.This was made in order to ensure that test specimens actually matched the intended tolerances. It was observed that the actual Y measure didn't match the intended offset, whereas the X measure seemed to match the intended design very well. Measuring the X-measure was difficult as weld faces and roots became wider than the X measure. Observations indicate that sheets A, E and I seems to match the intended nominal. All other sheets with X > 0 have a weld with waist like shape. The bigger the X the smaller the waist, which was expected. For the largest X, 225 μm, the actual distance between the plates could be measured indicating low deviation from the nominal horizontal offset.

Sheet	X [μm]	Y [μm]	Actual X [μm]	Actual Y [μm]
BOP	0	0	0	0
A	0	0	-	49
B	75	0	-	41
C	150	0	-	36
D	225	0	237	25
E	0	75	-	47
F	75	75	-	41
G	150	75	-	43
H	225	75	230	65
I	0	150	-	108
J	75	150	-	76
K	150	150	-	103
L	225	150	224	78

Table 6: Actual measures of X and Y
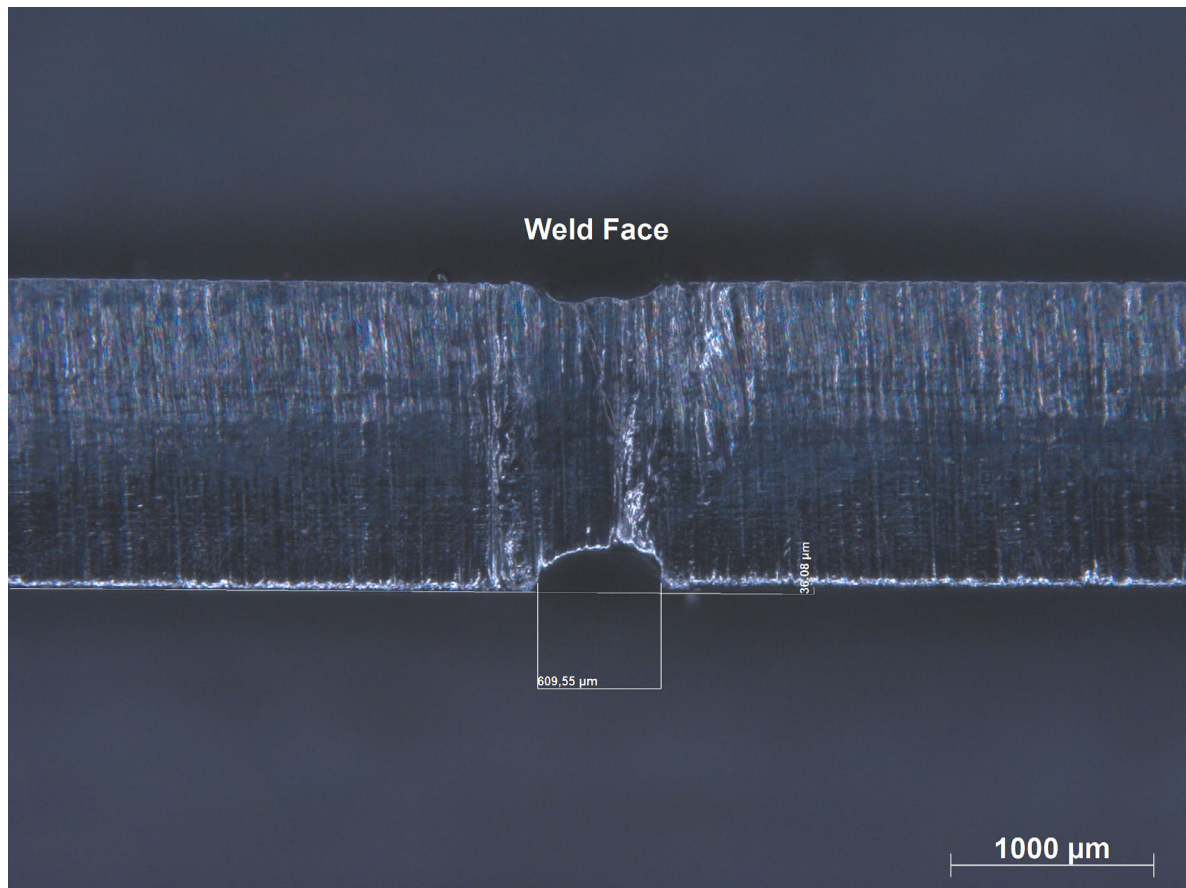
Table 7: Cross section of sheet C

4.2 Tensile Test

The tensile testing showed very positive results for tensile strength and elongation at break. Results (see Appendix II) show good repeatability with very little deviation for all test series. Tensile strength and elongation results in the same range as for the reference tests ($R_m \approx$ 620 MPa and $A_t \approx$ 55%) were achieved with the exception for sheets D, H and L. These sheets are the ones with biggest offsets and lower values were expected due to them having less material at the weld, thus creating a stress concentration.

	$R_{p0.2}$	R_m	A_t
	MPa	MPa	%
BOP 1	290,9	621,4	54
BOP 2	294,6	622,8	56
BOP 3	289,3	619,9	55
BOP 4	288,0	619,1	55

Fracture occurred in the weld for most specimens as expected. Specimens from sheets BOP, A, I and E all had fractures situated below or above the weld.

4.3 Bending Test

Inspection with the unaided eye showed no results of fracture except for specimens from sheet L. This applied to both of the two cases of bend testing. No surface irregularities or discontinuities as a result of the bending could be found during inspection. Inspection was extended to inspection under stereo microscope in order for closer evaluation. Inspection with stereo microscope was made (appendix IV) for 90° and 180° bends. Stereo microscope confirmed what had been observed with the unaided eye. No cracks or surface irregularities were present upon inspection.
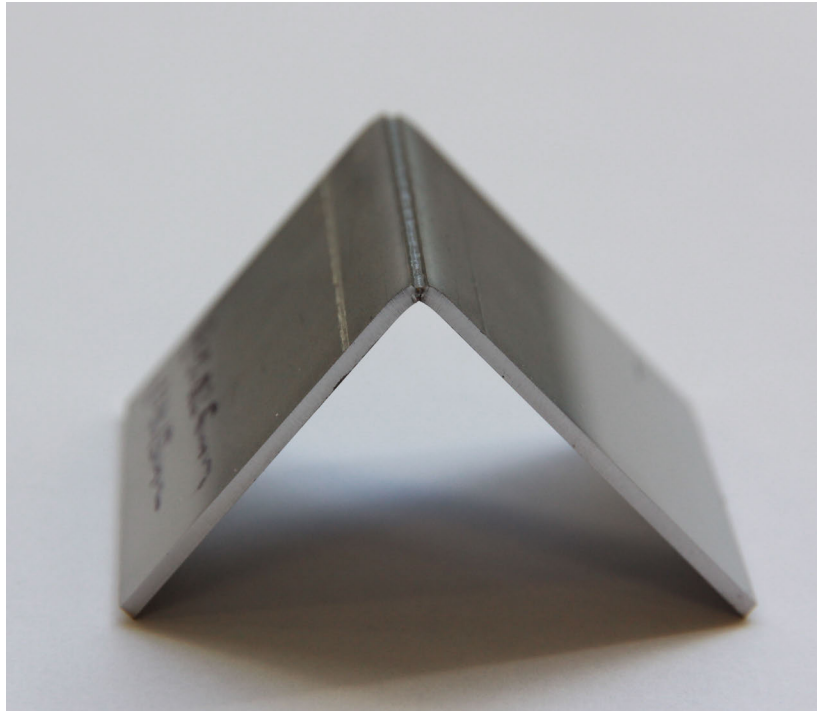
Figure 10: 90° bent test specimen
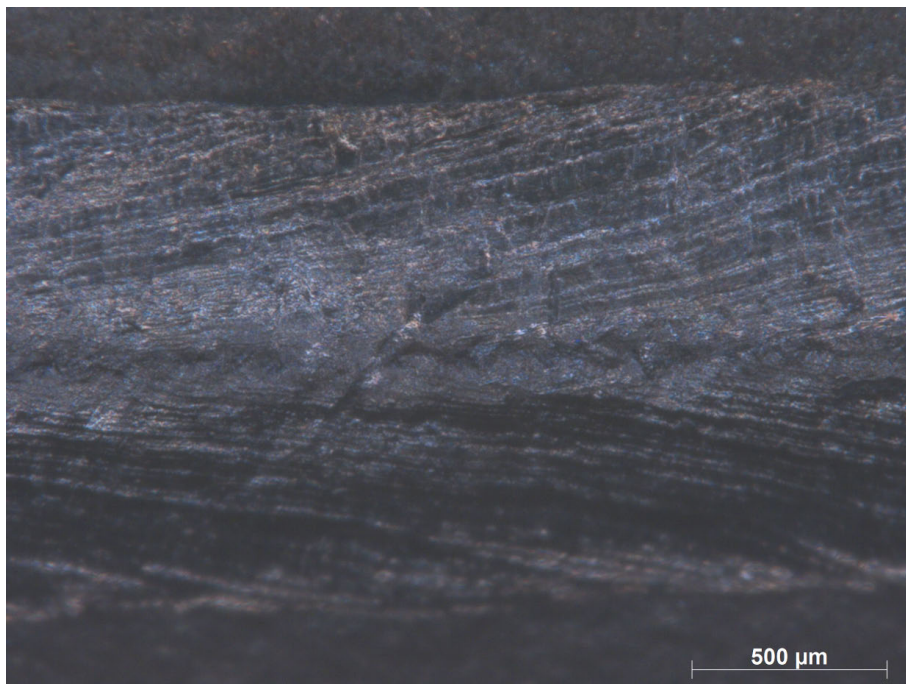
Figure 11: Bending Test 90° - Specimen A (Weld Face)

4.4 Vickers Hardness Test

The Vickers hardness tests (Appendix III) shows a local max in hardness situated at the center of the weld, with values ranging from approximately 180 to 200 HV1. This goes for all the tested test specimens 1-13.

The reference test specimen measured a hardness of approximately 140 HV1. The peak hardness is increased by approximately 28-43 %.

4.4 MATLAB Simulations of Heat Affected Zone

Plots below present results from the heat distribution simulation. Results confirm that the chosen efficiency factor seems reasonable as a weld pool of 0.5-0.6 mm is achieved, which was to be expected and was measured from the topography study.

Figure 21 depicts the shape of the three dimensional temperature fields. Figure 22 depicts the isotherms. The isotherms represent a prediction of how the weld pool looks. They define the size and shape of the weld pool. The shape and size of the weld pool is affected by heat input and welding speed. Figure 23 shows the time-temperature curves of the thermal cycle in the heat affected zone.
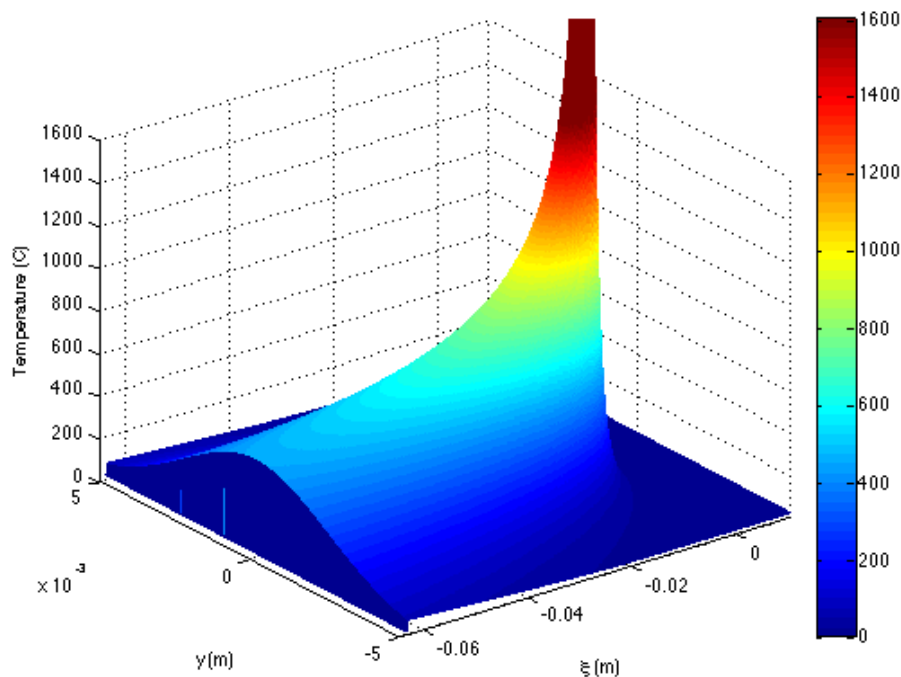
Figure 12: Three-dimensional temperature distribution
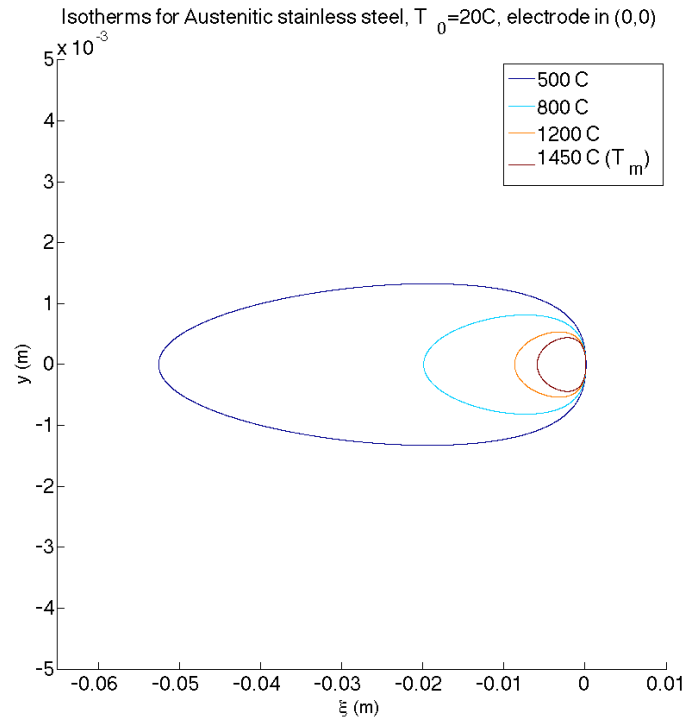
Figure 13: Isotherms
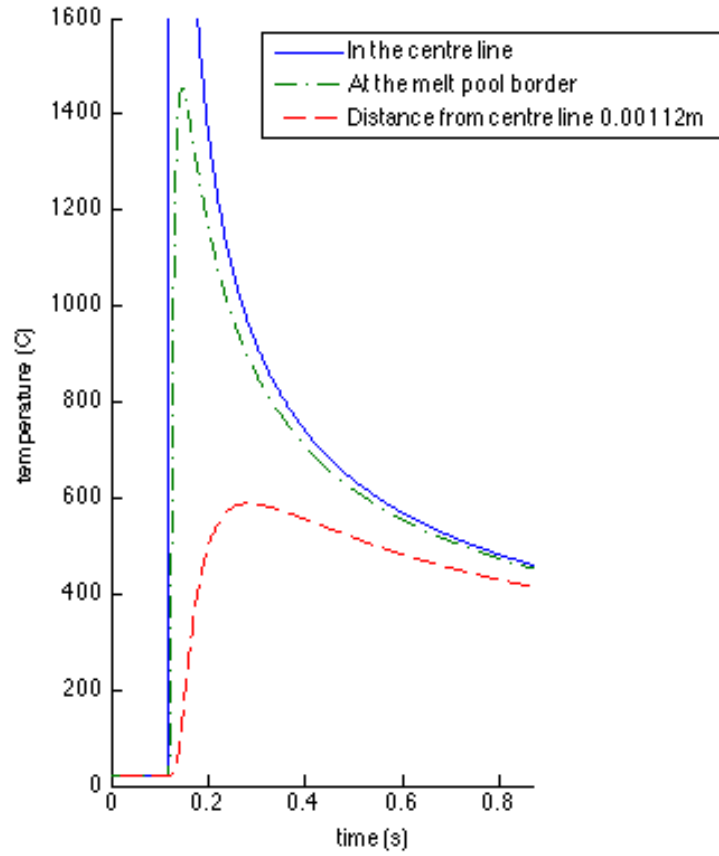
Figure 14: Temperature - Time curves

5. Discussion

Whereas conventional welding demands tolerances in the 1/10 mm range and is a very flexible process, laser welding demands tolerances in the 1/100 mm range in order to achieve good results. One of the biggest challenges that industries/producers may face lies in the adaption to a more demanding process control. Fixture optimization is crucial in order to successfully implement laser welding into a manufacturing line. The cross over from designing conventional fixtures to fixtures for laser welding requires decreased tolerances in most cases.

Tensile tests show that for tolerance offsets in the range 0-150 μm, both the elongation at break and tensile strength were fairly unaffected and very similar results were achieved. Since there is no infusion of material with laser welding (unless, hybrid welding) this poses requirements that tolerances must be kept in this range if the same tensile strength and ductility is to be achieved. A horizontal offset (X measure) of 225 μm showed a very pronounced waist like shape of the weld. The waist like shape is a direct result of the laser only hitting the sides of the sheets without infusion of filler material. The insufficient amount of melt sinks towards the middle as it solidifies, creating the waist. It becomes clear that the process window regarding geometric tolerance deviations lies in the $\mp$0.15 mm range for 1.5 mm thick sheets of EN 1.4301. It could generally be assumed that Cr-Ni steels with similar compositions will respond similarly, as fairly forgiving and easy to weld.

Stereo microscopy measurements established that for sheets A-L, the vertical offset, the Y measures were not corresponding to the nominal values. This was also true for test specimens 1-13 where no shims were used. This clearly indicates that the welding fixture was not sufficient. Even though the Y values were shifted in relation to their nominal values, the deviation was close enough to obtain results. These deviations are probably a result from thermal distortion from the laser cutting and stud welding. It could as well be a result of tightening the bolts too hard and achieving elastic deformation in the shims. Another possibility could be that the used shim design for the Y measure is too rough and unable to support the sheet enough. The insufficient support results in the sheet bulging down upon tightening.

Hardness measures showed a very pronounced hardness increase in all tested specimens. Even if the increase should not be accounted for as negligible it does not seem have a critical effect on ductility, thus making laser welded EN 1.4301 very suitable for post-weld mechanical forming. Especially since 90° bends, which are the most common type are easily achieved without the presence of surface irregularities or cracks.

Simulation of the HAZ is a fast method evaluating material and weld parameters. However uncertainties concerning efficiency factor and other variables need to be investigated further and accounted for. If this could be achieved, the simulations could be an early and accurate method for fast and cost effective evaluation of material and weld parameters. For example, by finding more accurate representations, models or measurements of the efficiency factor simulations could be a quick method for those interested in committing to laser welding.

6. Conclusions

The weld weldability of 1.4301, stainless steel has been made. Main focus has been process sensitivity against geometrical deviations in the weld joint. Test specimens with horizontal and vertical offset in the butt joint was manufactured, tested and analyzed. Performing ASTM standardized mechanical testing; tensile testing, bend testing and Vickers hardness data were obtained and analyzed. The heat HAZ have also been studied with the help of computer simulations based on the Rosenthal equations. Here are the compiled conclusions of the experiments:

- Solid state laser welding is a very favorable joining process for 1.4301

- For 1.5mm thick EN 1.4301 sheets optimum optics focus and weld speed seems to be -1 mm and 5 m/min respectively.

- Horizontal offset in the weld butt joint up to $\mp$0.15 mm can be achieved without any significant loss of mechanical properties in 1.4301 sheets. The weld will however act as a stress concentration.

- Tensile testing shows little to negligible effect in tensile strength and elongation to break with horizontal (X) and vertical (Y) offsets in the 0-150 μm range.

- Hardness testing shows a local increase of the peak hardness. Since the energy application is on such a small areas, a very small HAZ is achieved. Resulting in less thermal stressing and cracking than for conventional welding.

- Bend testing show that the local hardness increase does not crucially affect ductility. Laser welded 1.4301 can without any difficulties be mechanically processed.

7. Recommendations

In order to improve results of the Y-offset, shim design optimized for the fixture could be made. Milling the upper plate could improve its accuracy. Tightening the bolts with a torque wrench could result in improved consistency in fixation. In order to avoid thermal deformation, stud welding could be replaced with NC drilled/milled threaded holes and the use of regular bolts and/or nuts.

The uncertainties regarding whether or not the efficiency factor lies in a trustworthy region could be investigated in order to improve accuracy. What other factors are there to take into account? Further studies based on observations from earlier publications and mathematical models could make for a more accurate representation. This could be complemented with experiments using thermocouples. Reflection is another important aspect to take into account. The EN 1.4301 sheets welded in this project were not polished. How would a polished surface react in comparison to a non-polished one? Investigations of surface treatments and different welding geometries could be made in order to evaluate their influence and if they need to be accounted for in computer simulations.

Investigating the microstructure and by extension the HAZ, the validity of the computer simulations and its accuracy could be correlated. It could also be of great interest to further investigate other weld geometries as these behave differently i.e. in terms of thermal conduction.

It would be of great interest to further investigate if the optics focus of -1mm really is optimum. Even if this setting produces very desirable results, improvements are likely to be made if it was to be looked into further. An improved focus could potentially produce less spatters and/or achieve faster welding speeds, thus creating a more cost effective process.

Tests should be made investigating the effect of different sheet thicknesses in order to correlate how tolerance deviation corresponds to other dimensions as well.

EN 1.4301 being a stainless steel, it is of interest to evaluate the post weld corrosion properties after welding. Two big fields of use for thin laser welded EN 1.4301 sheets are medical and large scale catering applications (i.e. large dish washers and boiling pots, etc), both with strict requirements on corrosion due to strict demand on hygiene and aggressive environments that can be present.

8. References

1. A K Nath, R Sridhar, P Ganesh & R Kaul, Laser Power coupling efficiency in conduction and keyhole welding of austenitic stainless steel. Sādhanā, vol. 27, Part 3, June 2002

2. ASTM A 370-77 Mechanical Testing of Steel products. From 1997 ANNUAL BOOK OF ASTM STANDARDS VOLUME 01.02. J. Azara (ed), N. Baldini (ed), E. Barszczewski, L. Bernhardt (ed), E. Gutman (ed), J. Kramer (ed), C. Leinweber, V. Mayer, P. McGee (ed) T. Sandler, R. Wilhelm, pages 314-369, West Conshohocken, PA: AMERICAN SOCIETY FOR TESTING AND MATERIALS, 1997

3. ASTM E 8M-00b Standard Test Methods for Tension Testing of Metallic Materials. From 2001 ANNUAL BOOK OF ASTM STANDARDS VOLUME 03.01, R. Allen (ed), N. Baldinin (ed) E. Gotman (ed), E. Keefe (ed), C Leinweber (ed) V. Mayer (ed), P. McGee (ed), K. Peters (ed), T. Sandler (ed) E. Whealen (ed), R. Wihelm (ed), pages 77-98, West Conshohocken, PA: AMERICAN SOCIETY FOR TESTING AND MATERIALS, 2001

4. ASTM E 190-92 Standard Test Method for Guided Bend Test for Ductility of Welds. From 2001 ANNUAL BOOK OF ASTM STANDARDS VOLUME 03.01. R. Allen (ed), N. Baldinin (ed) E. Gotman (ed), E. Keefe (ed), C Leinweber (ed) V. Mayer (ed), P. McGee (ed), K. Peters (ed), T. Sandler (ed) E. Whealen (ed), R. Wihelm (ed), pages 354-360 West Conshohocken, PA: AMERICAN SOCIETY FOR TESTING AND MATERIALS, 2001

5. ASTM E 290-97a Standard Test Methods for Bend Testing of Material for Ductility. From 2001 ANNUAL BOOK OF ASTM STANDARDS VOLUME 03.01. R. Allen (ed), N. Baldinin (ed) E. Gotman (ed), E. Keefe (ed), C Leinweber (ed) V. Mayer (ed), P. McGee (ed), K. Peters (ed), T. Sandler (ed) E. Whealen (ed), R. Wihelm (ed), pages 354-360 West Conshohocken, PA: AMERICAN SOCIETY FOR TESTING AND MATERIALS, 2001

6. Buchfink, Gabriela. The Laser as a Tool. Würzburg: Vogel Buchverlag, 2007.

7. Demmeler, D28/D16 3-D clamping system. 2013. Demmeler Maschinenbau GmbH & Co. http://www.demmeler.com/en/products/d28-d16-3-d-clamping-system.html (Accessed 2013-08-28)

8. Easterling, Kenneth. Introduction to the Physical Metallurgy of Welding. Oxford: Butterworth-Heinemann Ltd, 1992.

9. M. F. McGuire, Stainless Steels for Design Engineers
    Materials Park, Ohio: ASM International, 2008

10. Outukumpu, EN 1.4301, AISI 304, Product Information, April, 2009
    https://www.outokumpu.com/SiteCollectionDocuments/Austenitic-Stainless-Steel-
    1.4304-1.4307_Datasheet.pdf (Downloaded 2013-06-10)

11. Shapiro, Eugene. Bend Testing, Mechanical Testing and Evaluation Volume 8, ASM
    Handbook. H. Kuhn (coord.) and D. Medlin (coord.), pages 172-184, ASM
    International, 2000

12. The MathWorks Inc, MATLAB Product Overview, 2013
    http://www.mathworks.se/products/matlab/index.html (Accessed 2013-08-28)

13. W. Mohr, Mechanical Testing of Welded Joints, *Mechanical Testing and Evaluation*,
    Volume 8, *ASM Handbook*. H. Kuhn (coord.) and D. Medlin (coord.), pages 845–852,
    ASM International, 2000

Appendices

Appendix I – Topography
Specimen 1
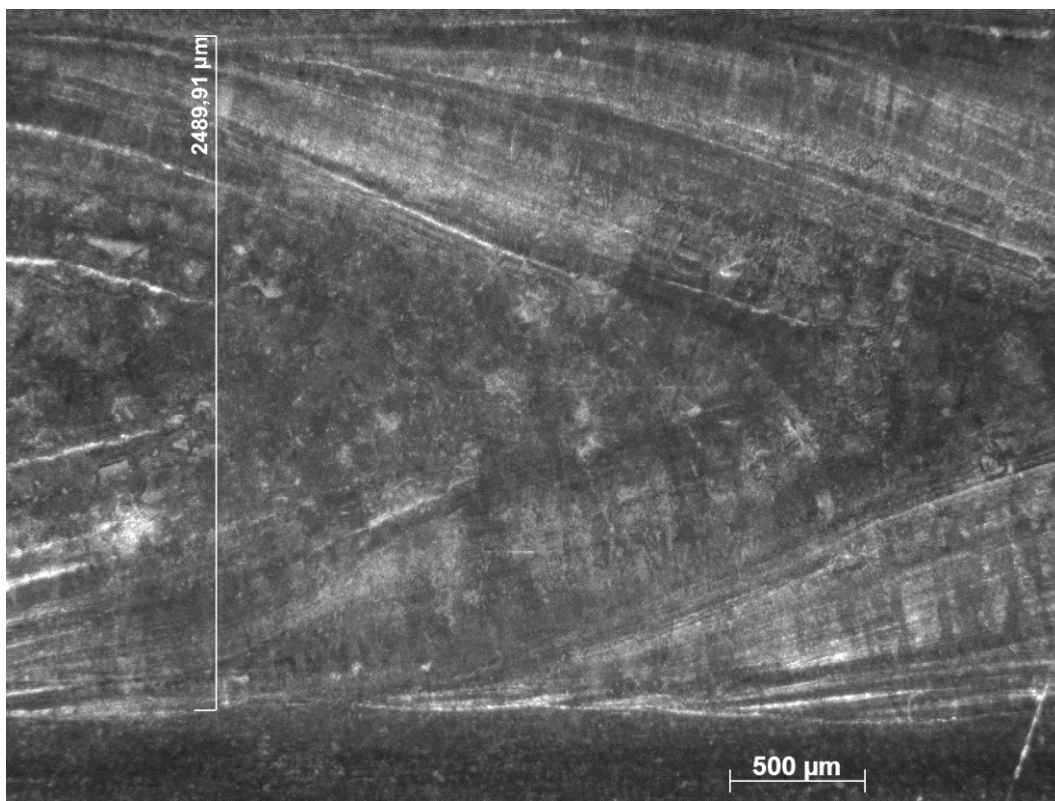
Specimen 1 (Weld Face)
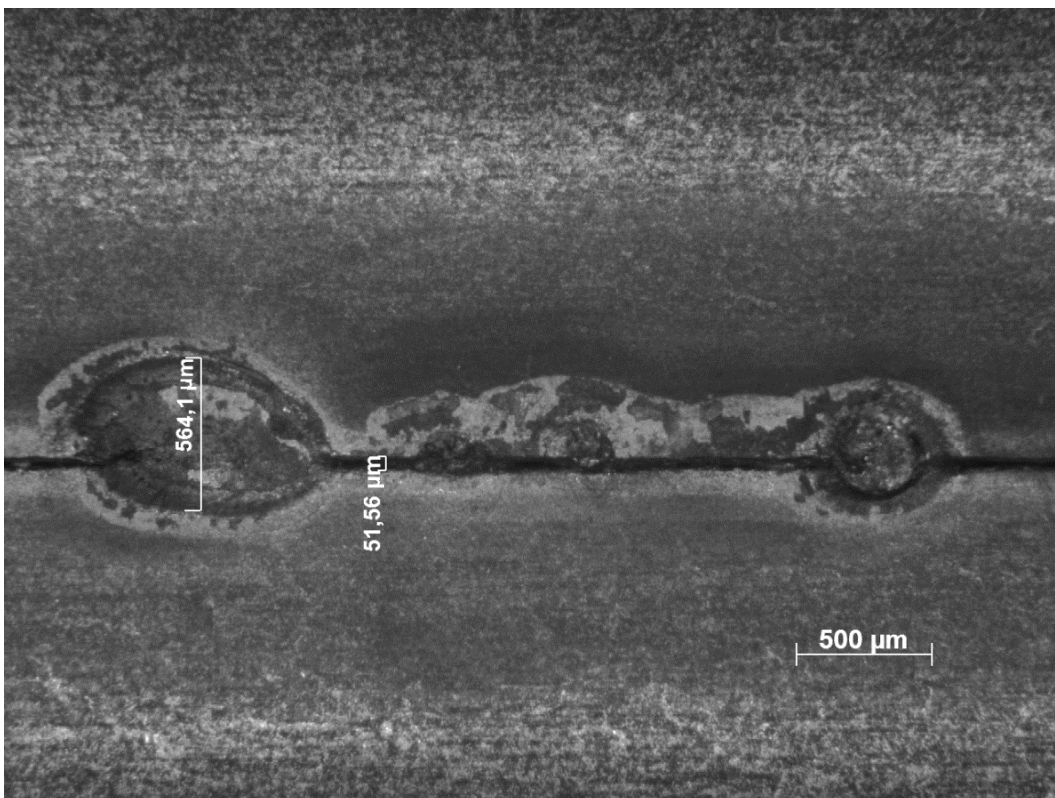
Specimen 1 (Weld Root)

Specimen 2
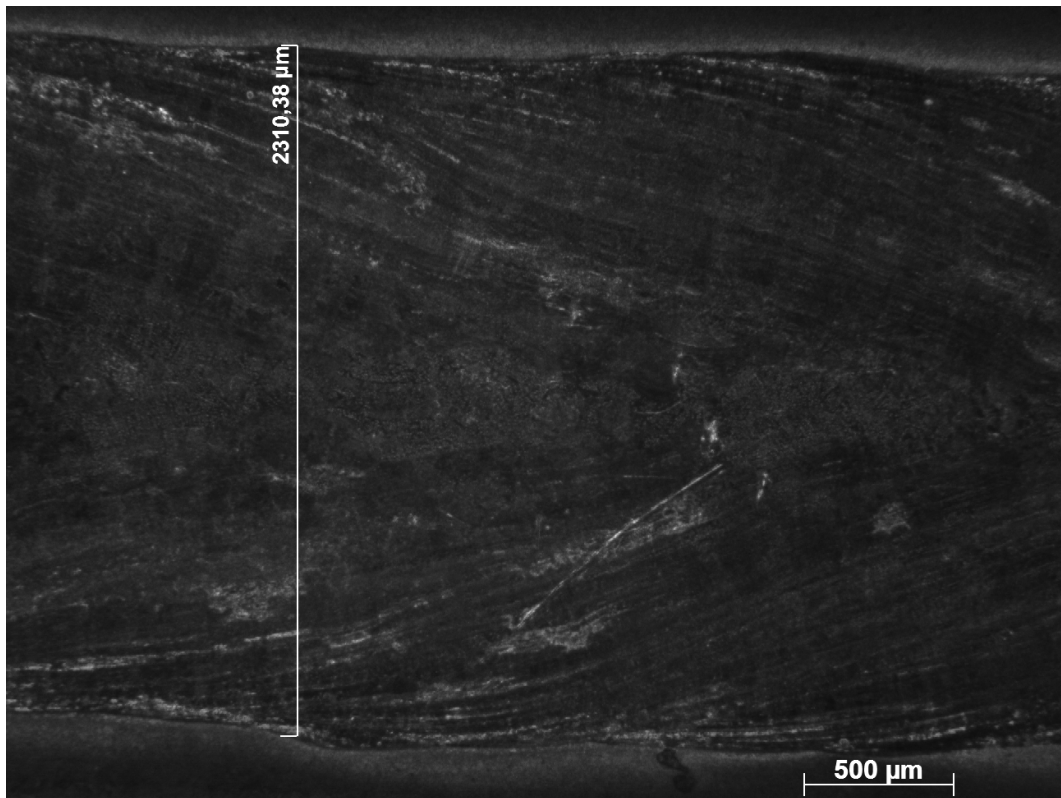
Specimen 2 (Weld Face)
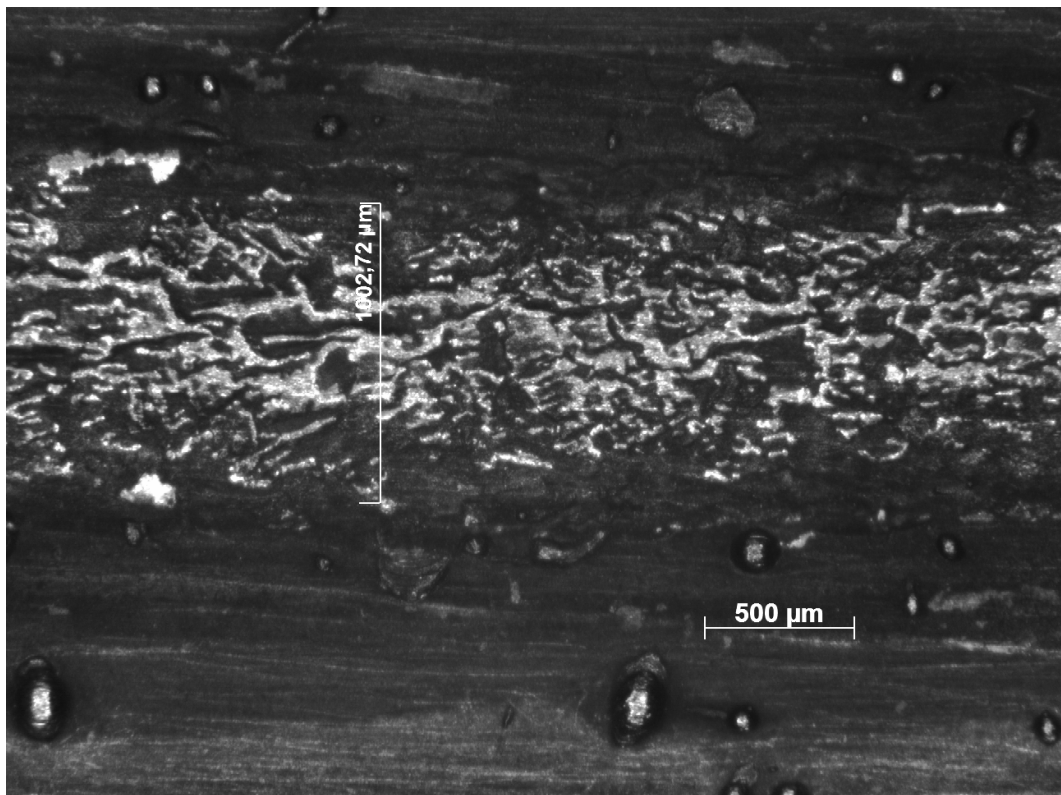
Specimen 2 (Weld Root)

Specimen 3
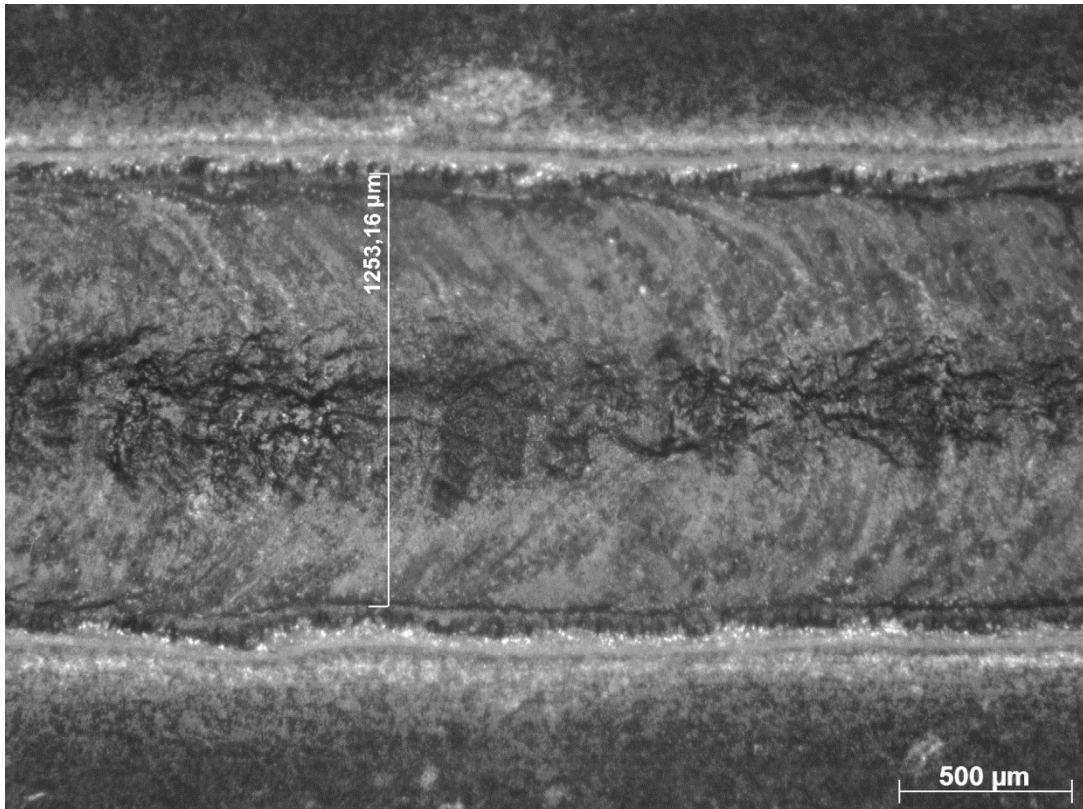
Specimen 3 (Weld Face)
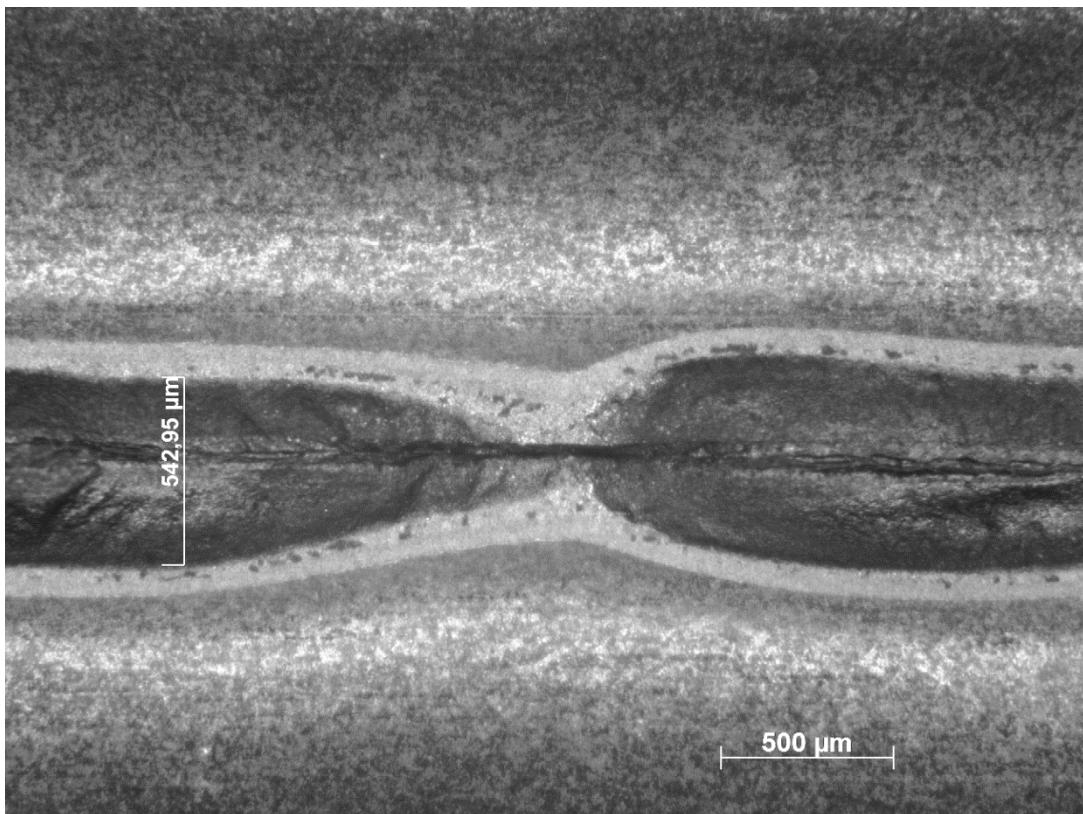
Specimen 3 (Weld Root)

Specimen 4
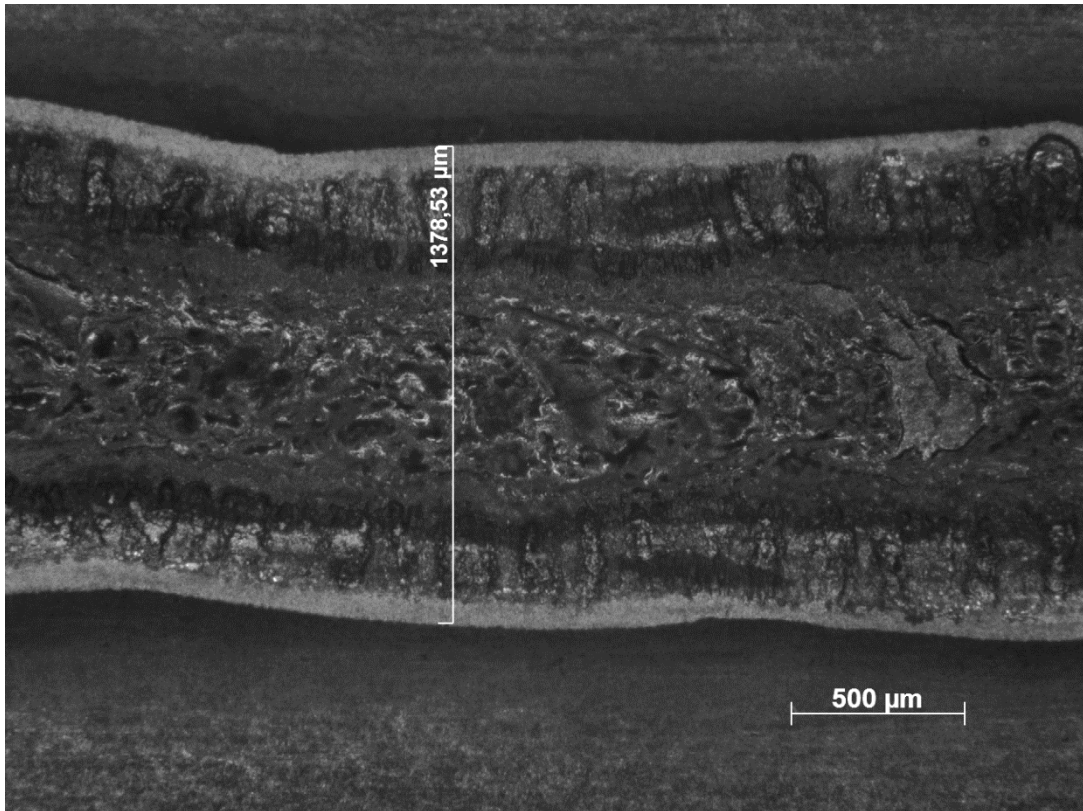
Specimen 4 (Weld Face)
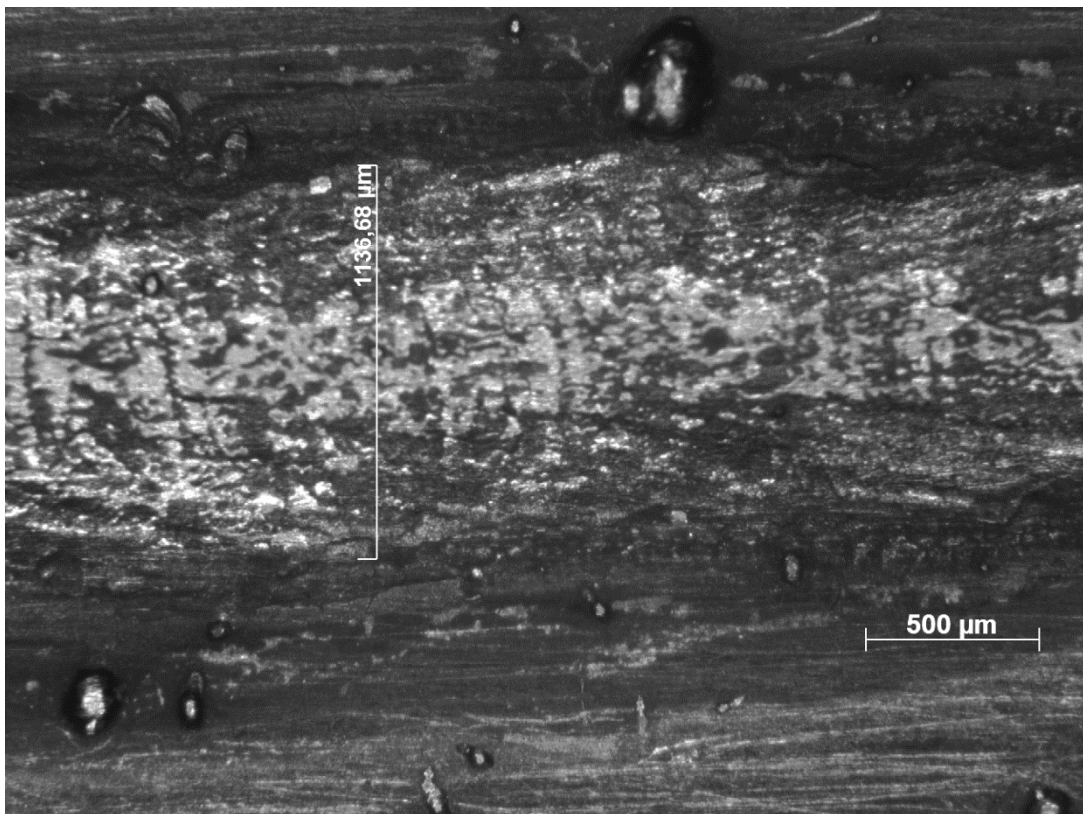
Specimen 4 (Weld Root)

Specimen 5
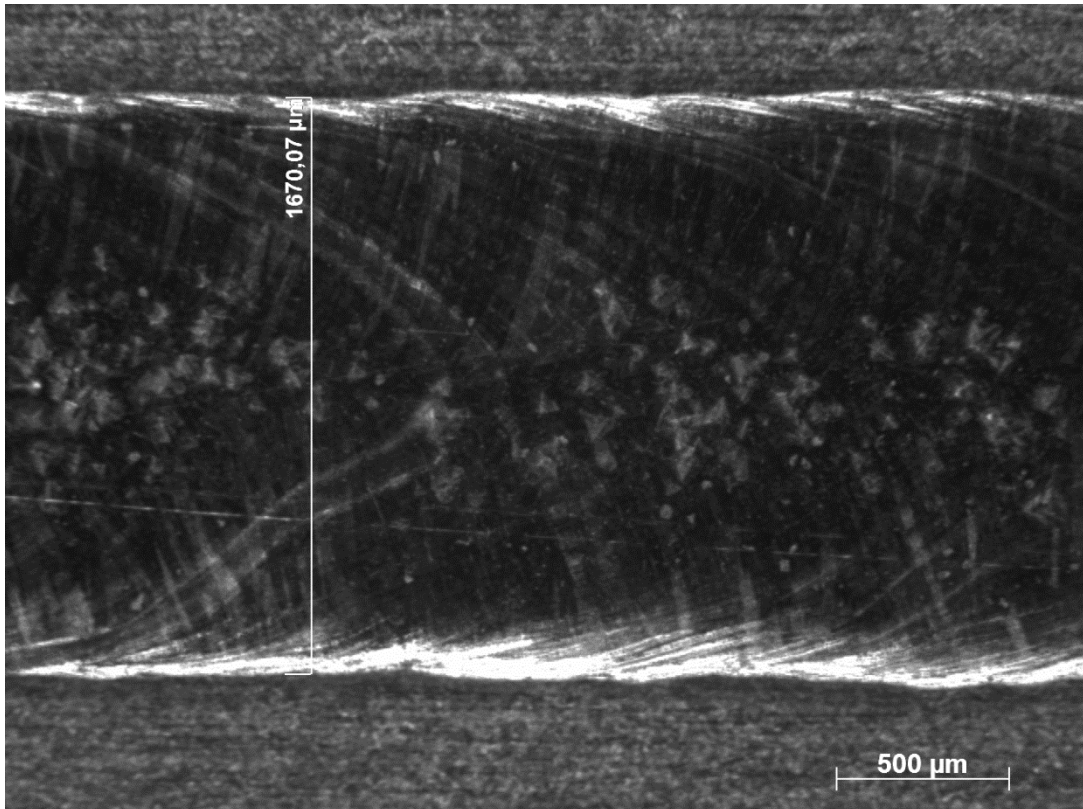
Specimen 5 (Weld Face)
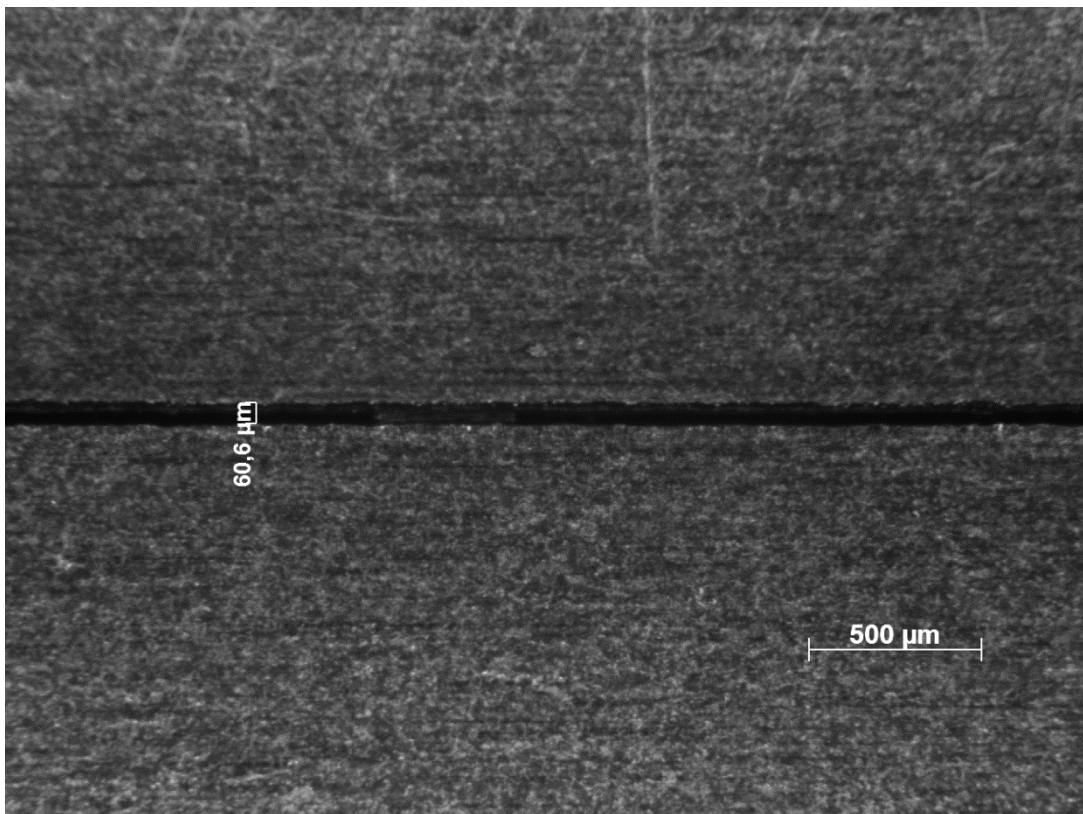
Specimen 5 (Bottom side)

Specimen 6
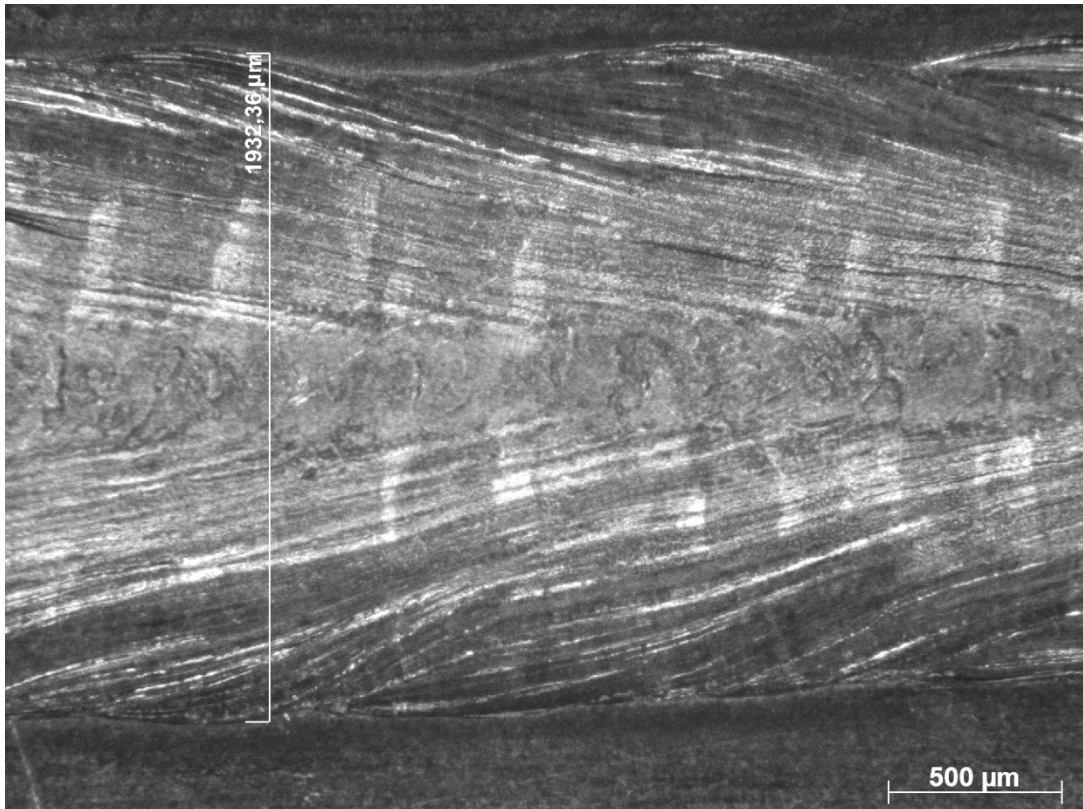
Specimen 6 (Weld Face)
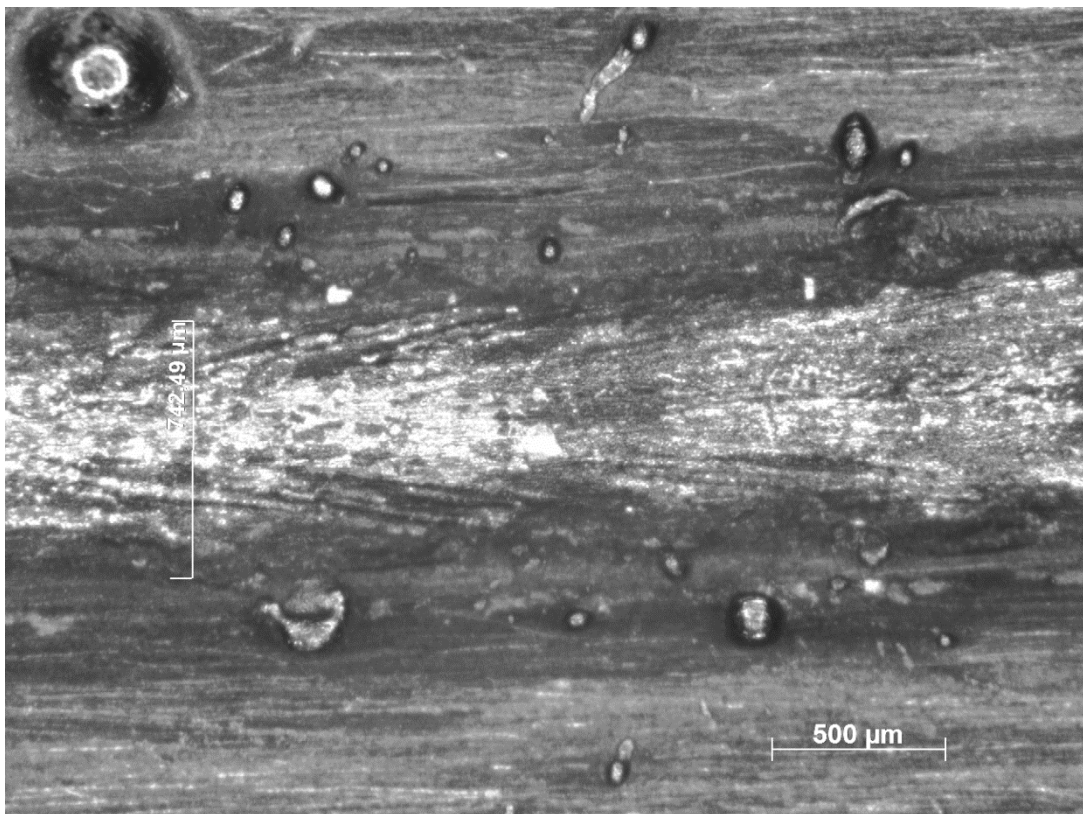
Specimen 6 (Weld Root)

Specimen 7
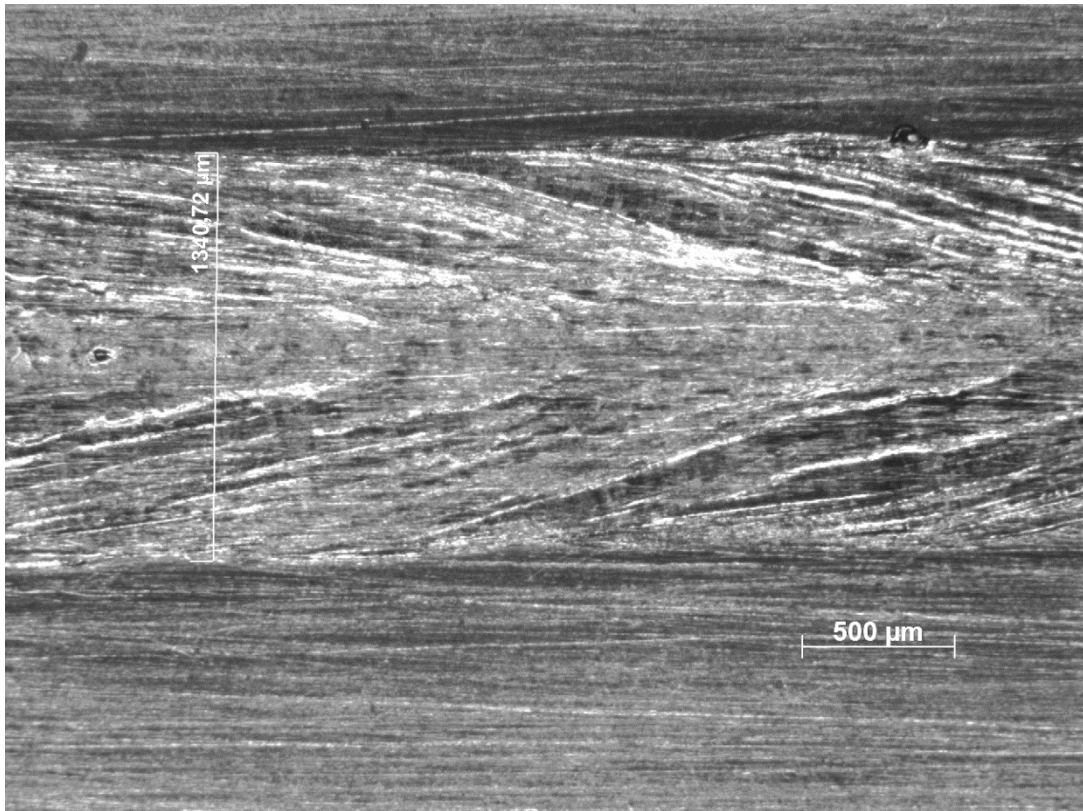
Specimen 7 (Weld Face)
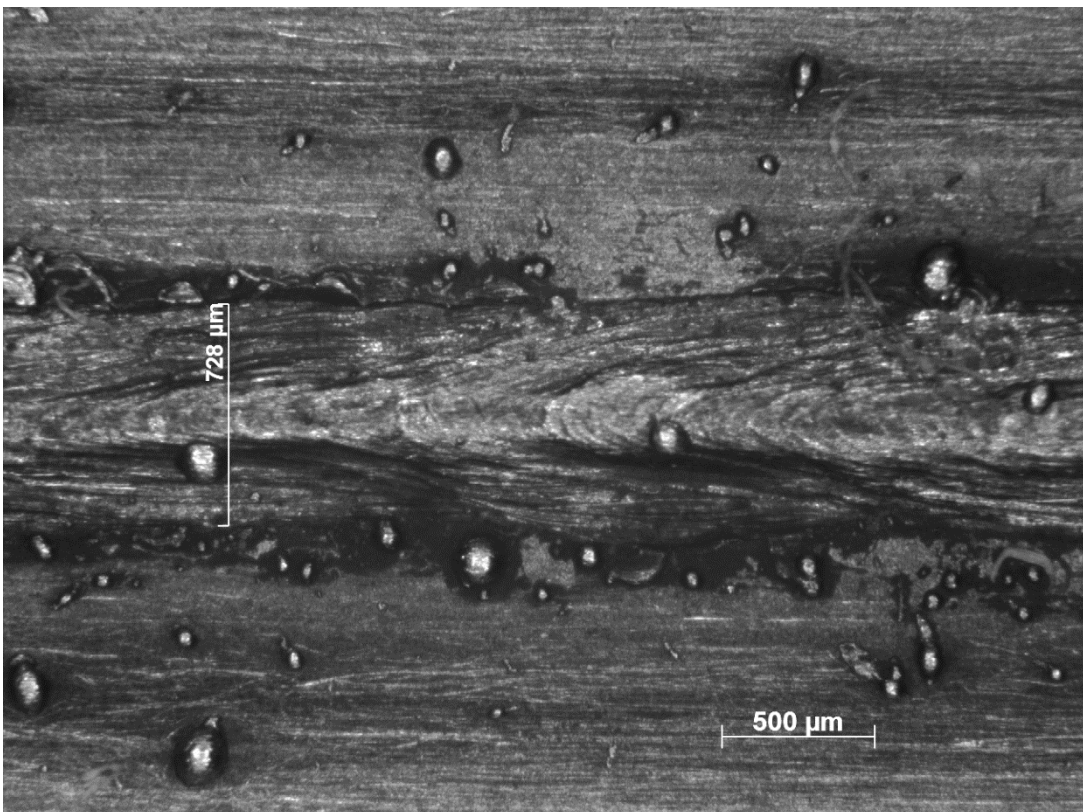
Specimen 7 (Weld Root)

Specimen 8
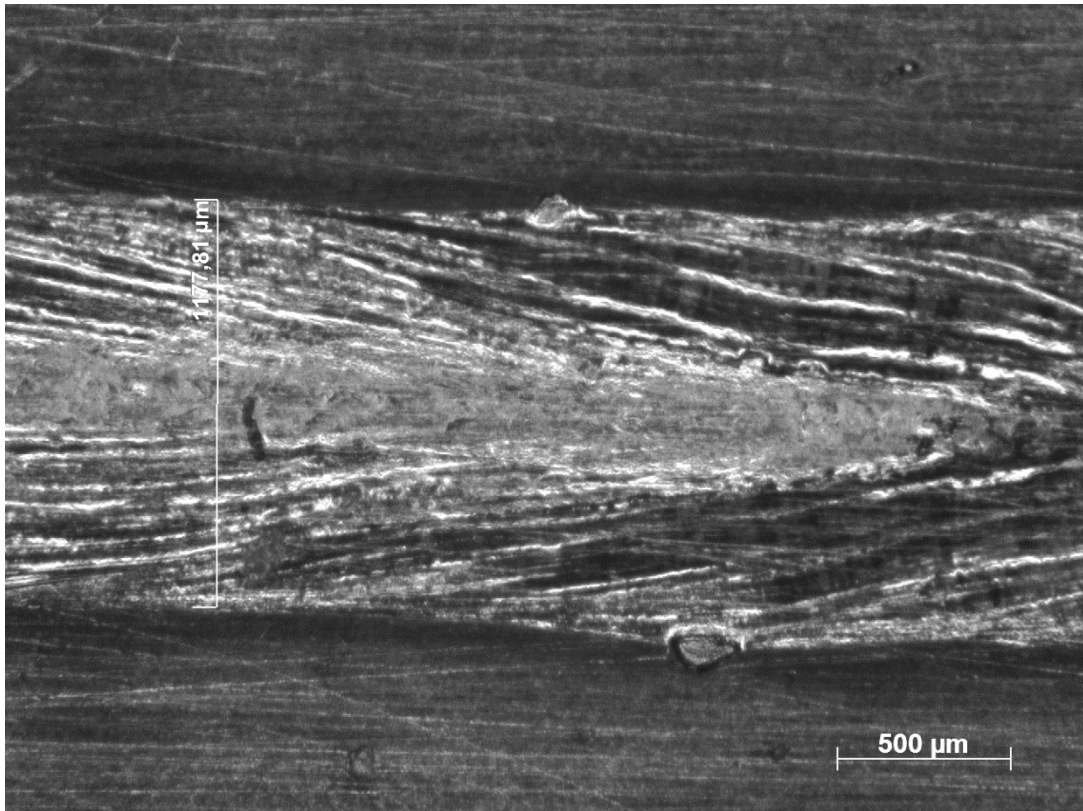
Specimen 8 (Weld Face)
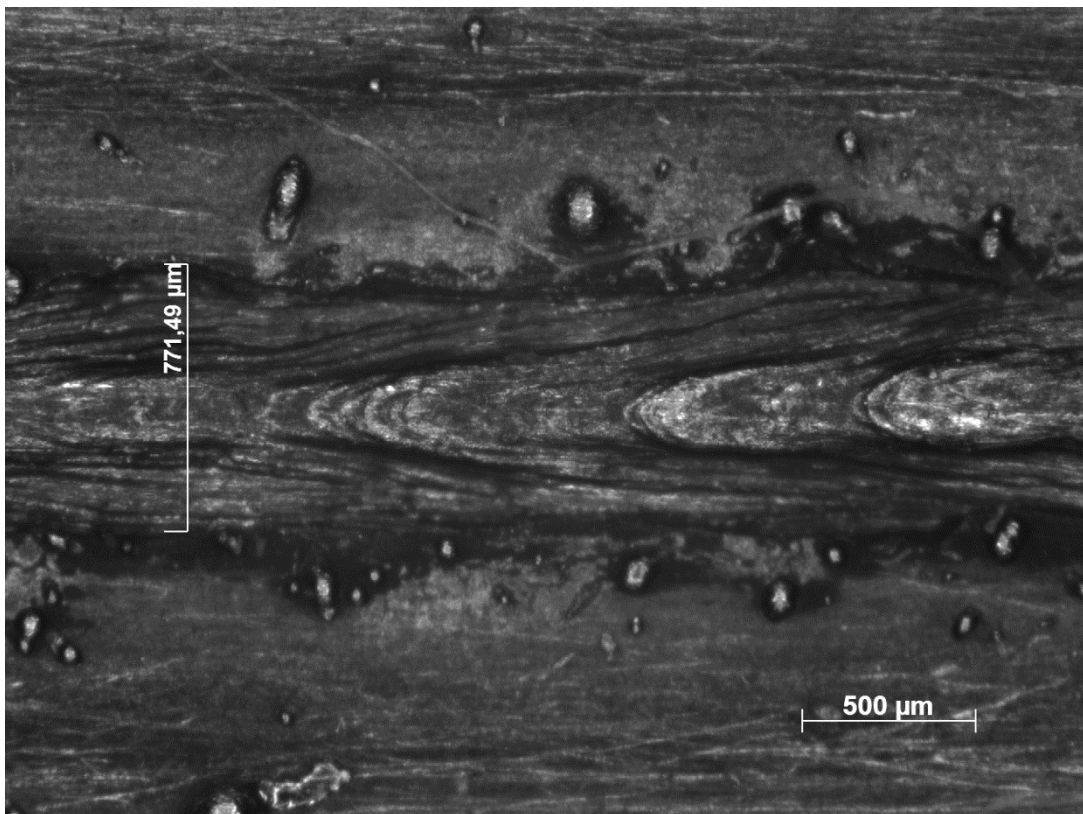
Specimen 8 (Weld Root)

Specimen 9
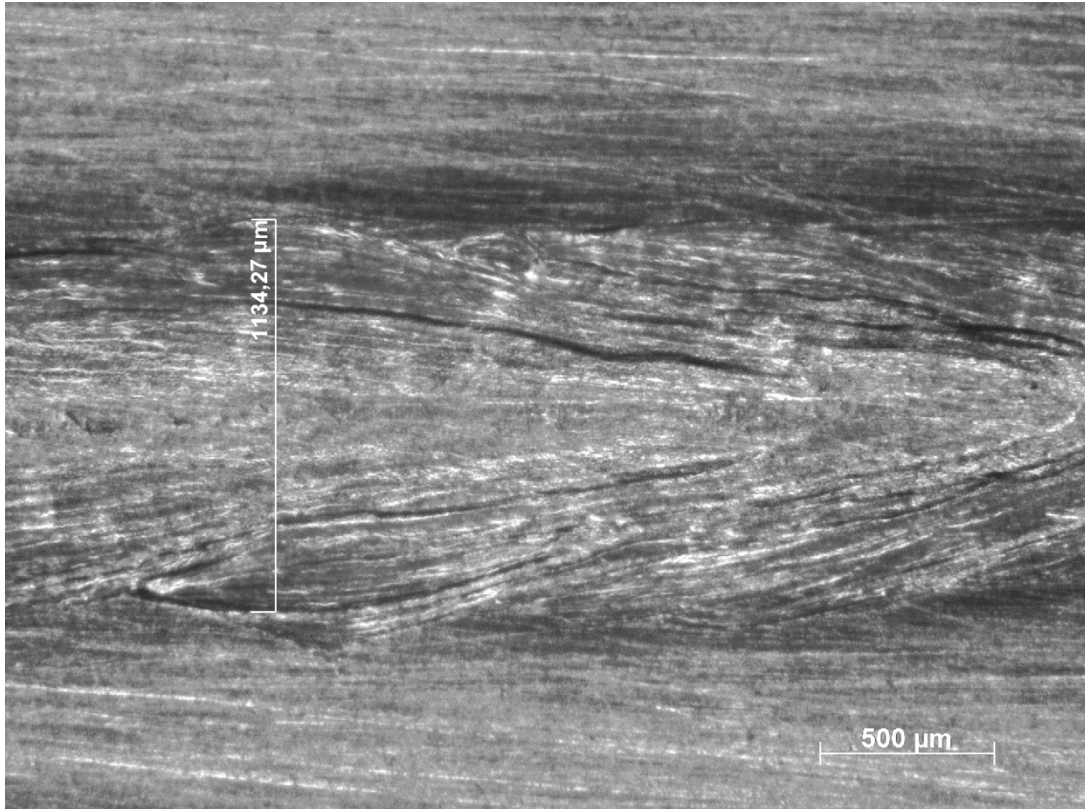
Specimen 9 (Weld Face)
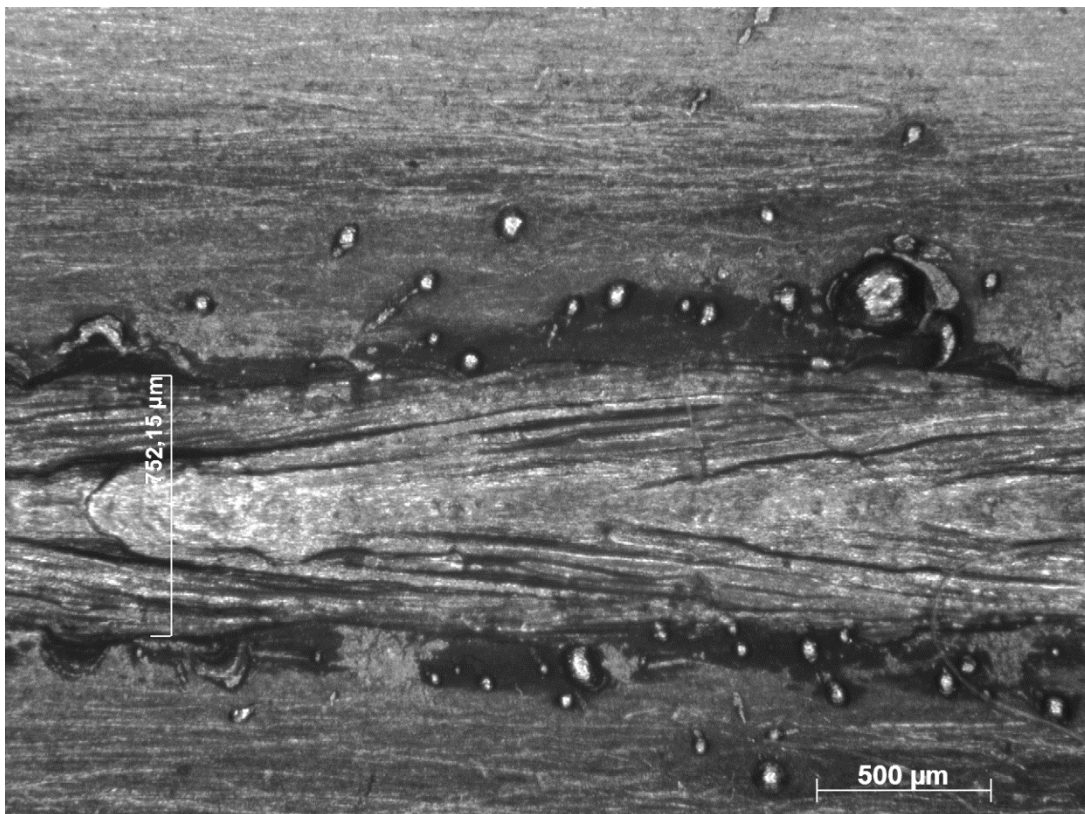
Specimen 9 (Weld Root)

9
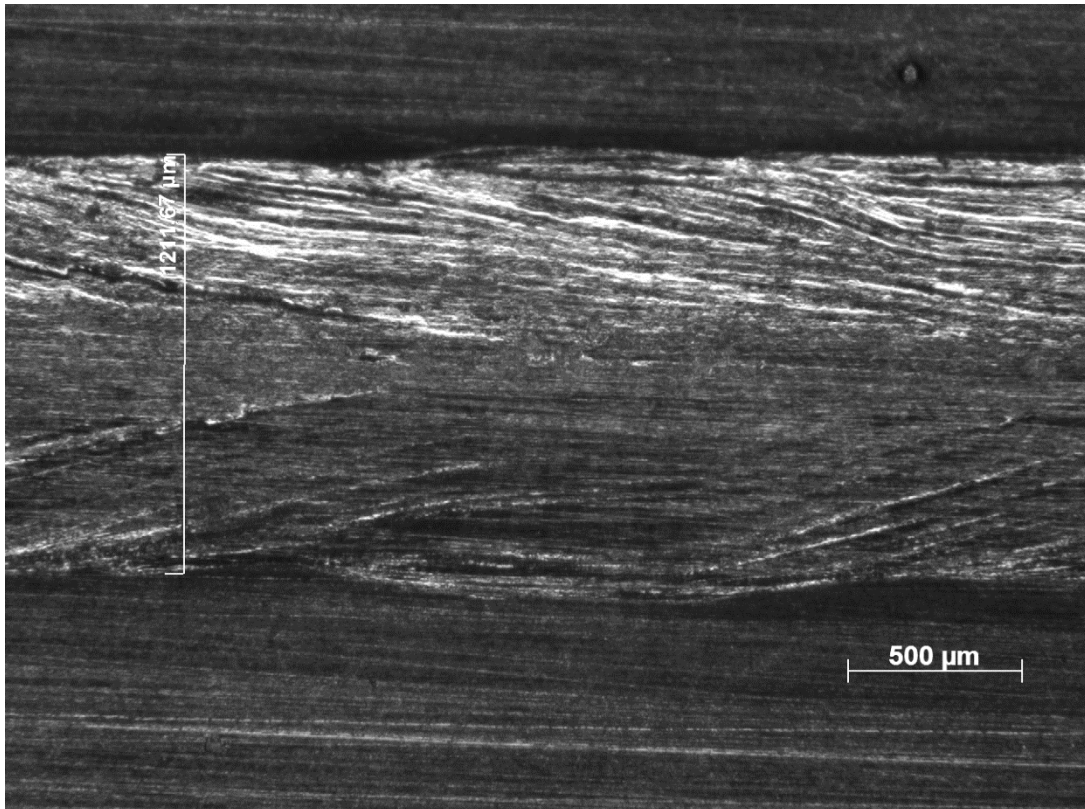
Specimen 10

Specimen 10 (Weld Face)
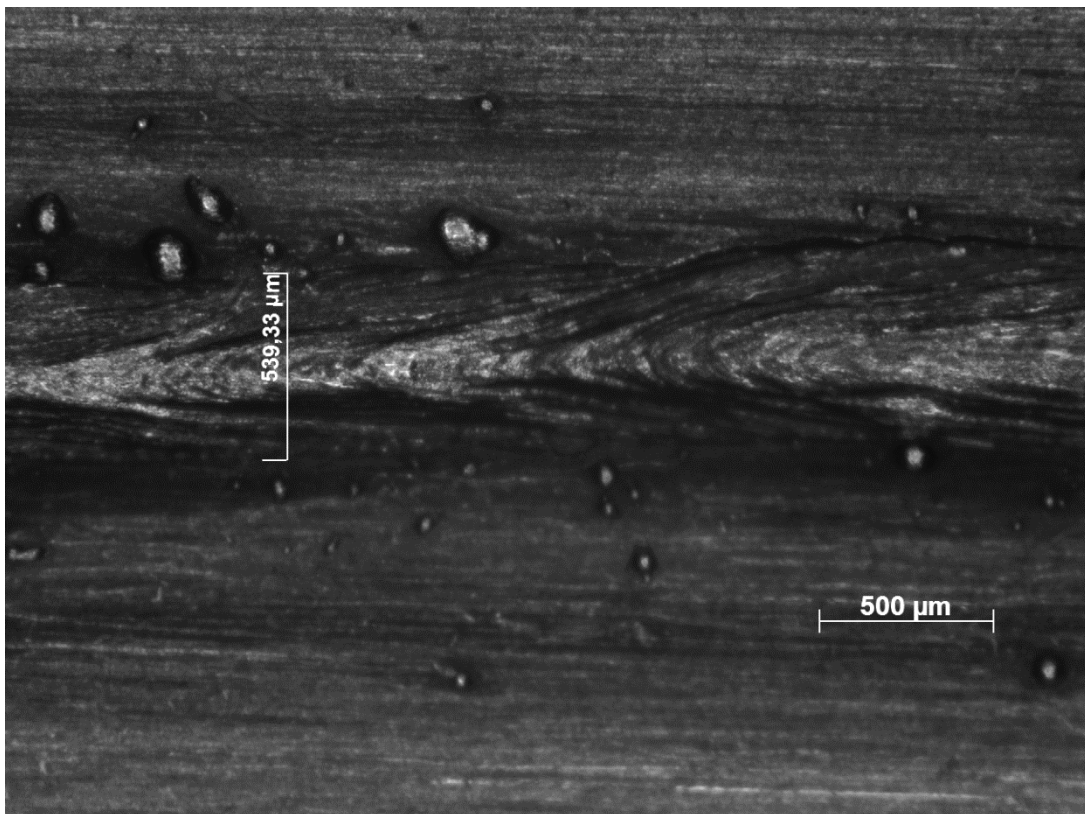
Specimen 10 (Weld Root)

Specimen 11
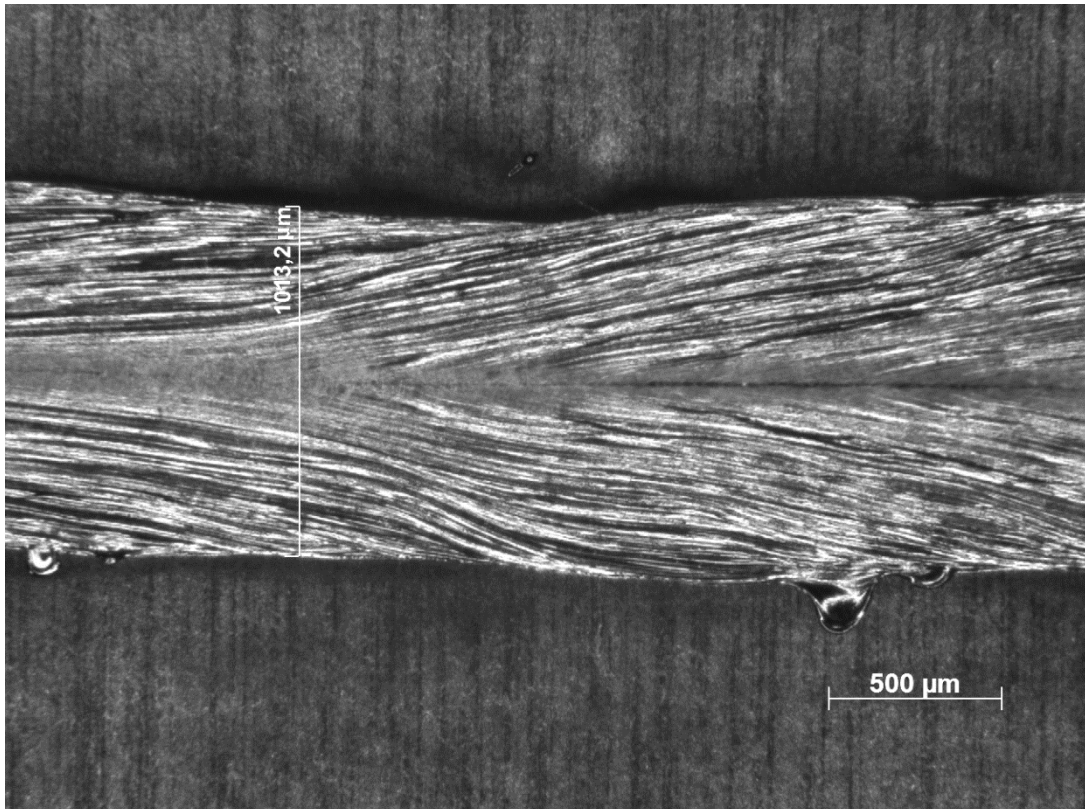
Specimen 11 (Weld Face)
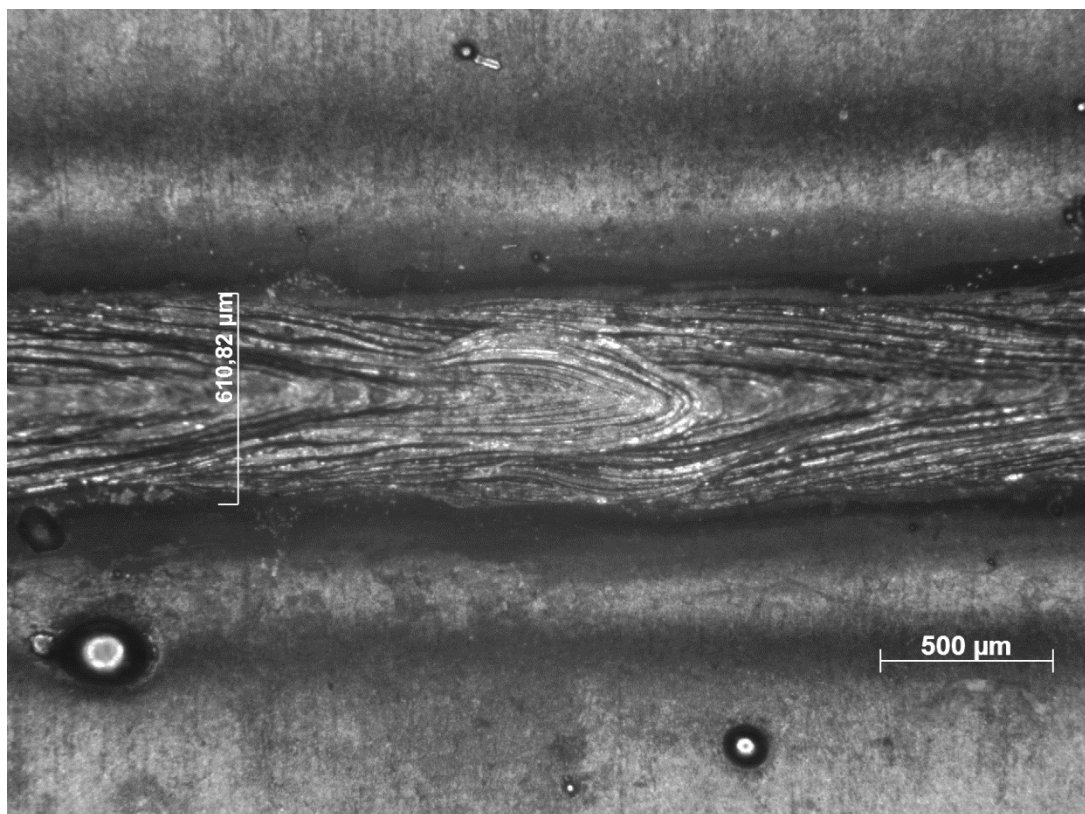
Specimen 11 (Weld Root)

11
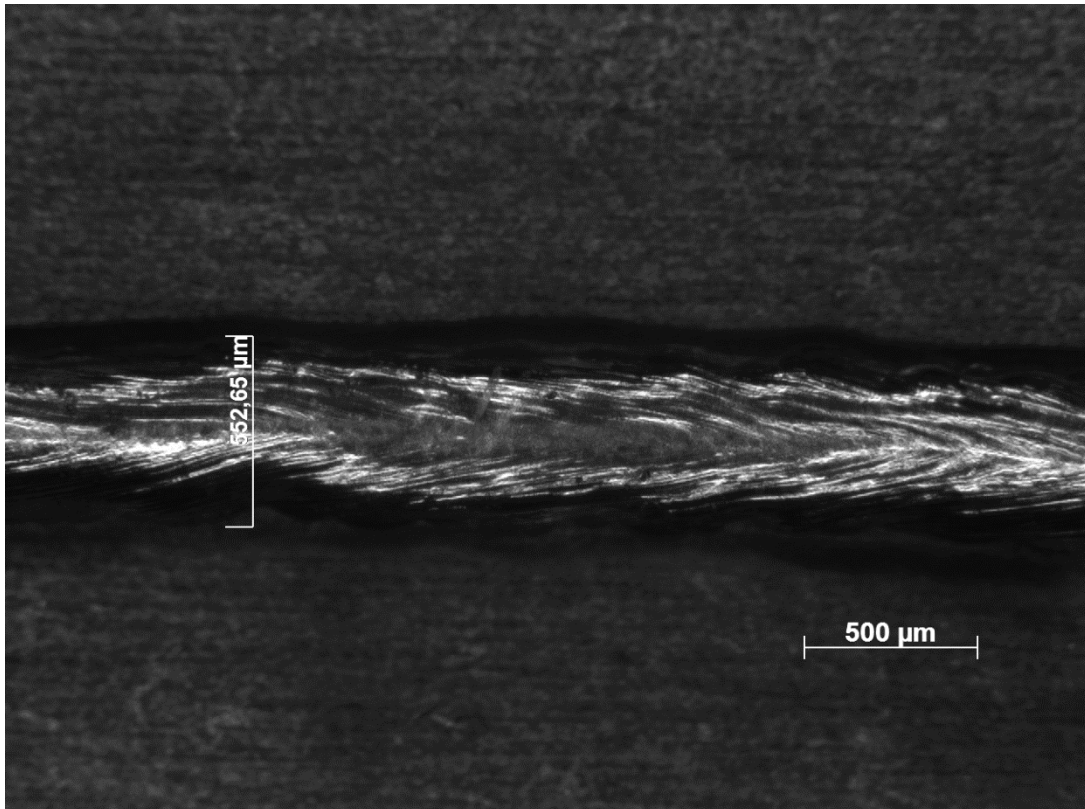
Specimen 12

Specimen 12 (Weld Face)
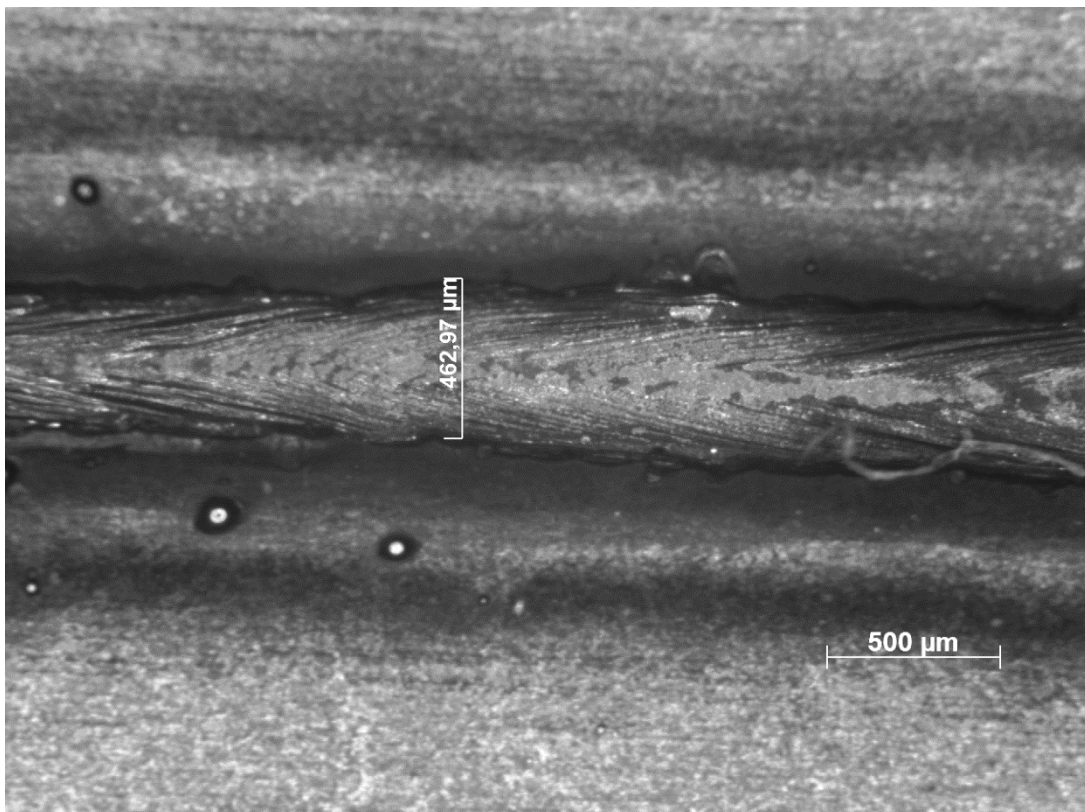
Specimen 12 (Weld Root)

Specimen 13
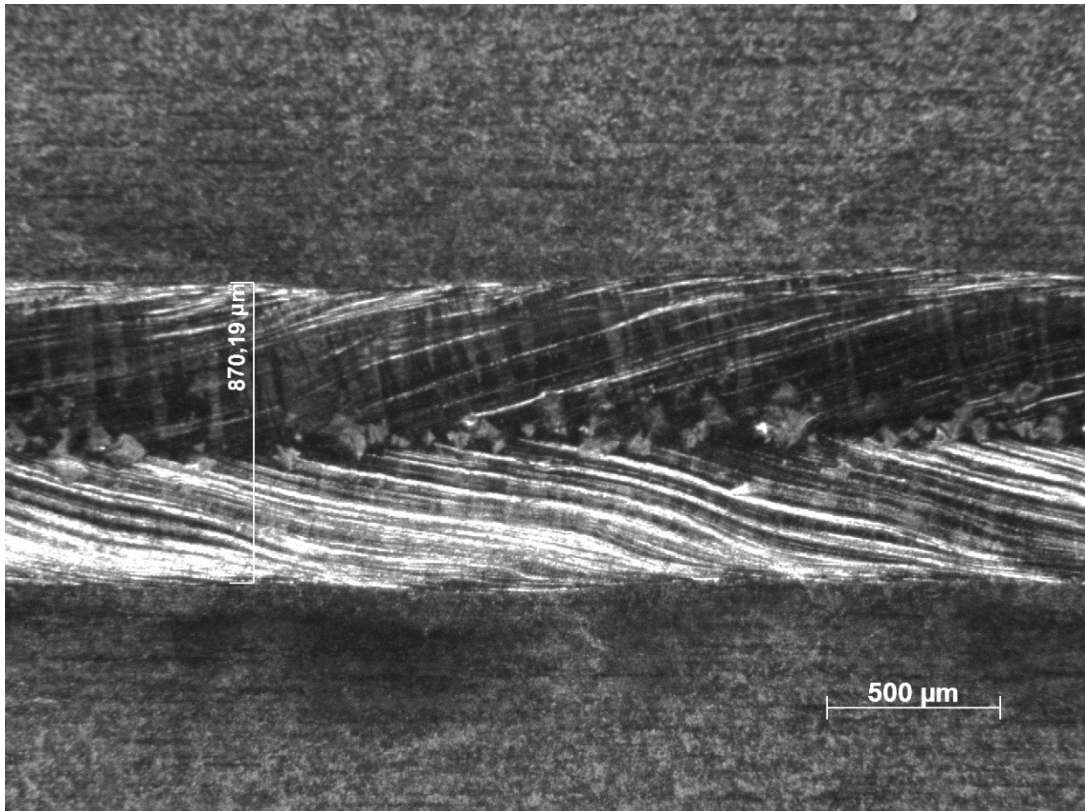
Specimen 13 (Weld Face)
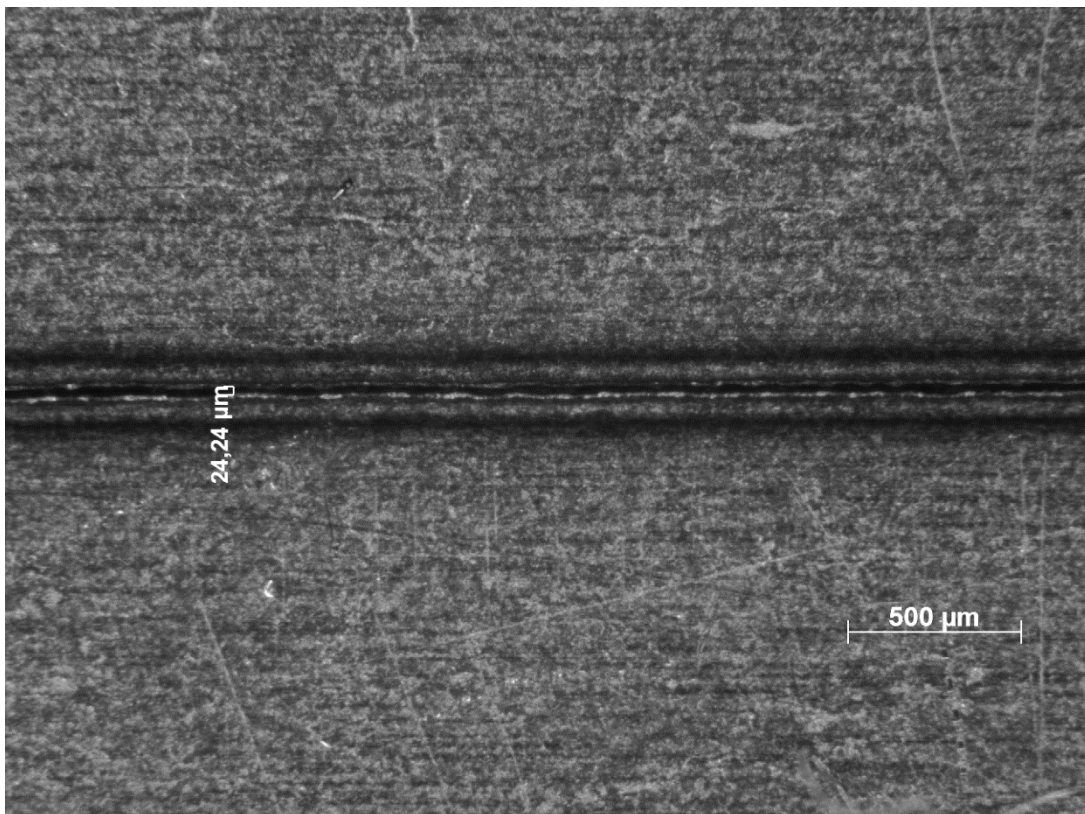
Specimen 13 (Weld Root)

13

Appendix II: Tensile Test Results

$R_{p0.2}$	-	0.2% offset yield strength
R_m	-	Maximum Tensile Strength
A_t	-	Elongation at Break

Tensile Test – Reference Test
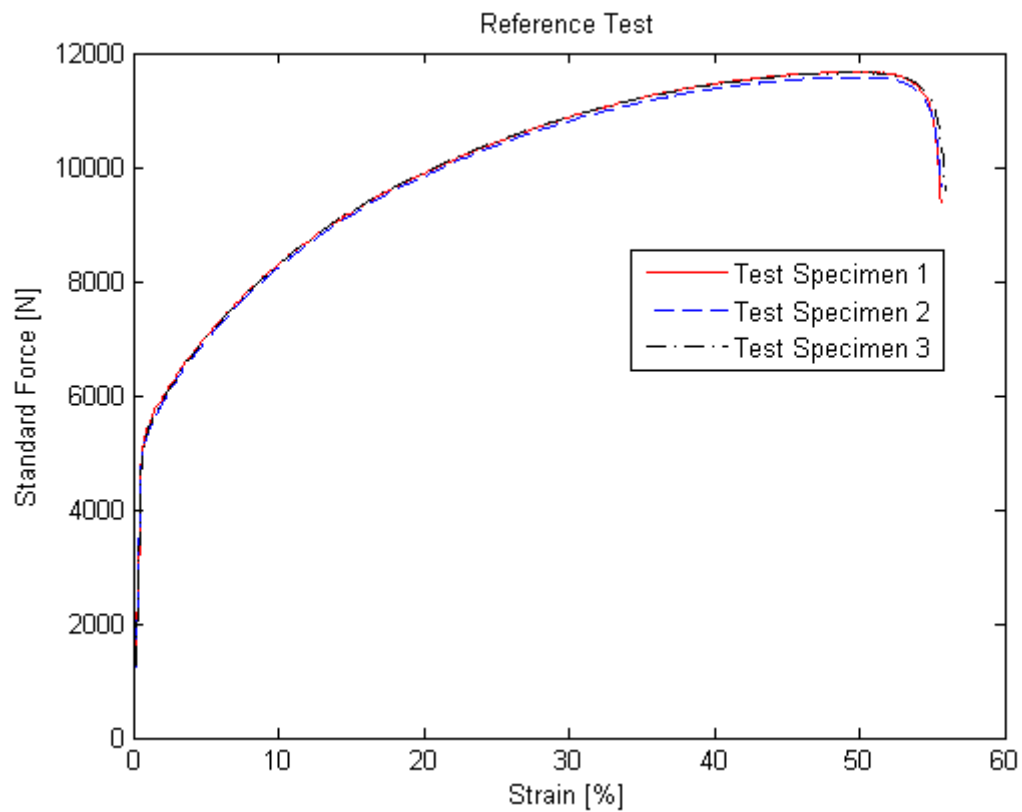
	$R_{p0.2}$	R_m	A_t
	MPa	MPa	%
1.	280,8977	622,3193	55,59645
3	279,8352	621,8579	55,92378
2	277,0134	617,5239	55,62672

Tensile Test – Bead on Plate
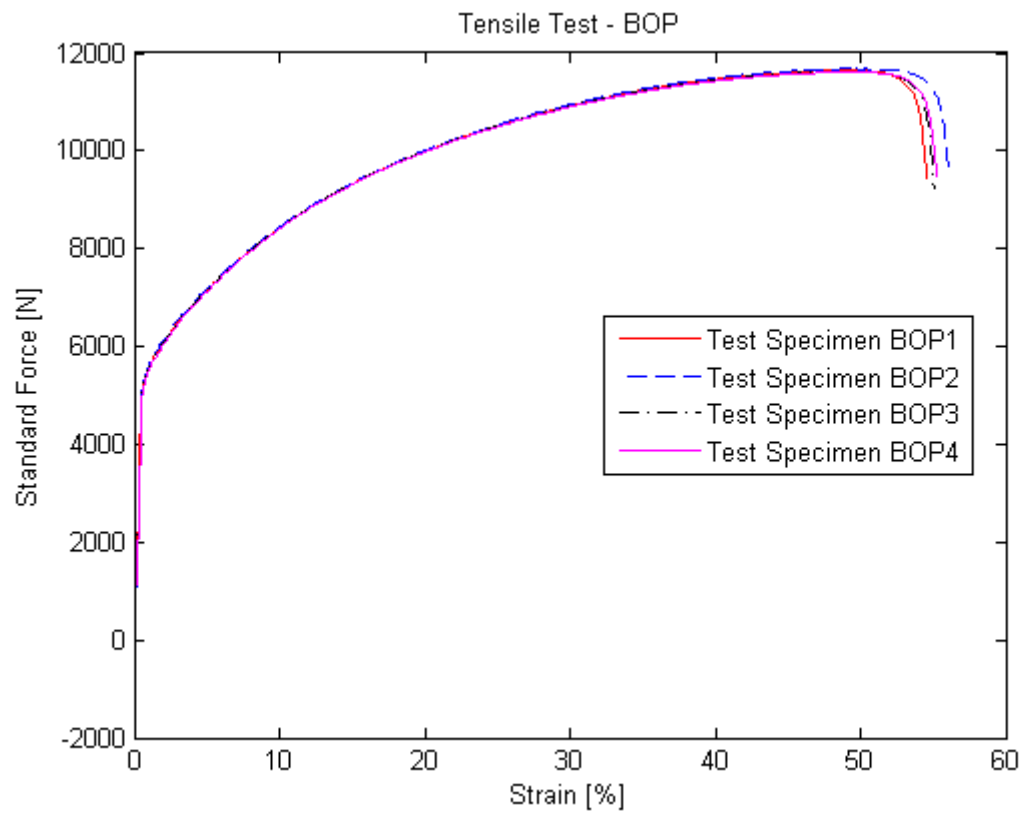
	$R_{p0.2}$	R_m	A_t
	MPa	MPa	%
BOP 1	290,8884	621,3804	54,55167
BOP 2	294,5759	622,798	56,05051
BOP 3	289,3435	619,9295	55,04705
BOP 4	287,9956	619,116	55,22312

Tensile Test – Bead on Plate

15

Tensile Test – Sheet A
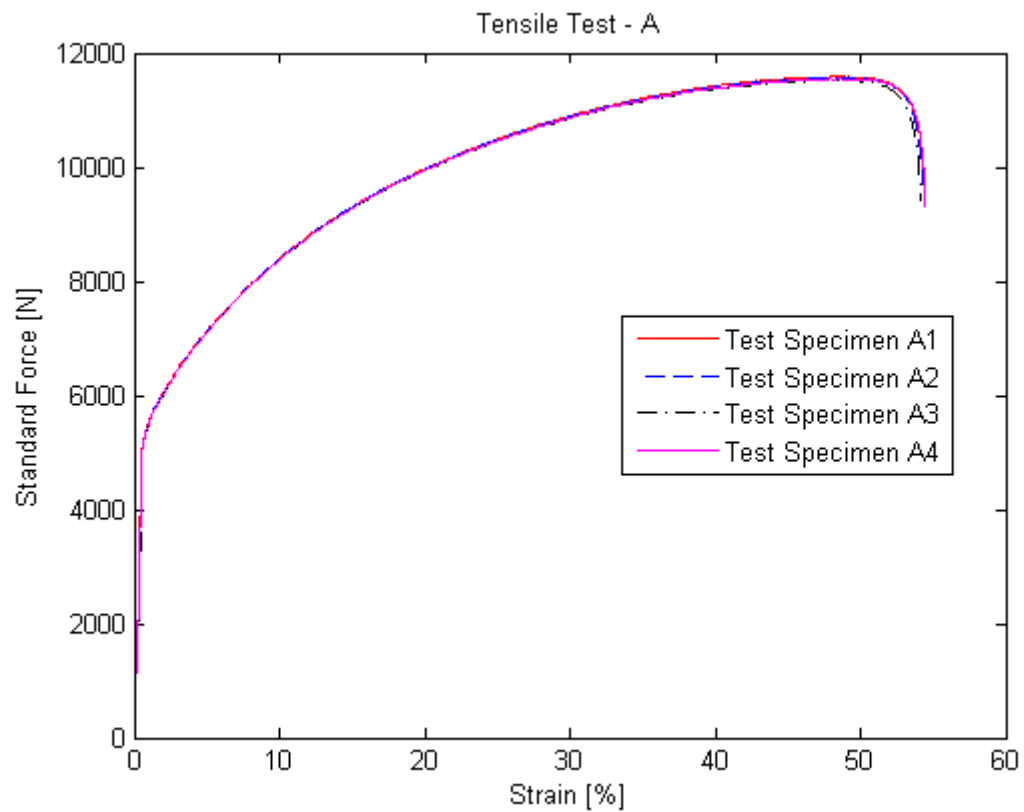
Tensile Test - A

	$R_{p0.2}$	R_m	A_t
	MPa	MPa	%
A1	290,4677	617,9949	54,426
A2	289,8387	616,9627	54,28474
A3	288,1106	614,508	54,19393
A4	289,3316	615,8447	54,44618

Tensile Test – Sheet B
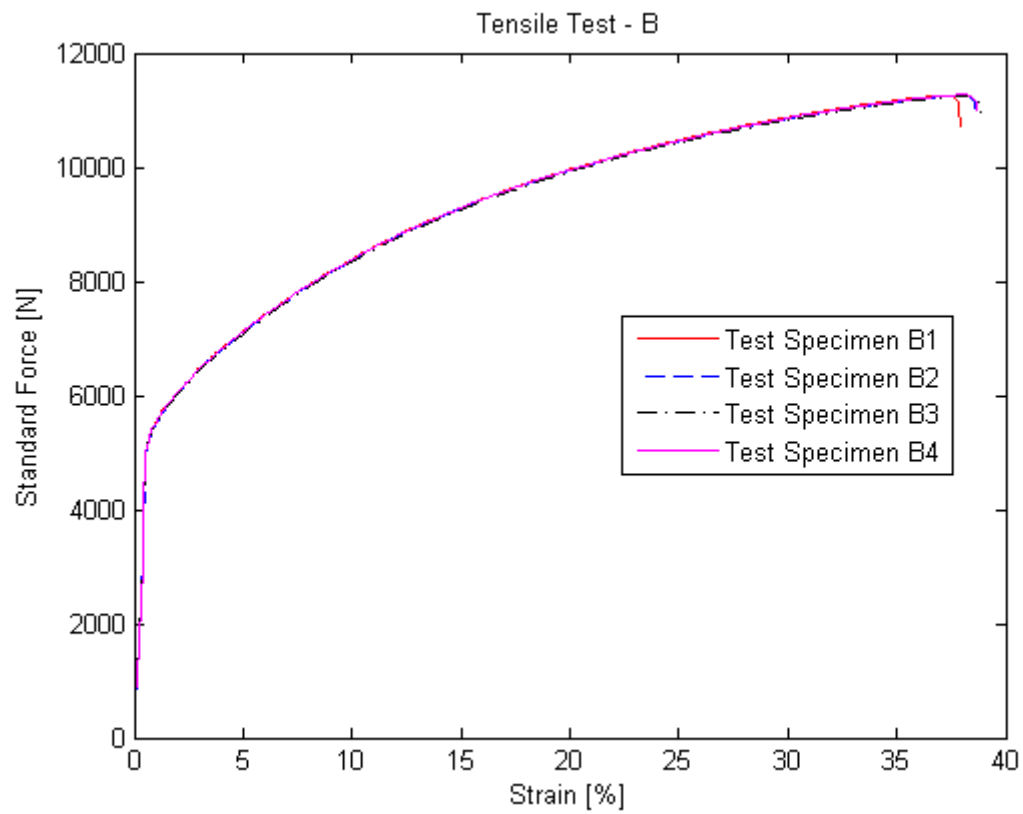
	$R_{p0.2}$	R_m	A_t
	MPa	MPa	%
B1	292,3111	600,2291	37,89841
B2	290,4693	600,3956	38,59463
B3	290,6618	600,0103	38,86707
B4	290,2431	601,2567	38,69553

Tensile Test – Sheet B

Tensile Test – Sheet C
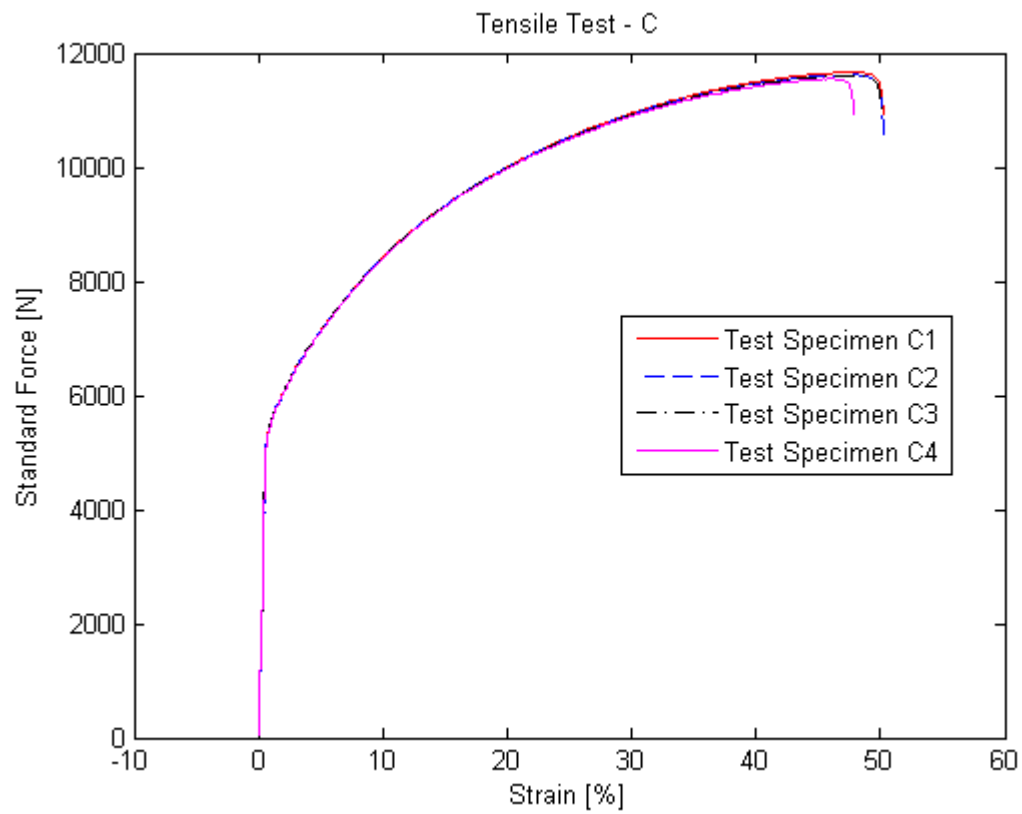
Tensile Test - C

	$R_{p0.2}$	R_m	A_t
	MPa	MPa	%
C1	289,1424	621,9467	50,22345
C2	290,1421	619,7727	50,25879
C3	289,5595	619,1353	50,07717
C4	286,4691	615,891	47,85735

Tensile Test – Sheet D
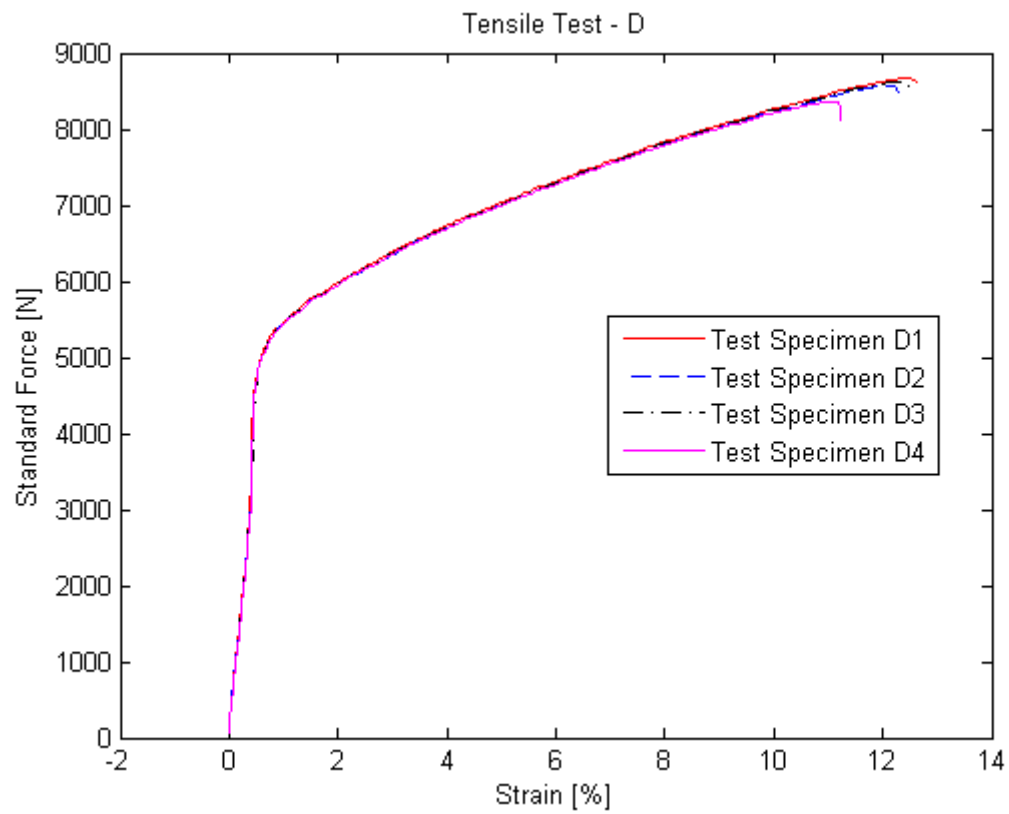
	$R_{p0.2}$	R_m	A_t
	MPa	MPa	%
D1	285,9009	462,386	12,60254
D2	283,536	457,3195	12,27841
D3	285,6119	460,0264	12,50163
D4	287,8779	446,1113	11,23028

Tensile Test – Sheet E
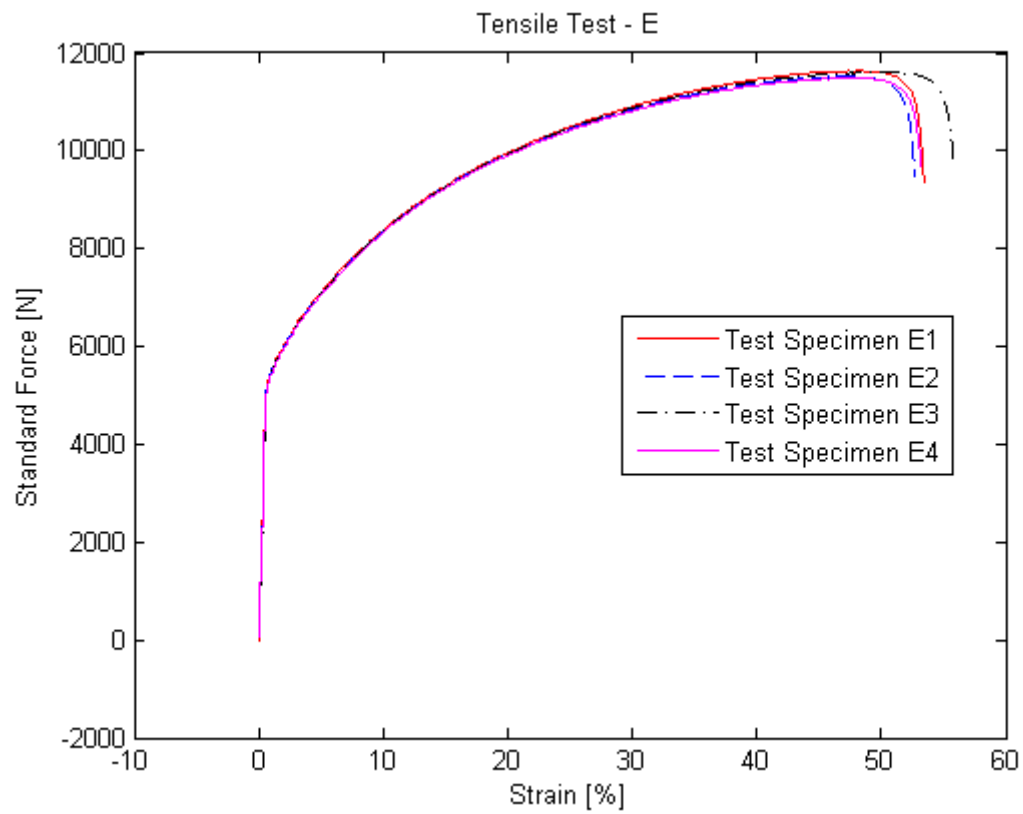
	$R_{p0.2}$	R_m	A_t
	MPa	MPa	%
E1	286,005	620,5042	53,4116
E2	286,8299	614,4432	52,71068
E3	287,6686	618,8676	55,77807
E4	283,5298	612,8351	53,21519

Tensile Test – Sheet F
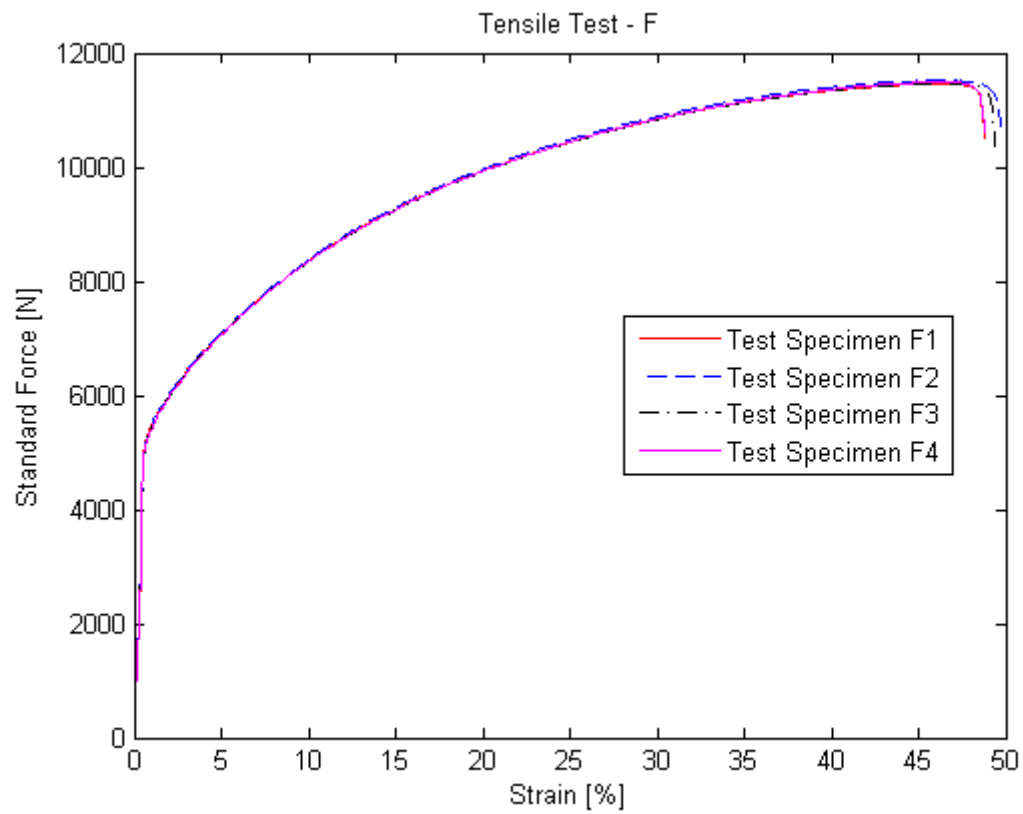
	$R_{p0.2}$	R_m	A_t
	MPa	MPa	%
F1	285,8911	611,4556	48,79572
F2	284,9534	614,4762	49,70383
F3	284,5091	611,9693	49,38095
F4	282,0895	613,1776	48,79572

Tensile Test – Sheet F

Tensile Test – Sheet G
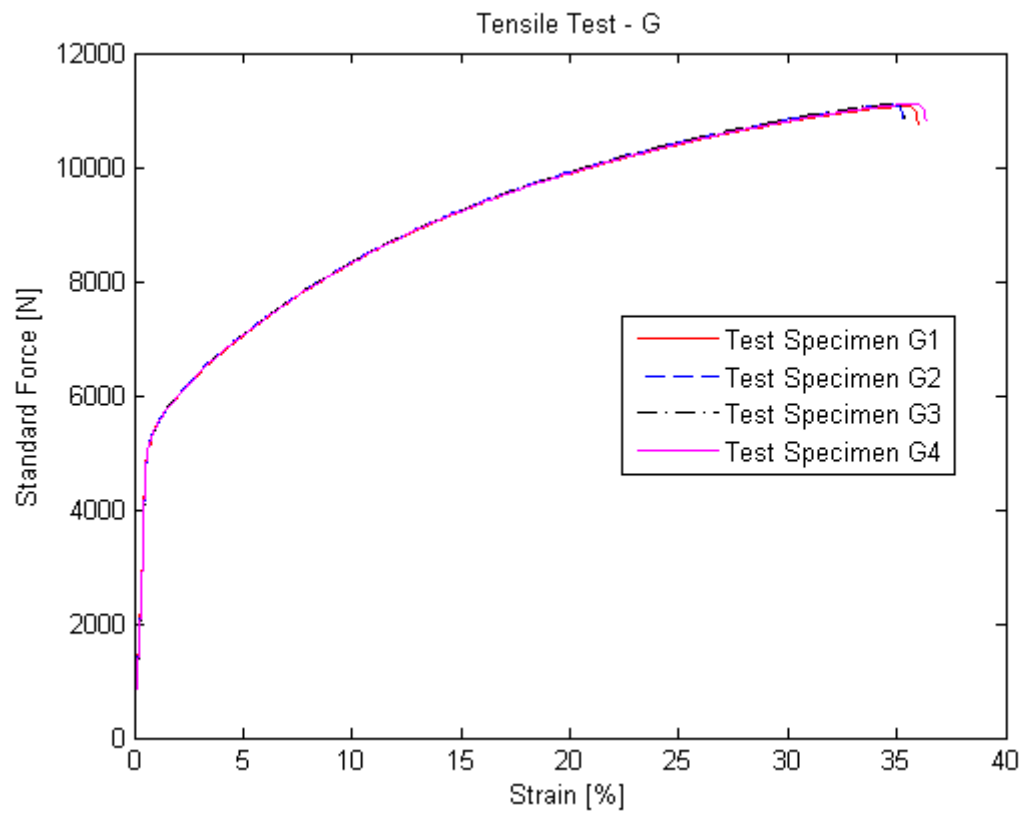
	$R_{p0.2}$	R_m	A_t
	MPa	MPa	%
G1	284,3204	590,5126	35,97121
G2	283,1163	591,7781	35,31535
G3	284,647	592,2491	35,39607
G4	286,8801	592,8533	36,33445

Tensile Test – Sheet H
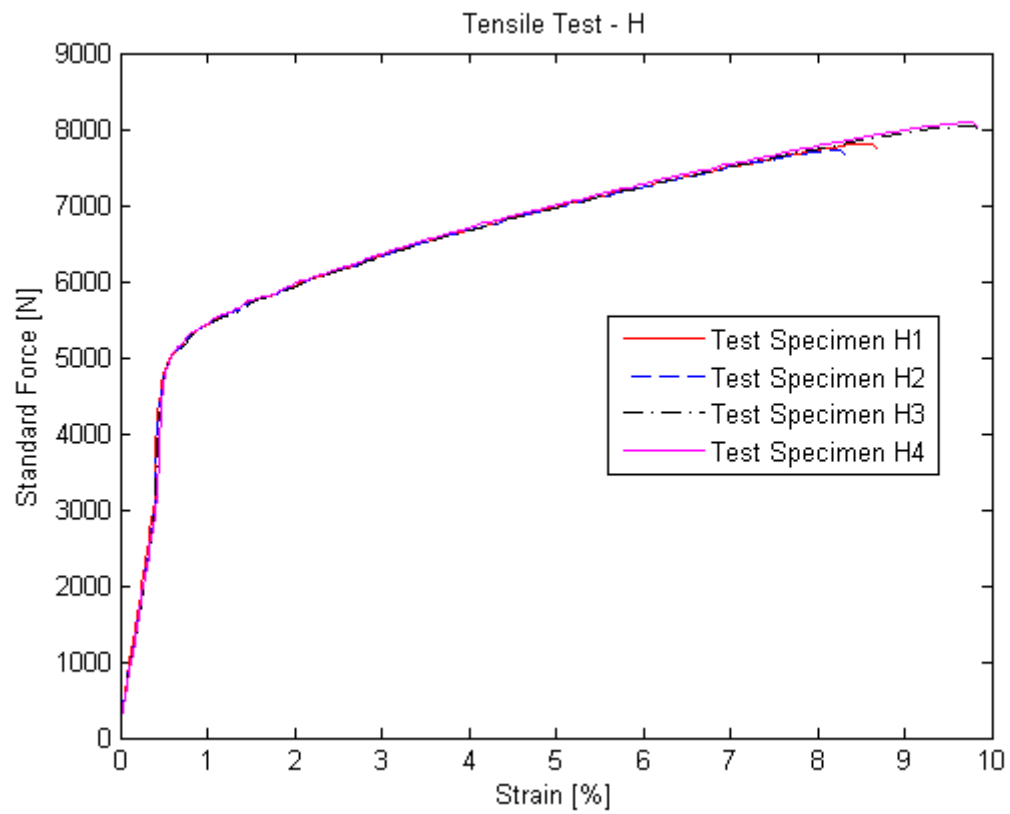
	$R_{p0.2}$	R_m	A_t
	MPa	MPa	%
H1	283,9409	416,4013	8,677486
H2	283,4333	412,0817	8,314242
H3	283,9558	429,1794	9,868118
H4	286,8173	431,3773	9,837848

Tensile Test – Sheet I
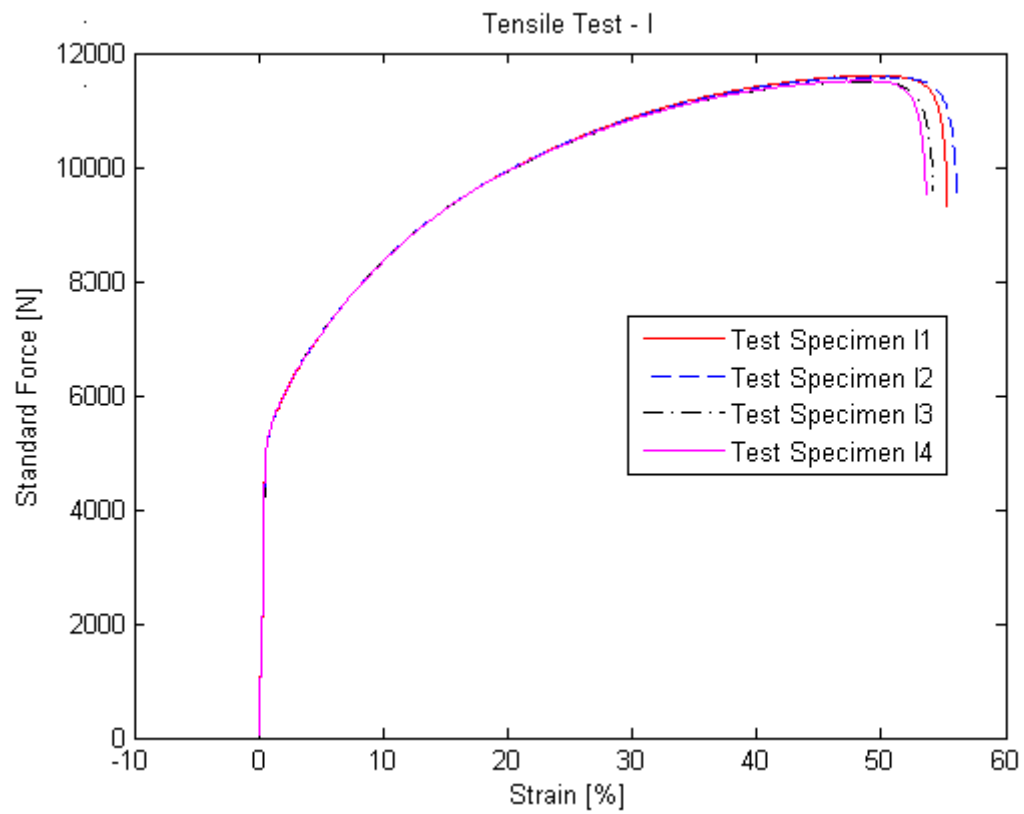
	$R_{p0.2}$	R_m	A_t
	MPa	MPa	%
I1	285,7238	618,8763	55,30384
I2	285,6429	617,6538	56,0606
I3	287,6289	613,8338	54,20402
I4	288,7119	614,2382	53,63897

Tensile Test – Sheet J
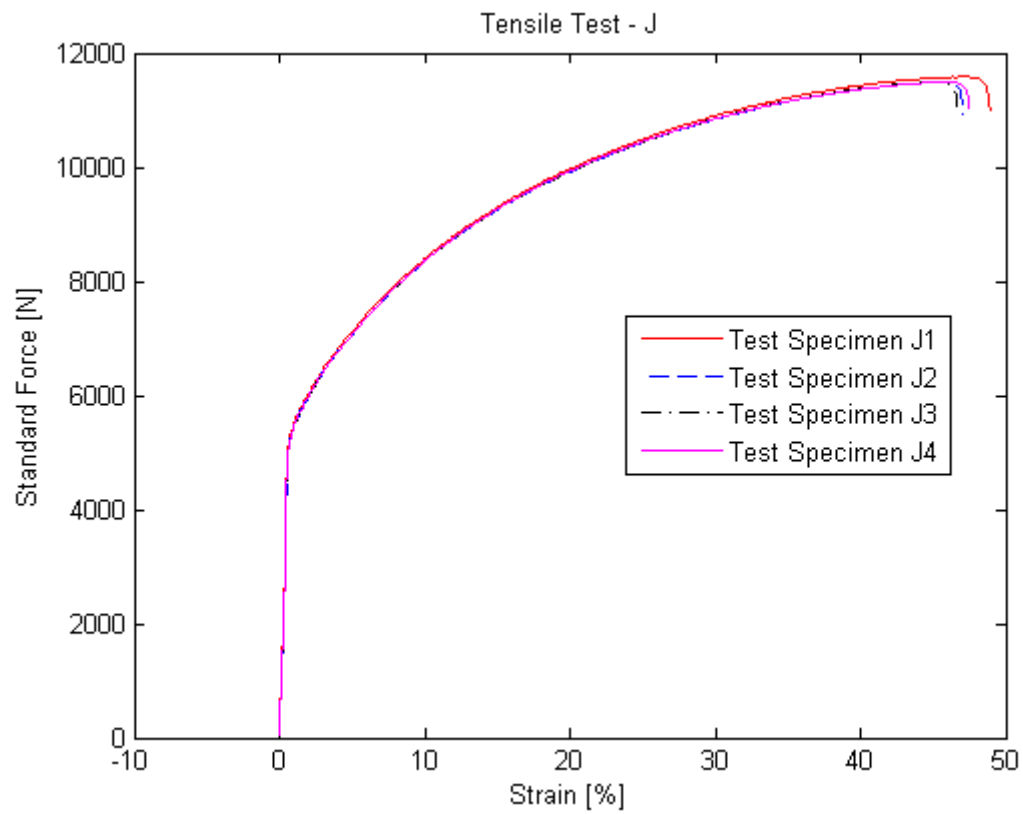
	$R_{p0.2}$	R_m	A_t
	MPa	MPa	%
J1	286,1729	617,784	48,89663
J2	287,2156	612,6649	47,06023
J3	287,7331	613,4167	46,60617
J4	287,0195	612,9932	47,48401

Tensile Test – Sheet J

Tensile Test – Sheet K
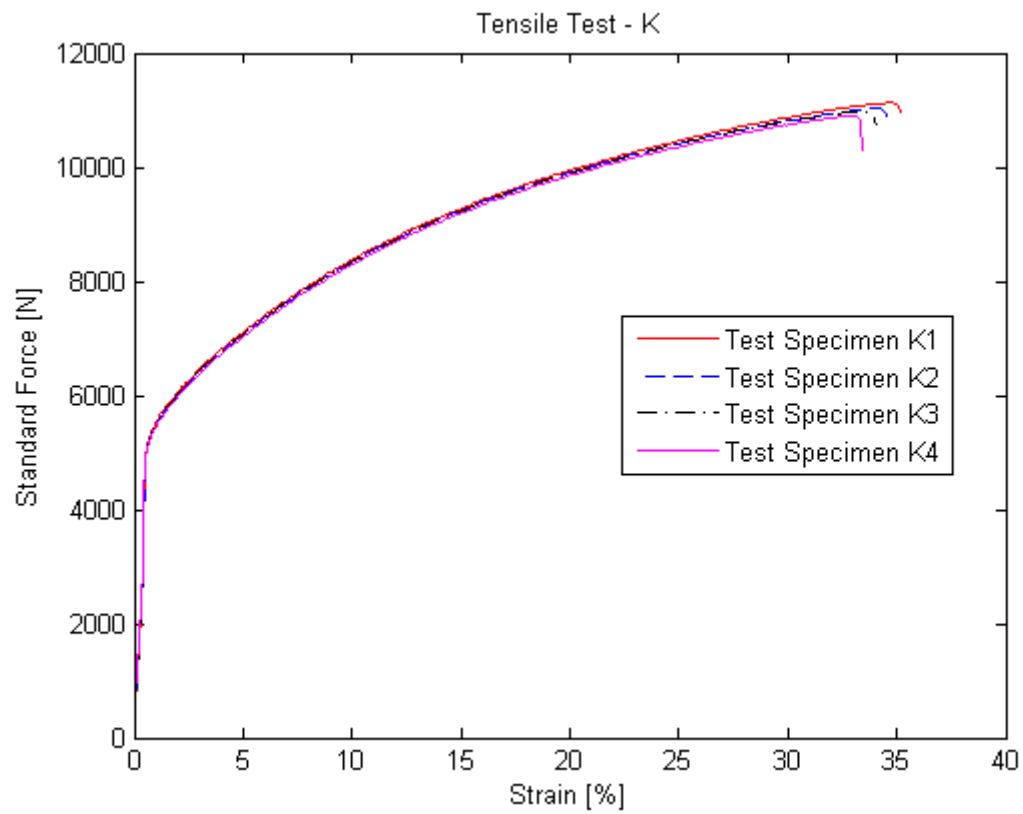
	$R_{p0.2}$	R_m	A_t
	MPa	MPa	%
J1	286,1729	617,784	48,89663
J2	287,2156	612,6649	47,06023
J3	287,7331	613,4167	46,60617
J4	287,0195	612,9932	47,48401

Tensile Test – Sheet L
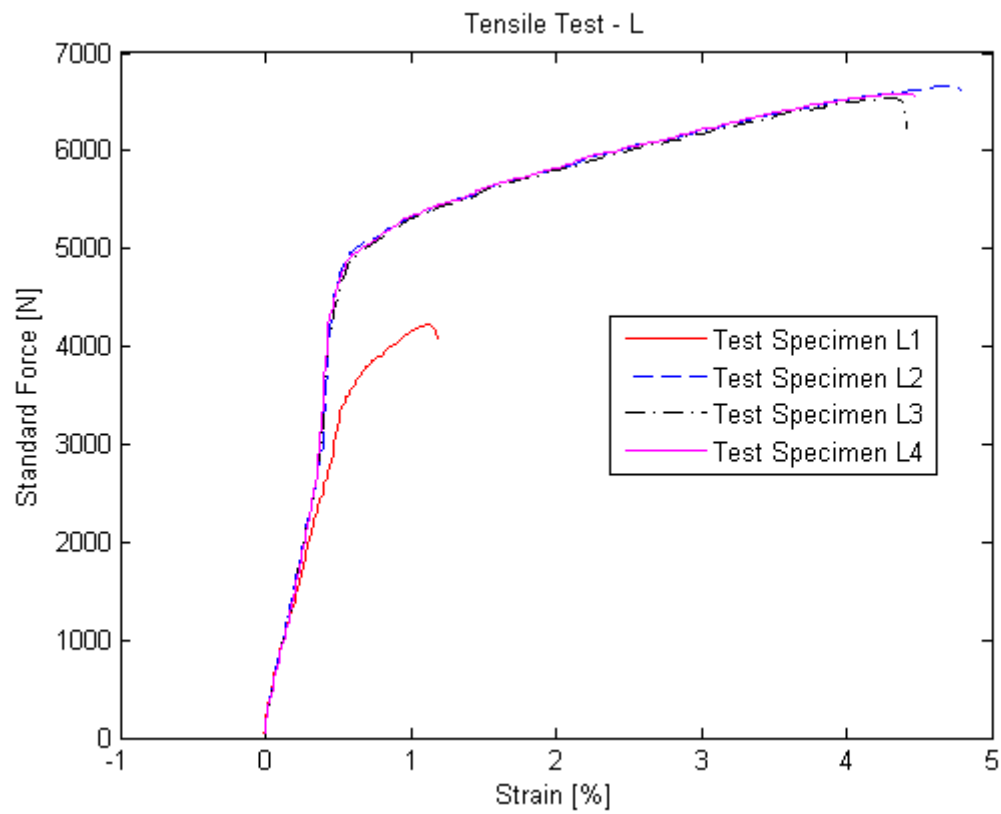
	$R_{p0.2}$	R_m	A_t
	MPa	MPa	%
L1	204,8478	224,8916	1,190632
L2	277,456	355,1372	4,782707
L3	277,7172	348,3054	4,409374
L4	281,1993	351,3835	4,469914

Appendix III – Vickers Hardness Test

Vickers Hardness Test – Specimen 2
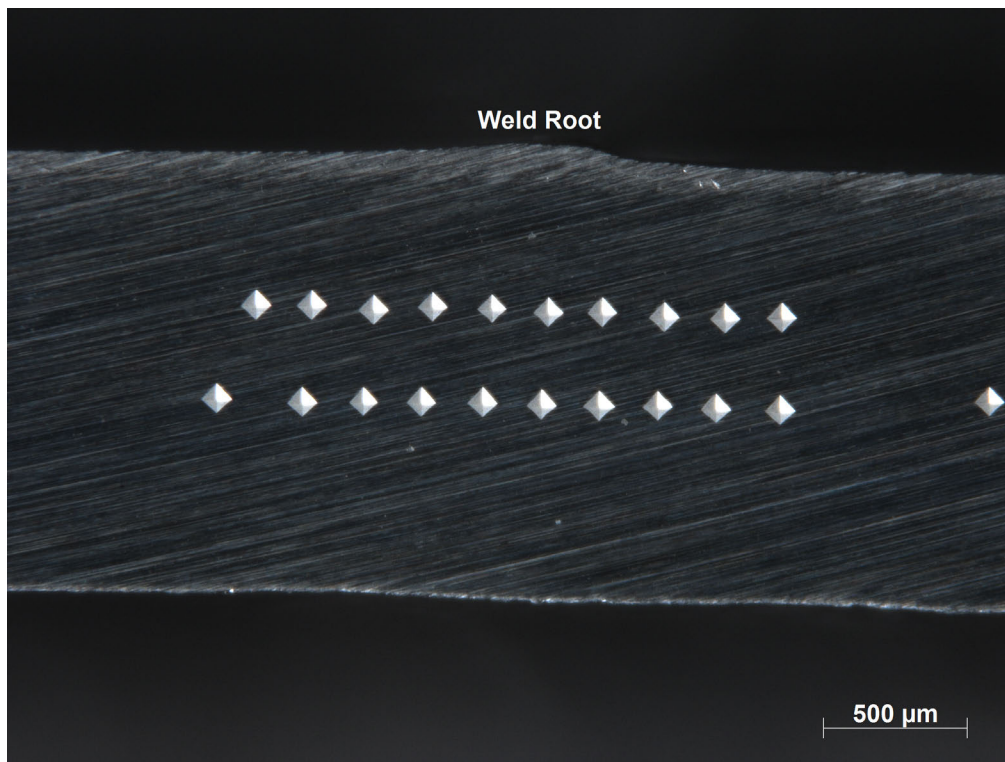
Vickers Indentation - Test specimen 1
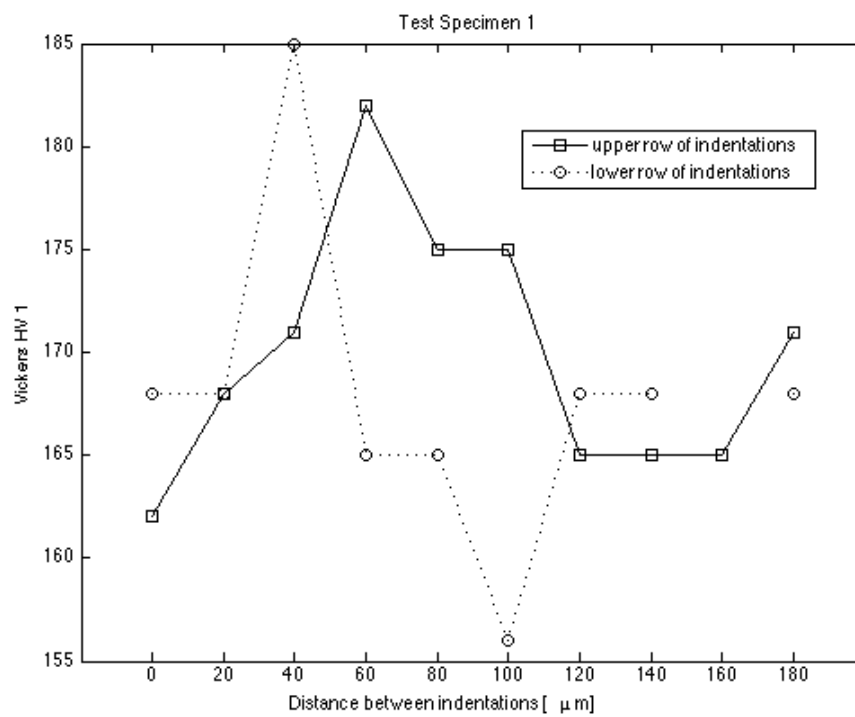
Vickers Hardness Measurements - Specimen 1

Vickers Hardness Test – Specimen 2
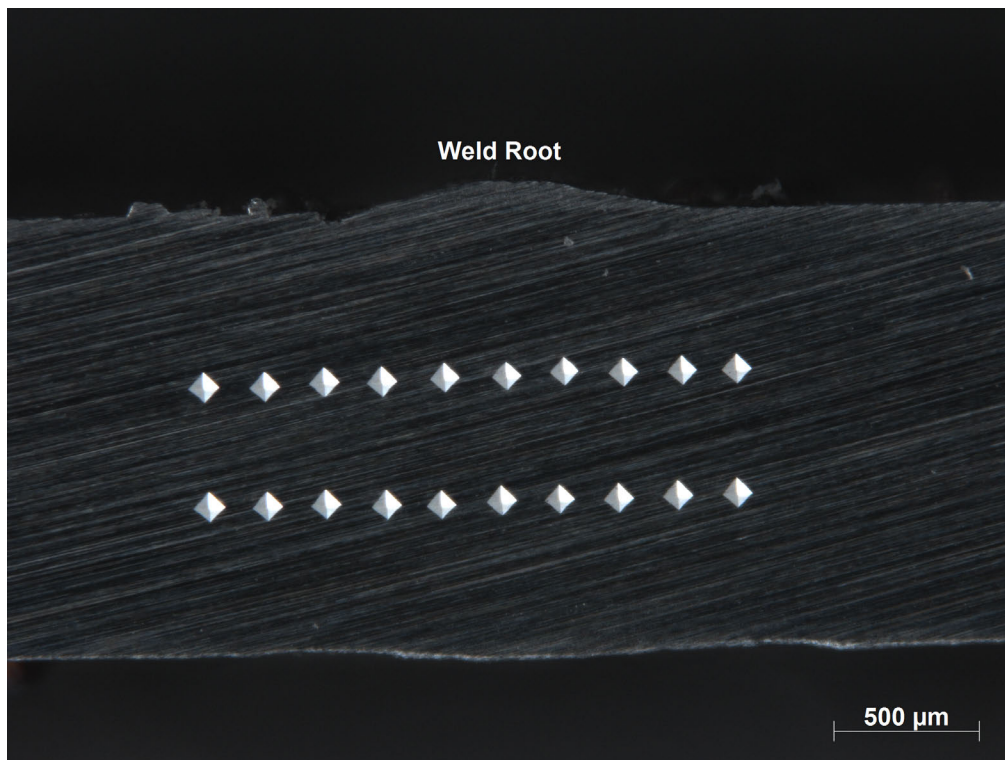
Vickers Indentation - Test specimen 2
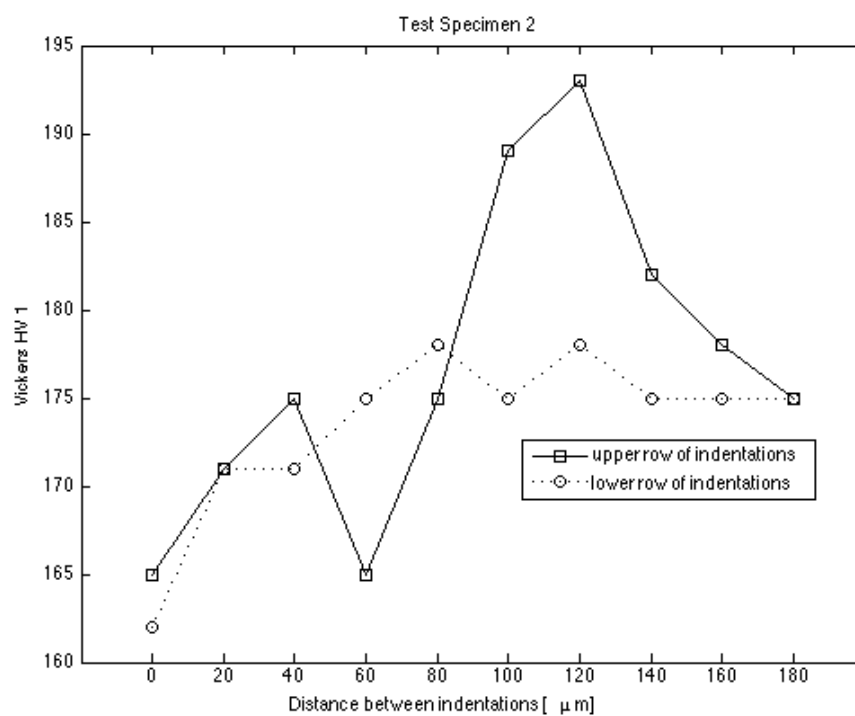
Vickers Hardness Measurements - Specimen 2

Vickers Hardness Test – Specimen 3
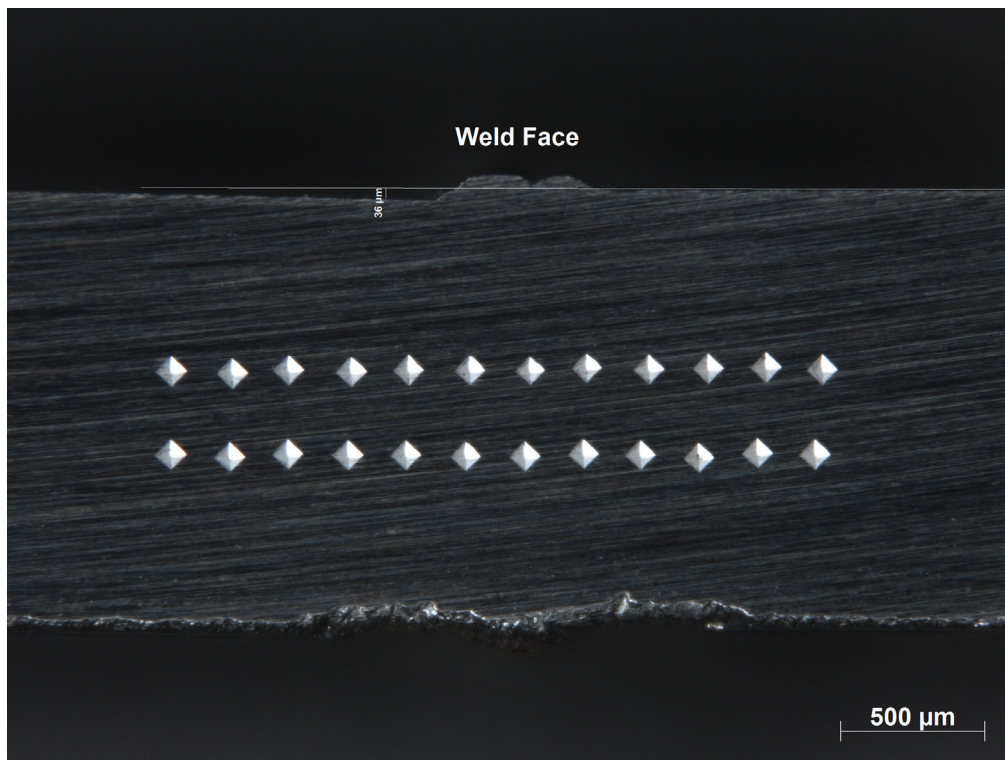
Vickers Indentation - Test specimen 3
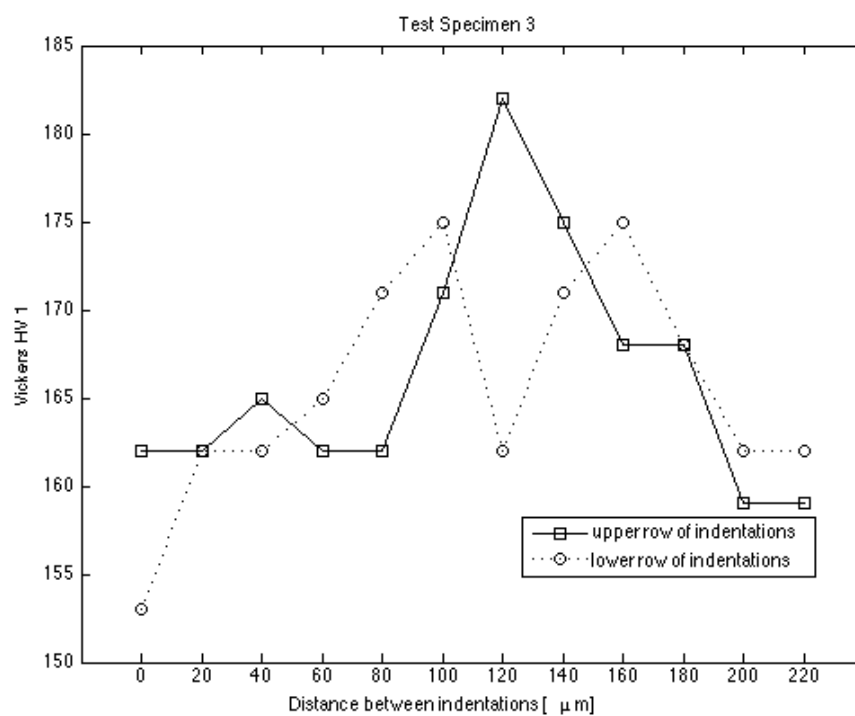
Vickers Hardness Measurements - Specimen 3

Vickers Hardness Test – Specimen 4
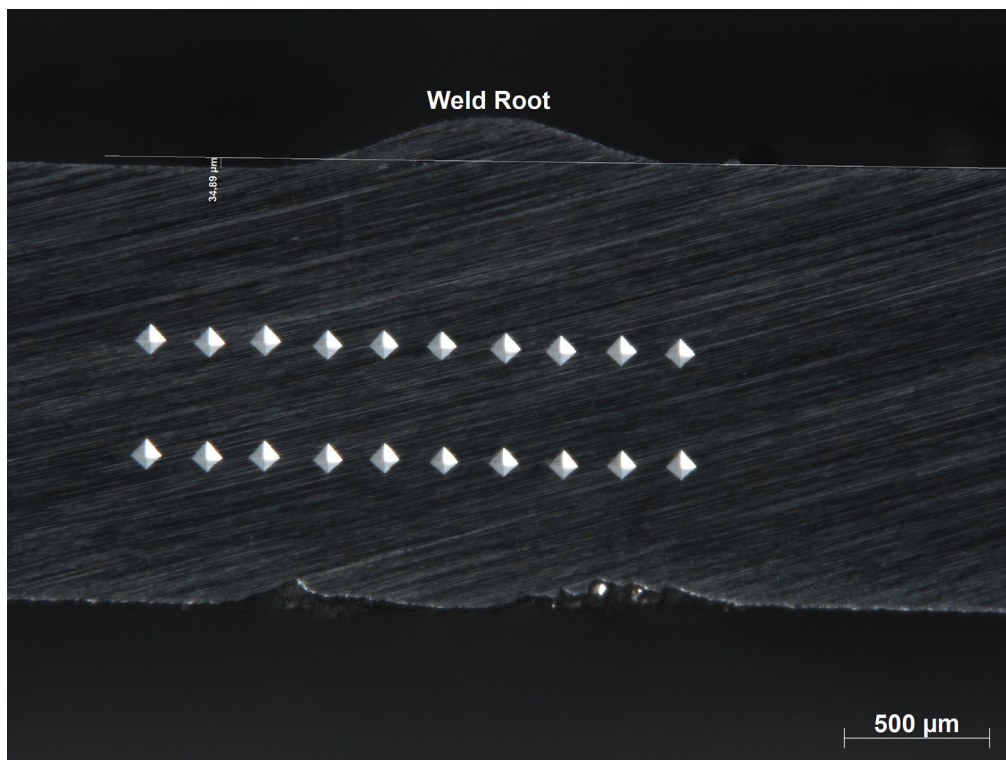
Vickers Indentation - Test specimen 4
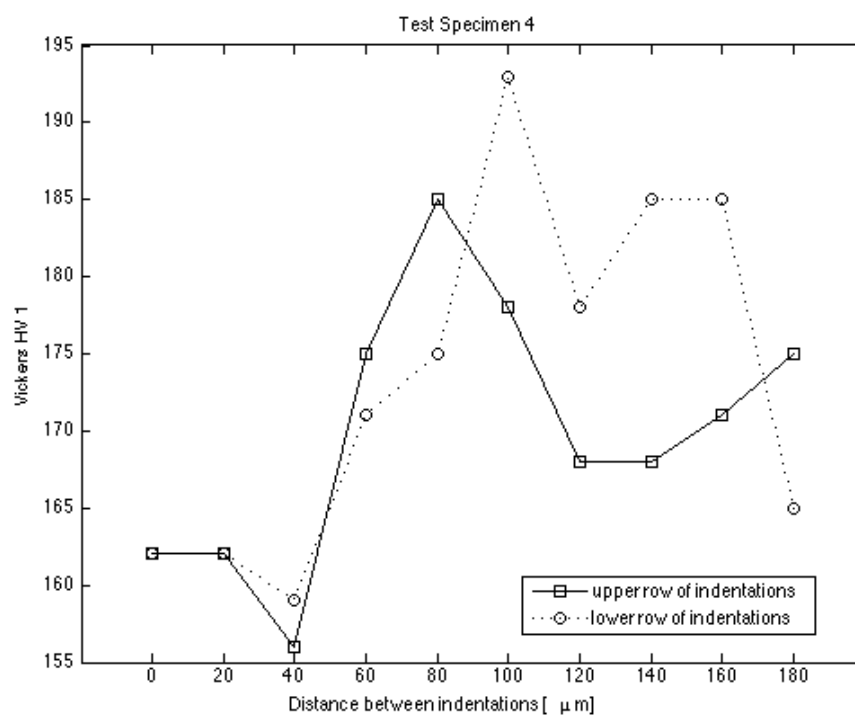
Vickers Hardness Measurements - Specimen 4

Vickers Hardness Test – Specimen 5
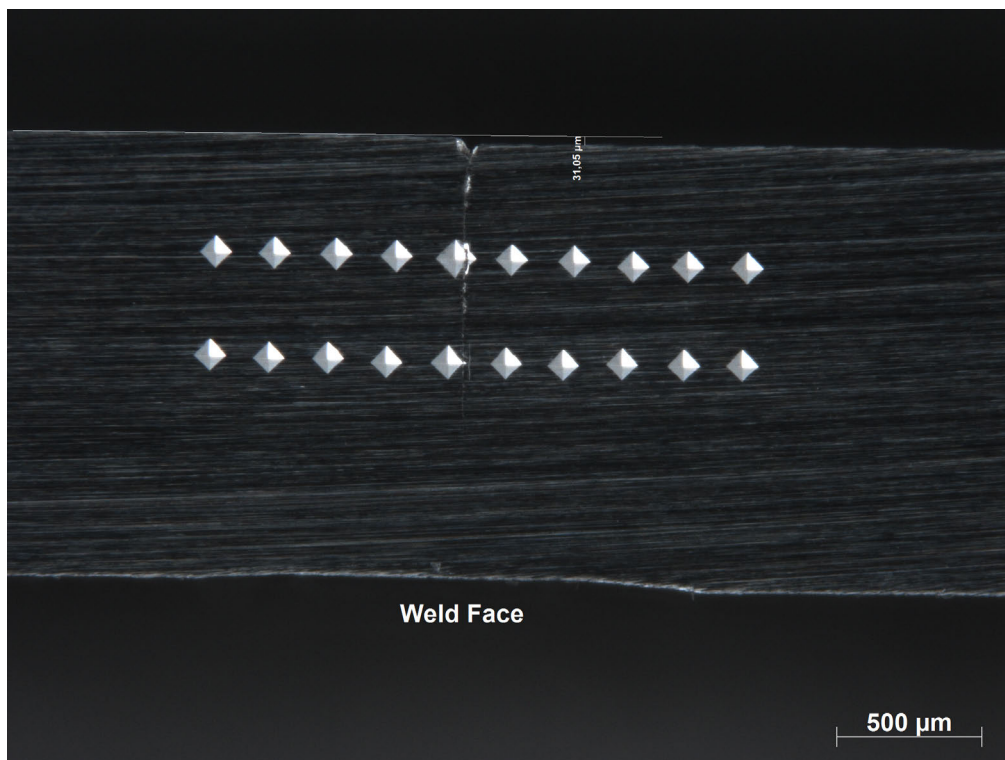
Vickers Indentation - Test specimen 5
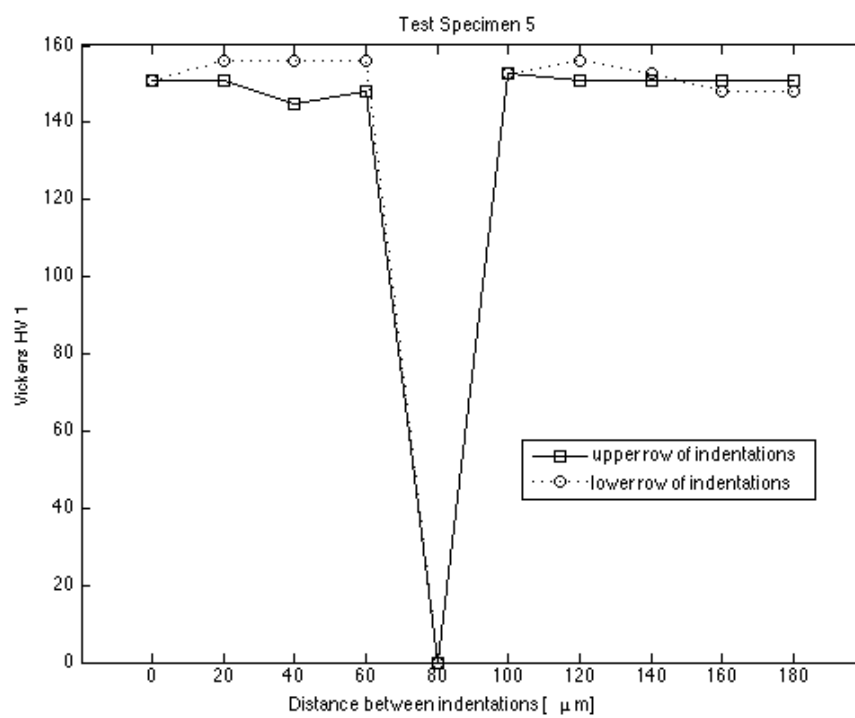
Vickers Hardness Measurements - Specimen 5

Vickers Hardness Test – Specimen 6
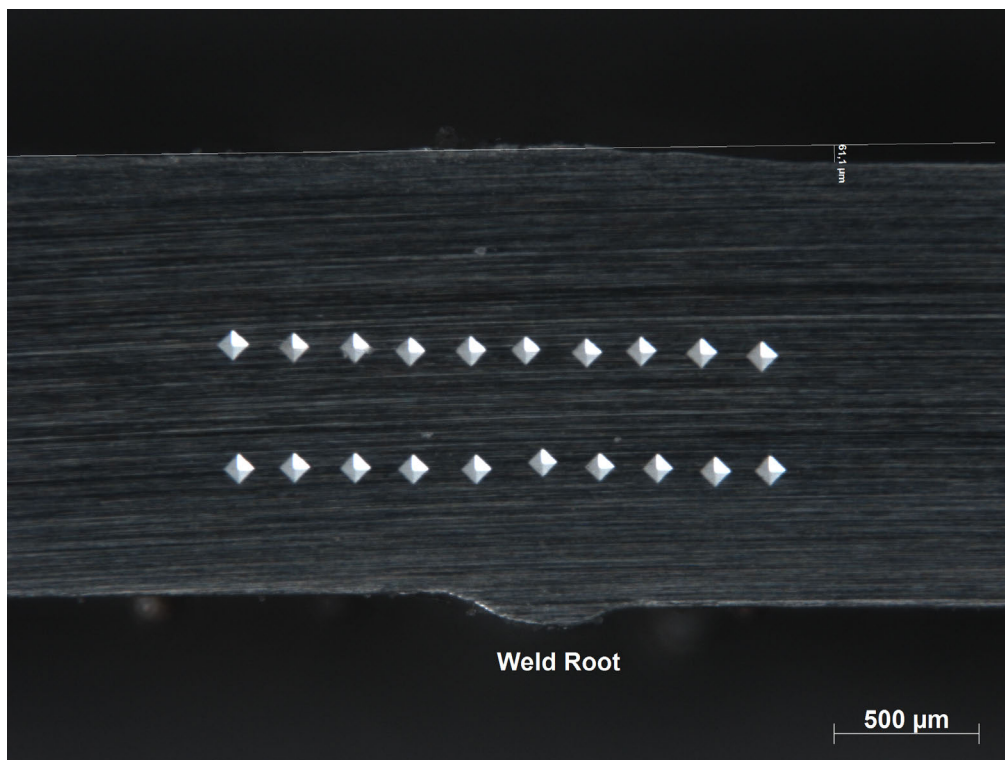
Vickers Indentation - Test specimen 6
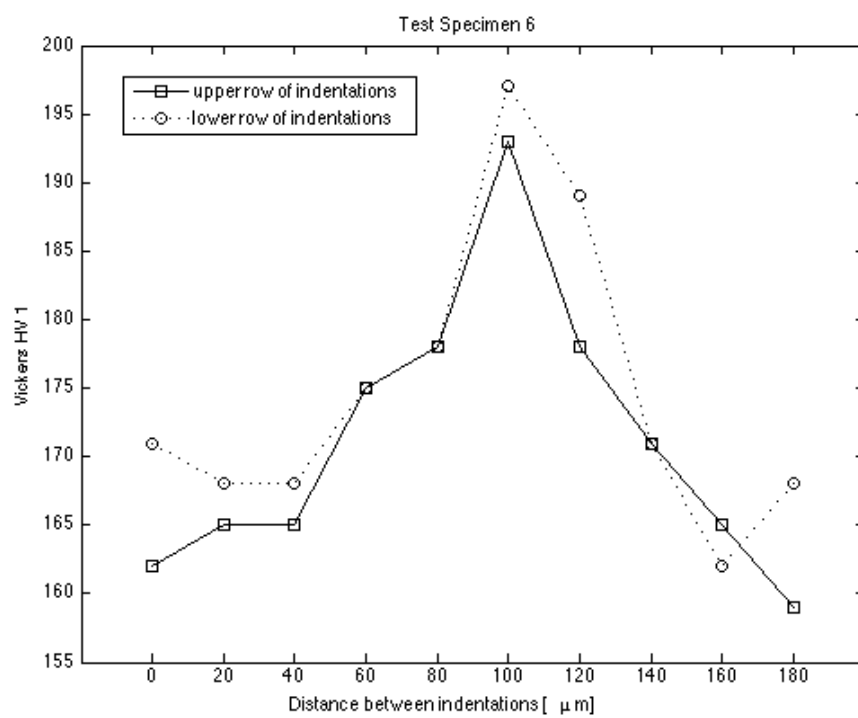
Vickers Hardness Measurements - Specimen 6

Vickers Hardness Test – Specimen 7
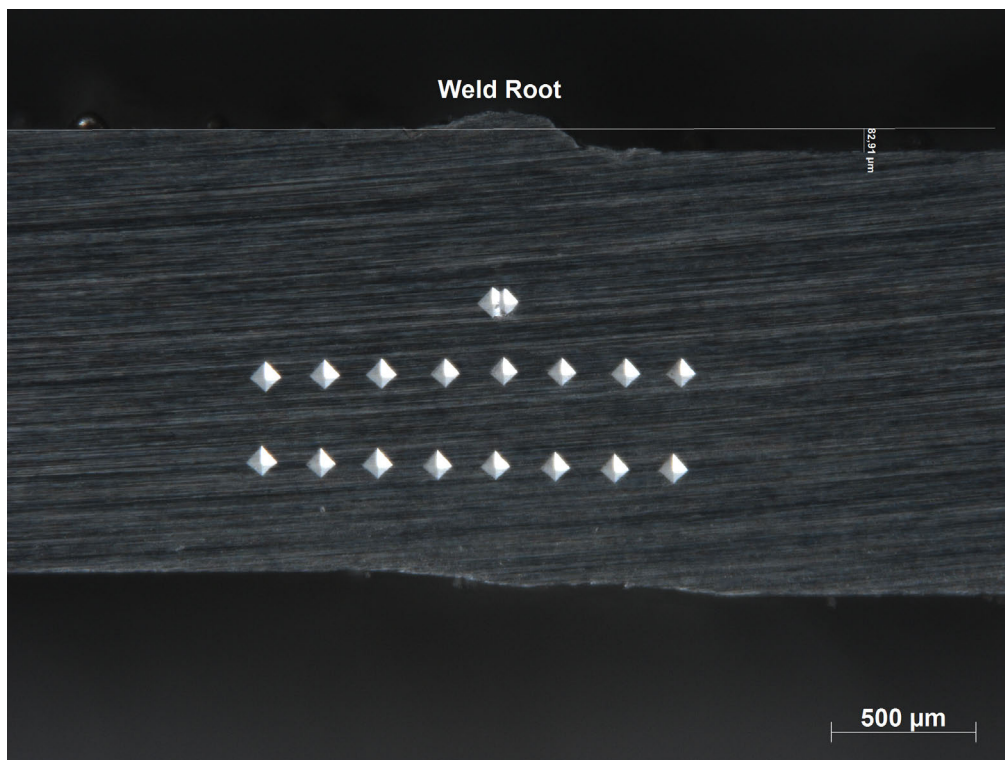
Vickers Indentation - Test specimen 7
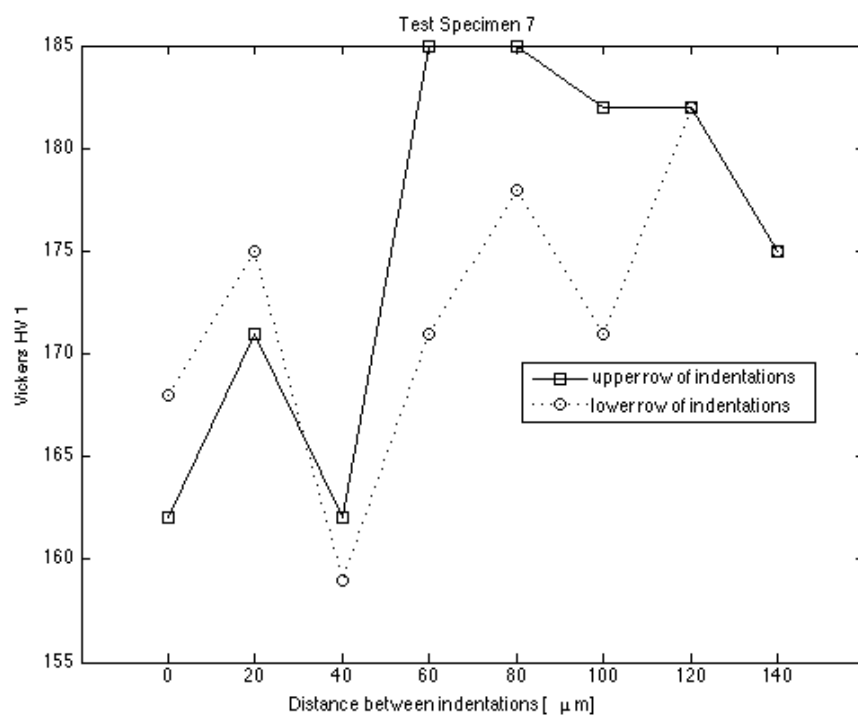
Vickers Hardness Measurements - Specimen 7

Vickers Hardness Test – Specimen 8

Vickers Indentation - Test specimen 8
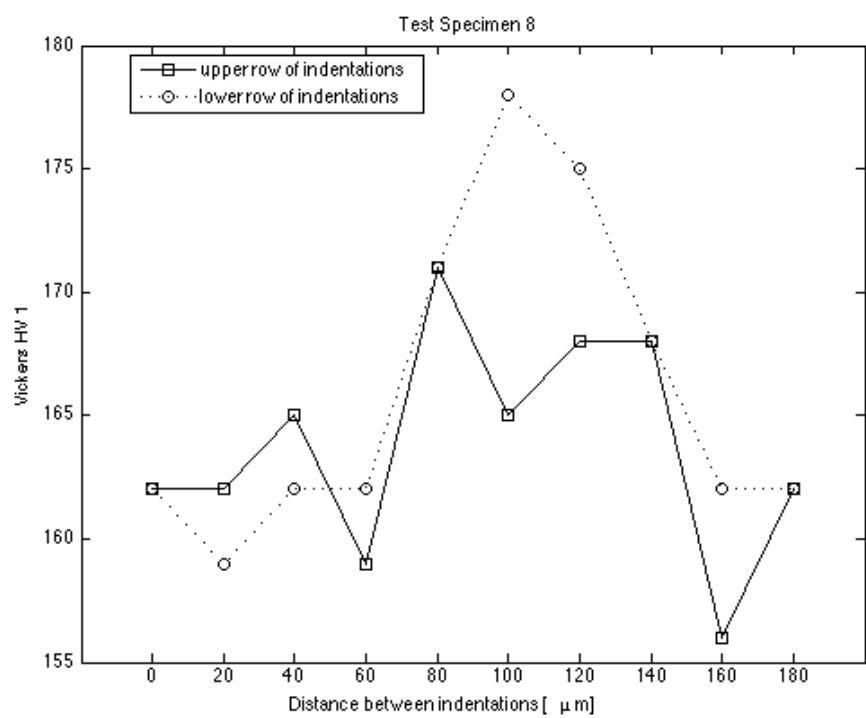
Vickers Hardness Measurements - Specimen 8

Vickers Hardness Test – Specimen 9
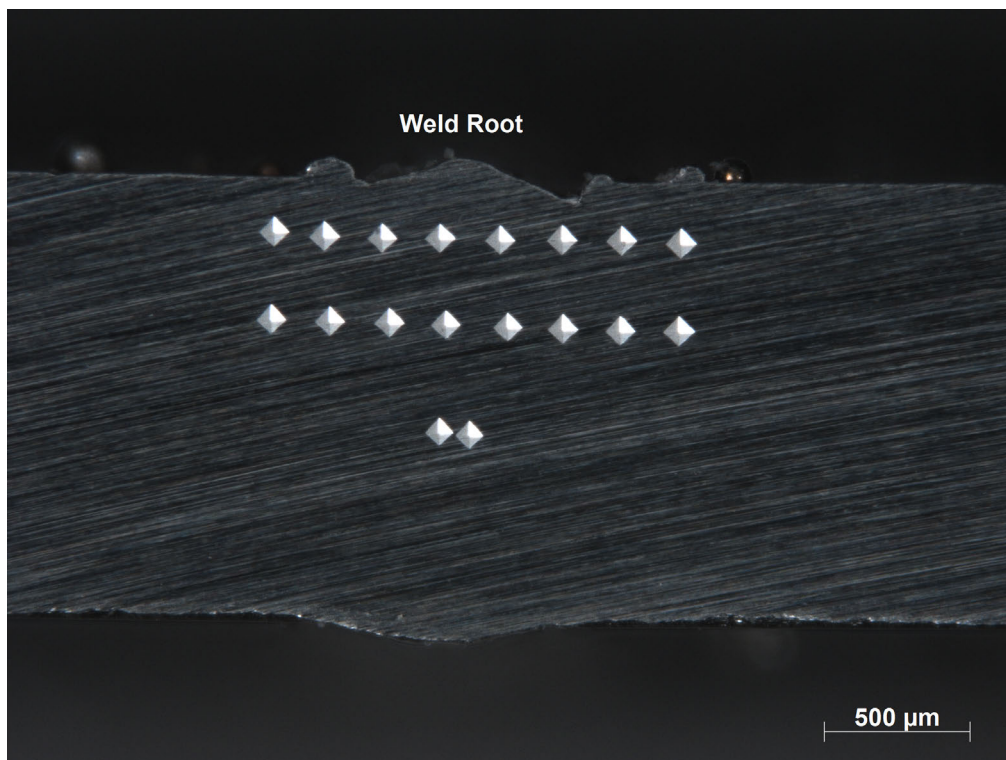
Vickers Indentation - Test specimen 9
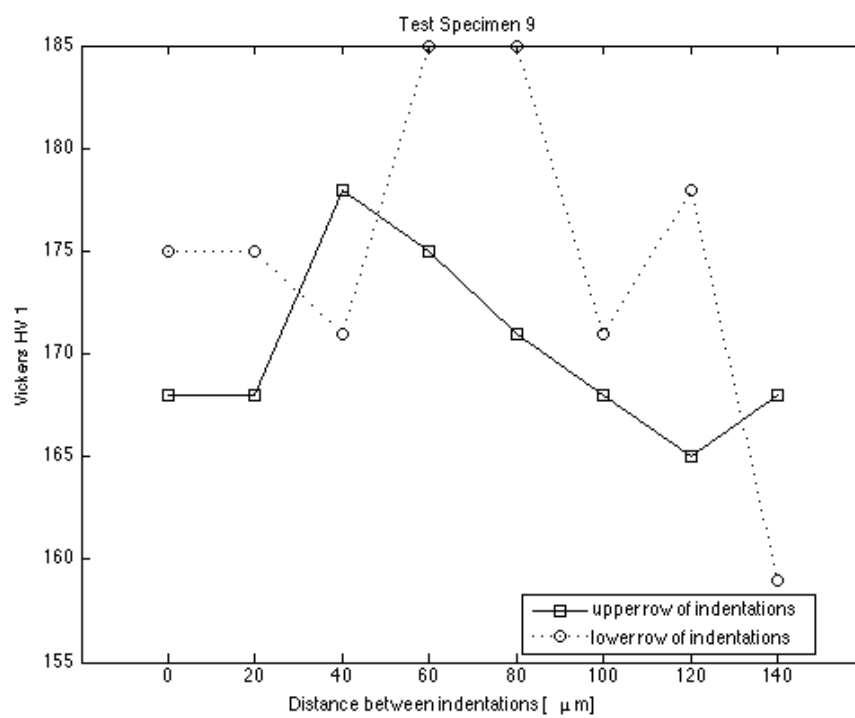
Vickers Hardness Measurements - Specimen 9

Vickers Hardness Test – Specimen 10

Vickers Indentation - Test specimen 10
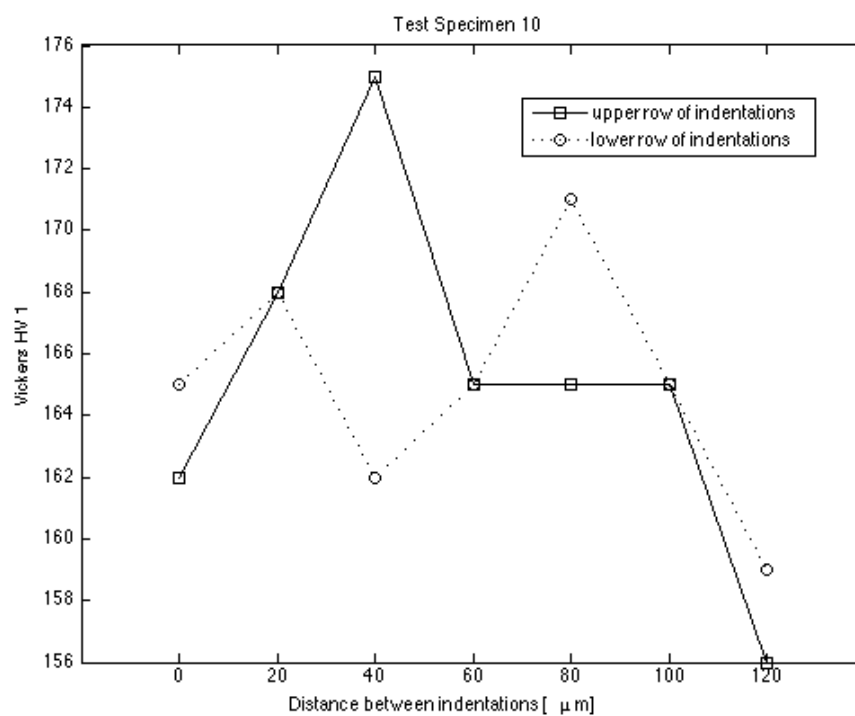
Vickers Hardness Measurements - Specimen 10

Vickers Hardness Test – Specimen 11

Vickers Indentation - Test specimen 11
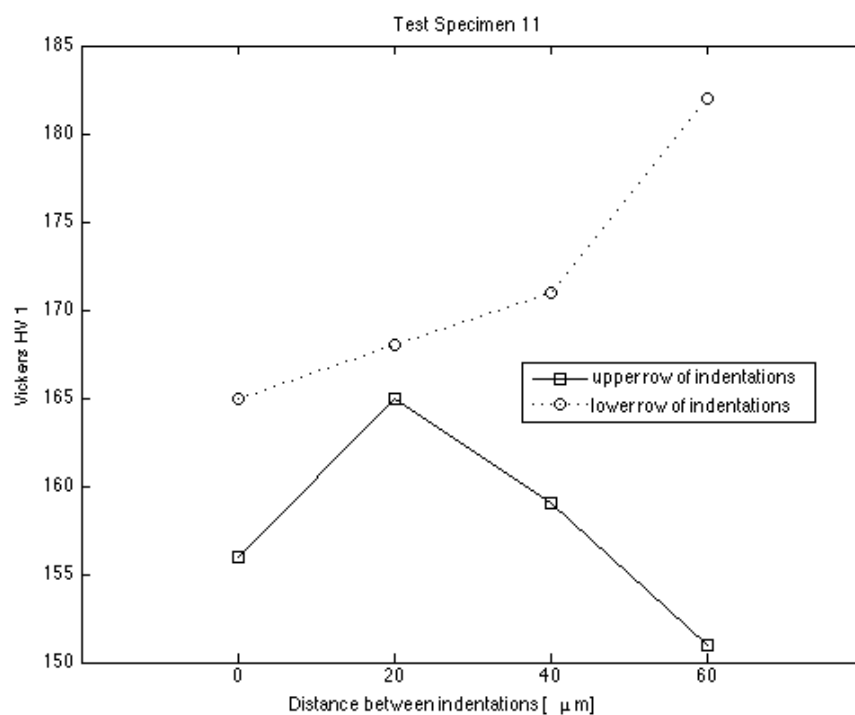
Vickers Hardness Measurements - Specimen 11

Vickers Hardness Test – Specimen 12

Weld Root

46,63 μm

514,18 μm

500 μm

Vickers Indentation - Test specimen 12

Test Specimen 12

upper row of indentations
····◇···· lower row of indentations

Vickers HV 1

Distance between indentations [μm]
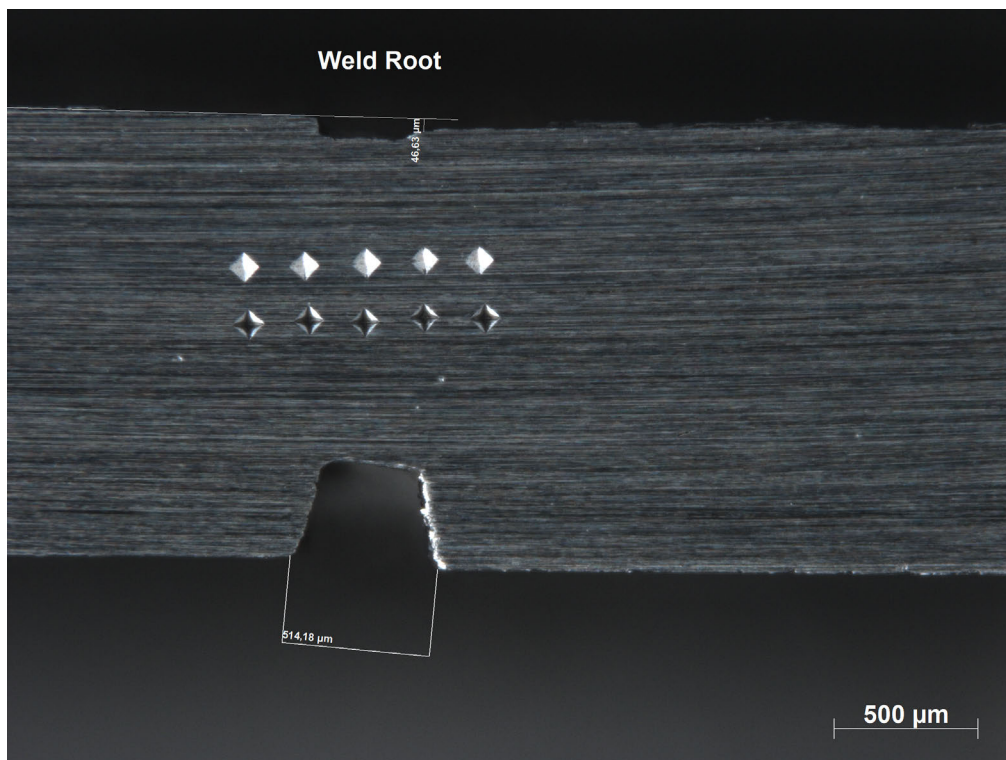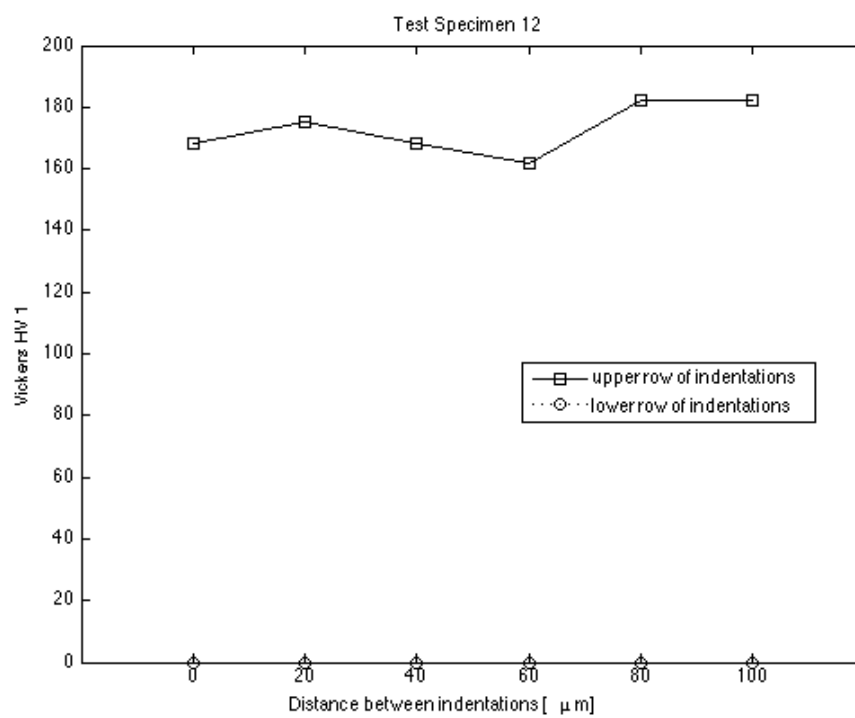
Vickers Hardness Measurements - Specimen 12

Vickers Hardness Test – Specimen 13
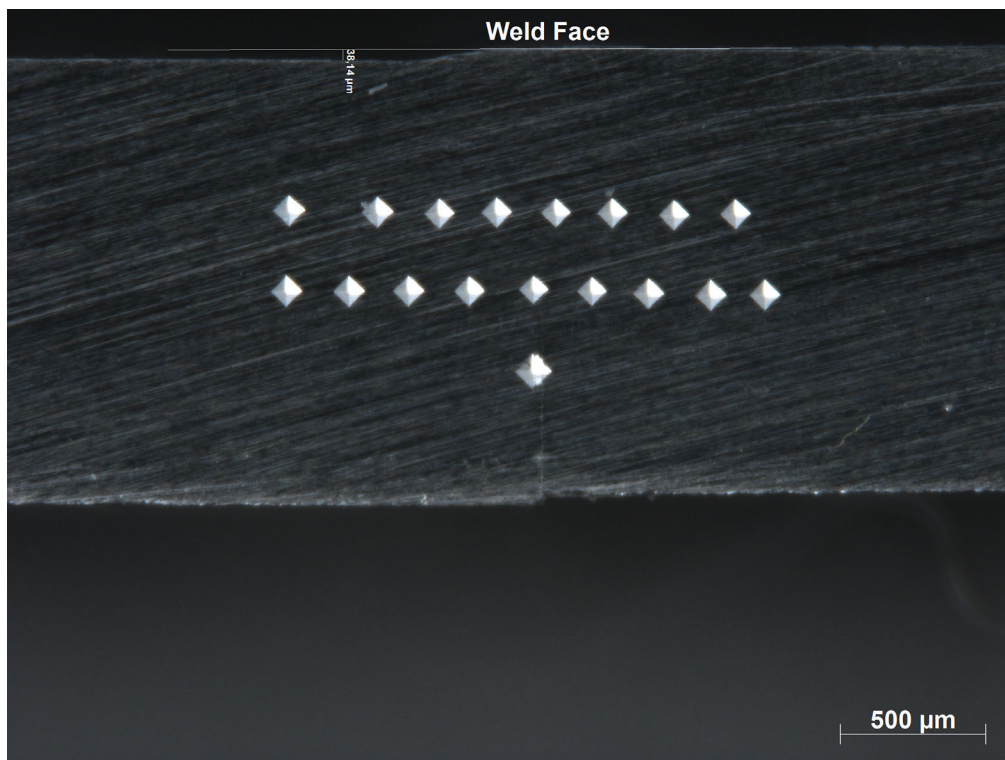
Vickers Indentation - Test specimen 13
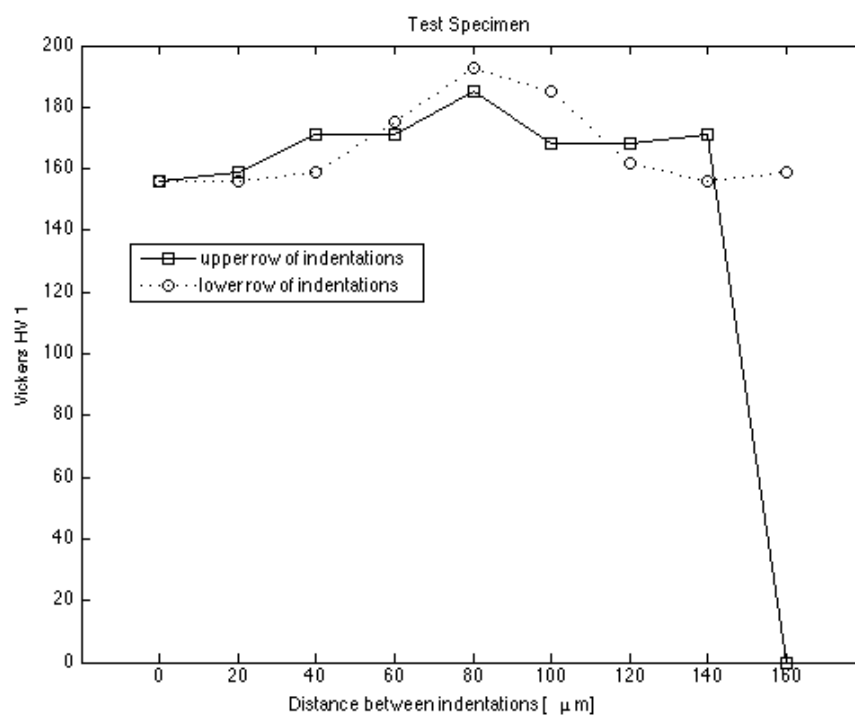
Vickers Hardness Measurements - Specimen 13

Appendix IV – Bend Testing

Bend Testing – Weld Face
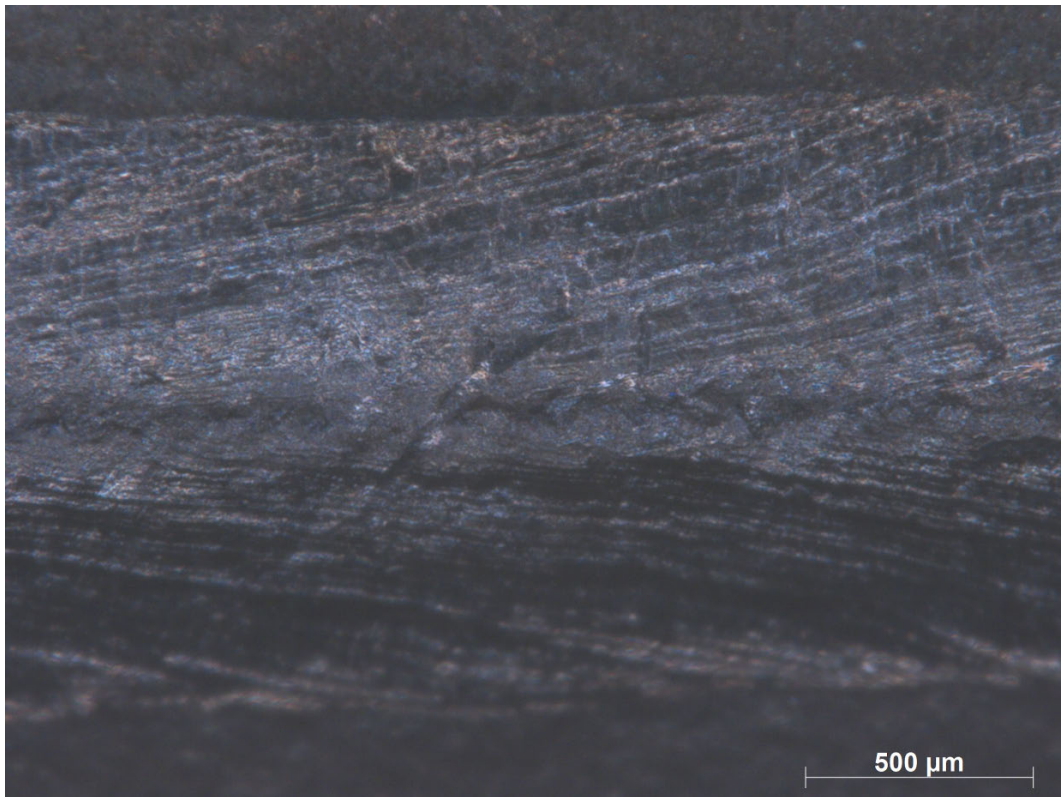
Bend Test 90° - Specimen A
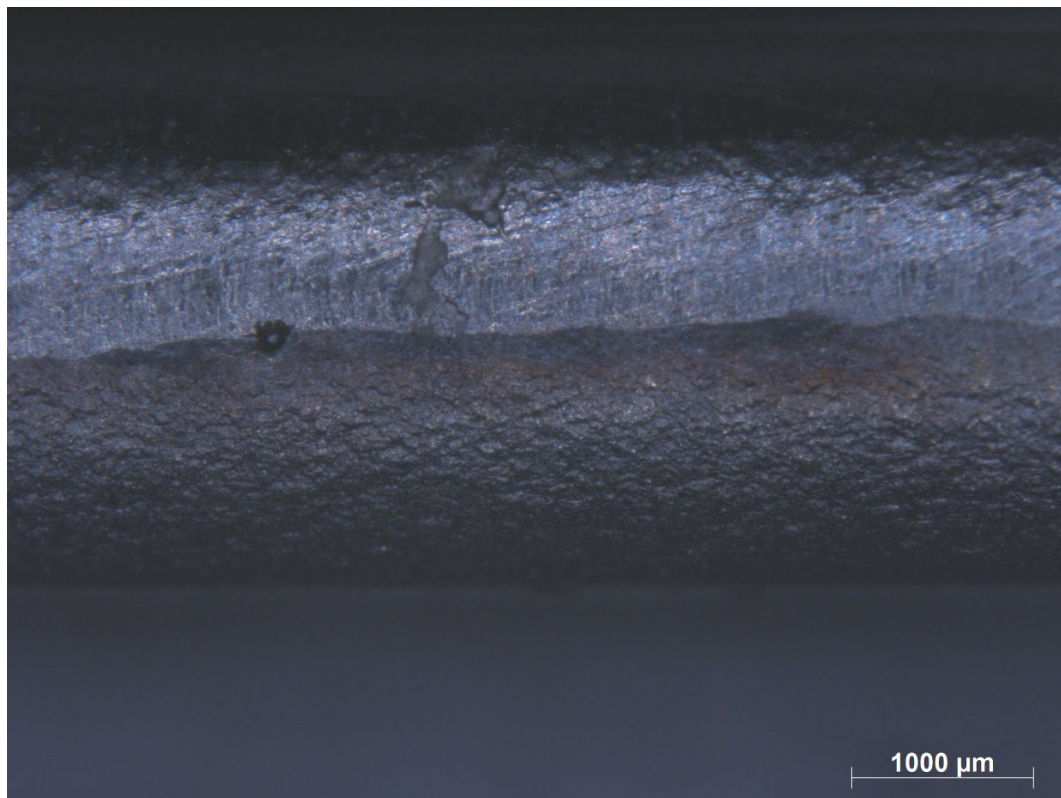
Bend Testing 180° - Specimen A
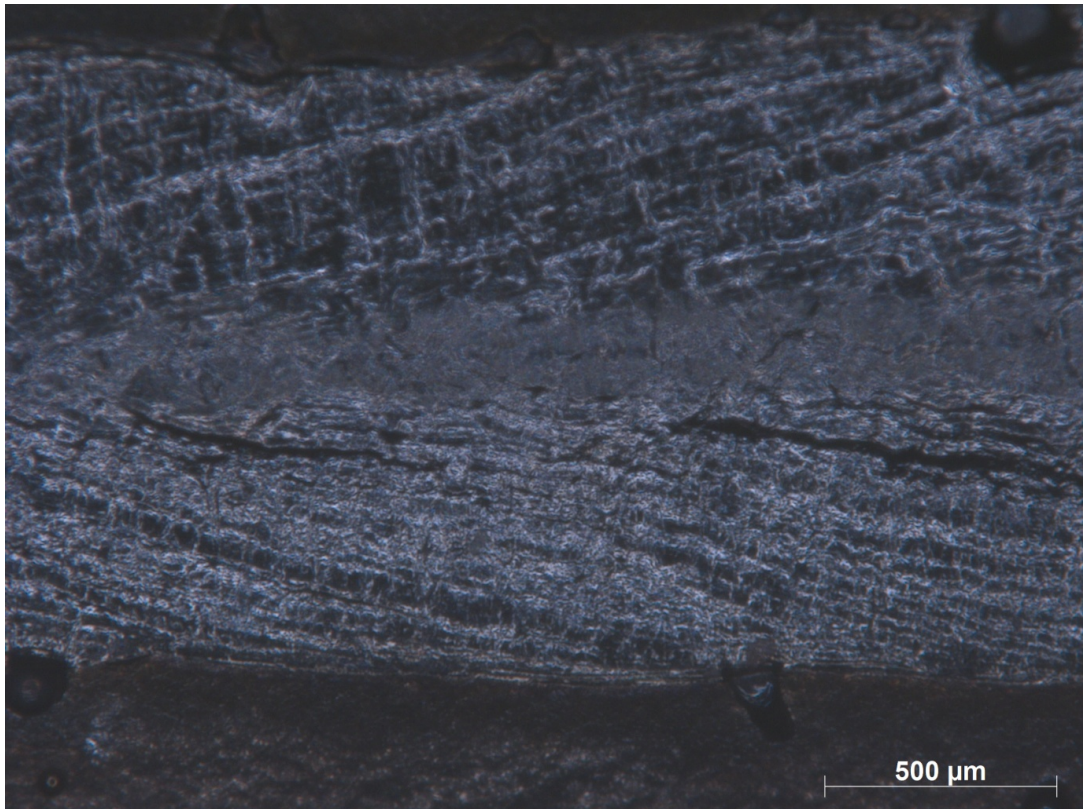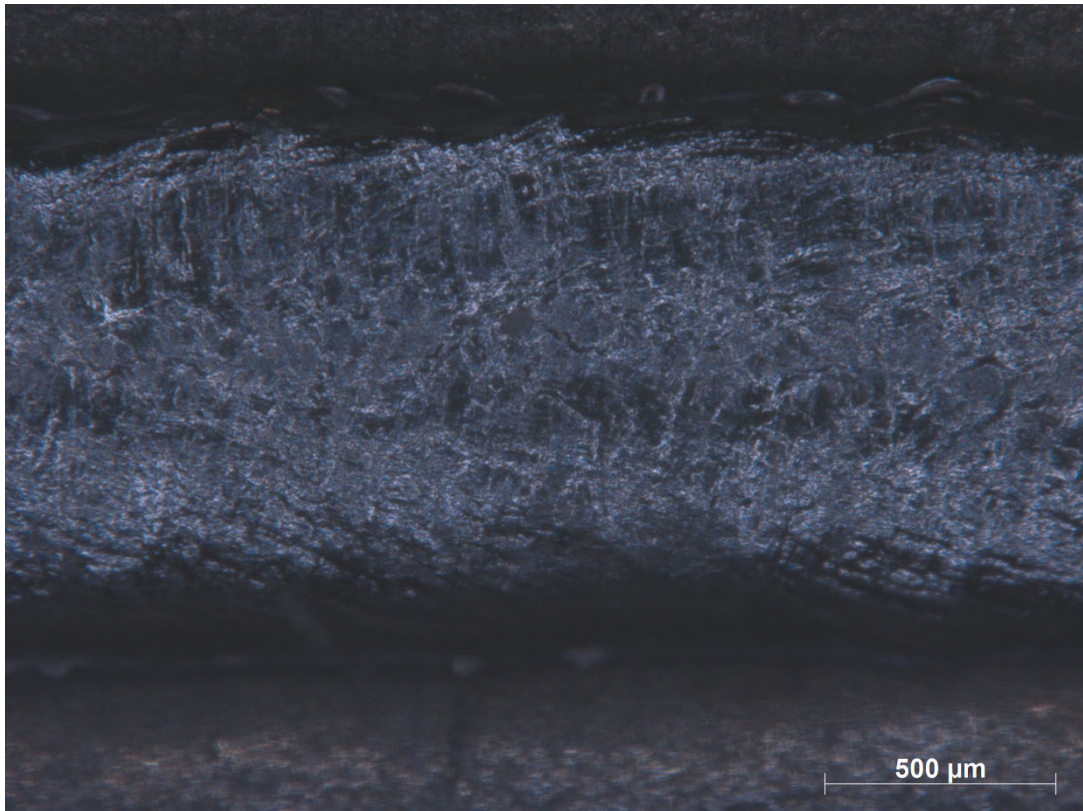
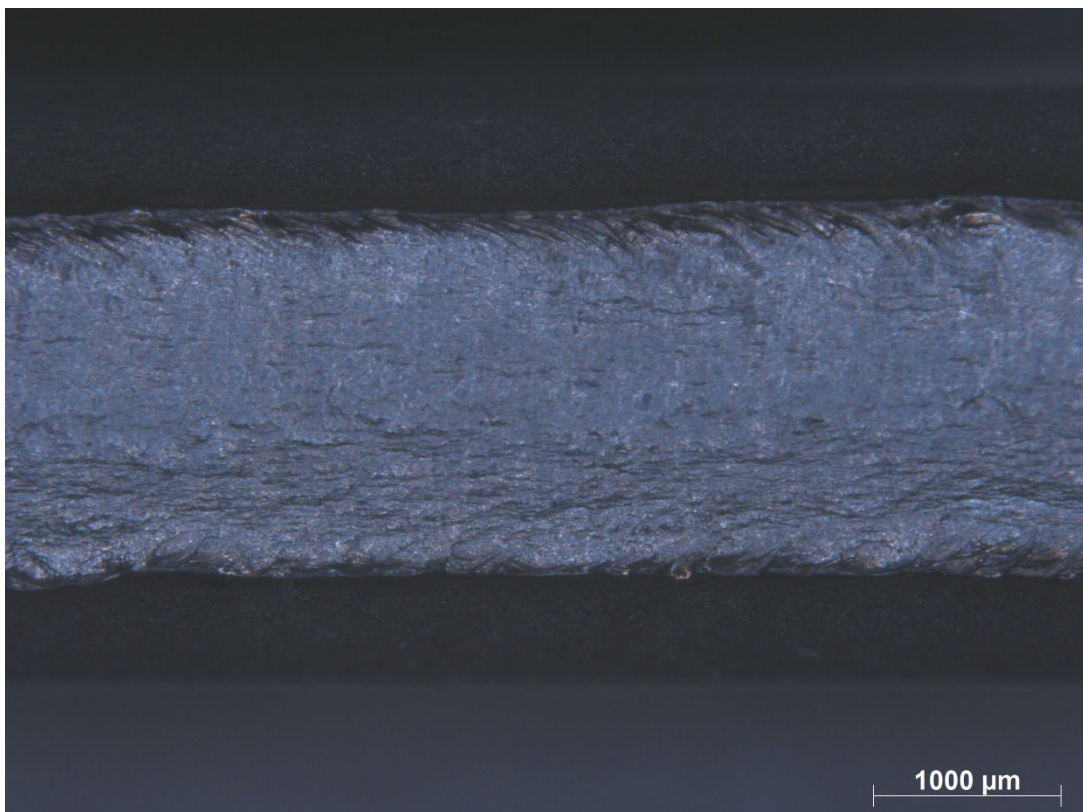**Bend Test 90° - Specimen B**
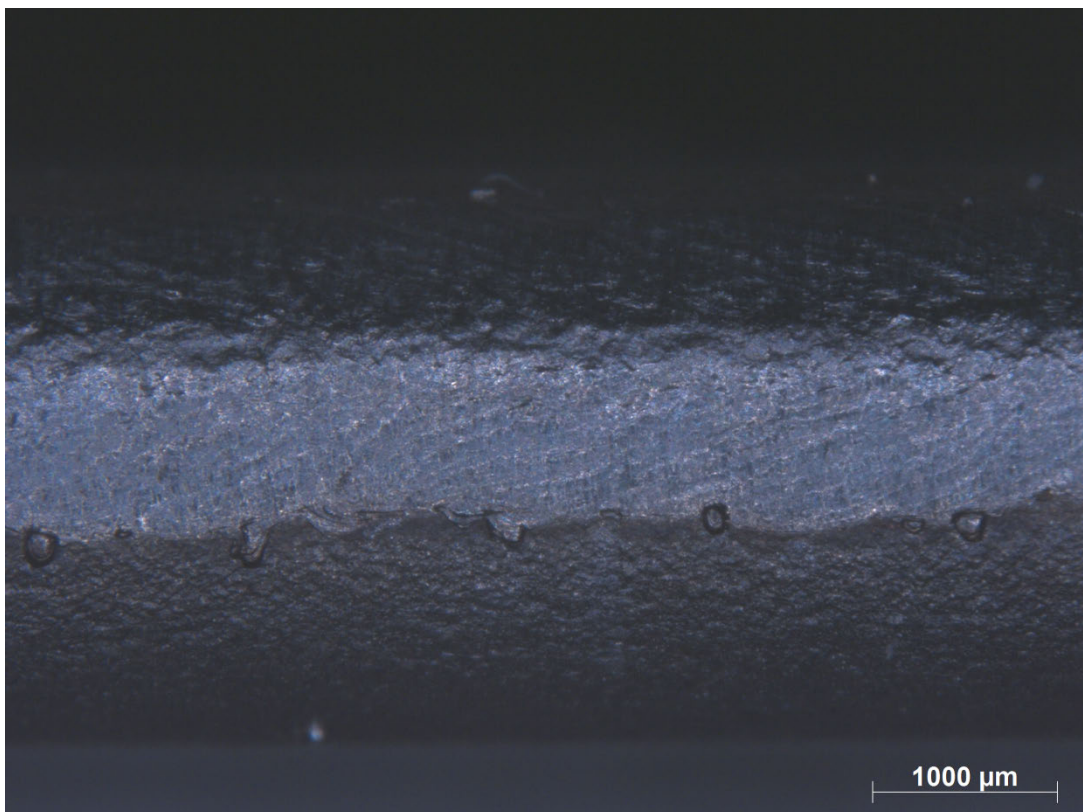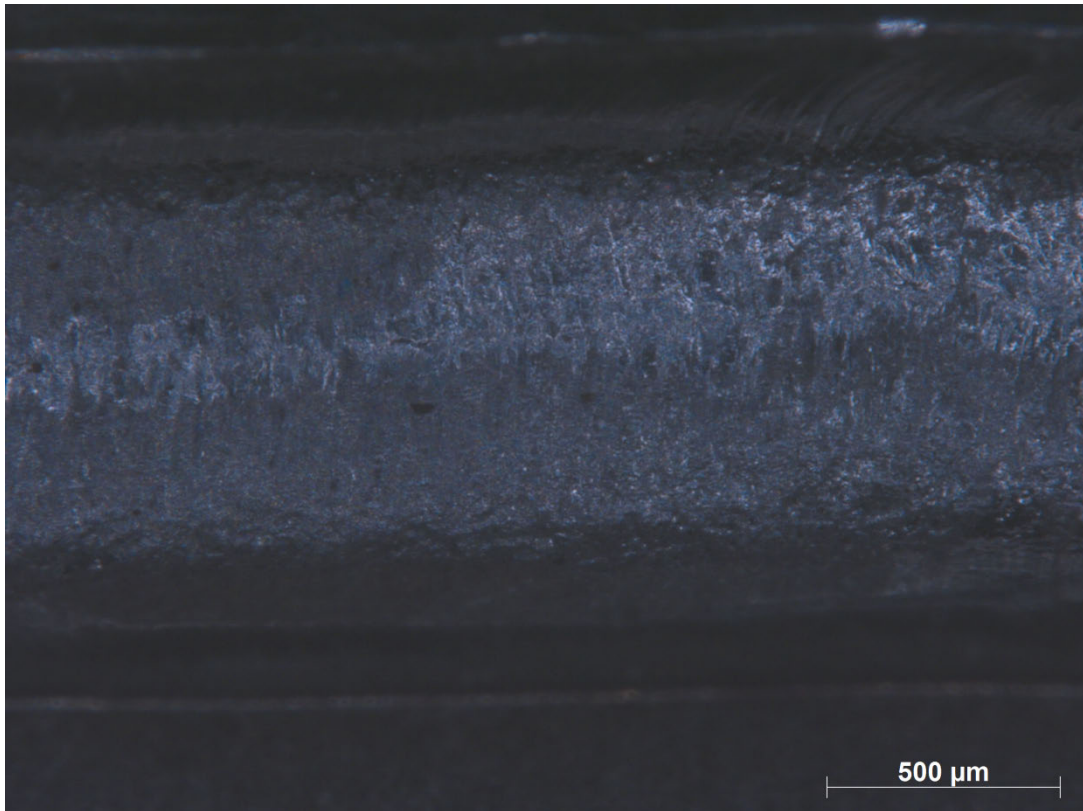

Bend Testing 180° - Specimen B
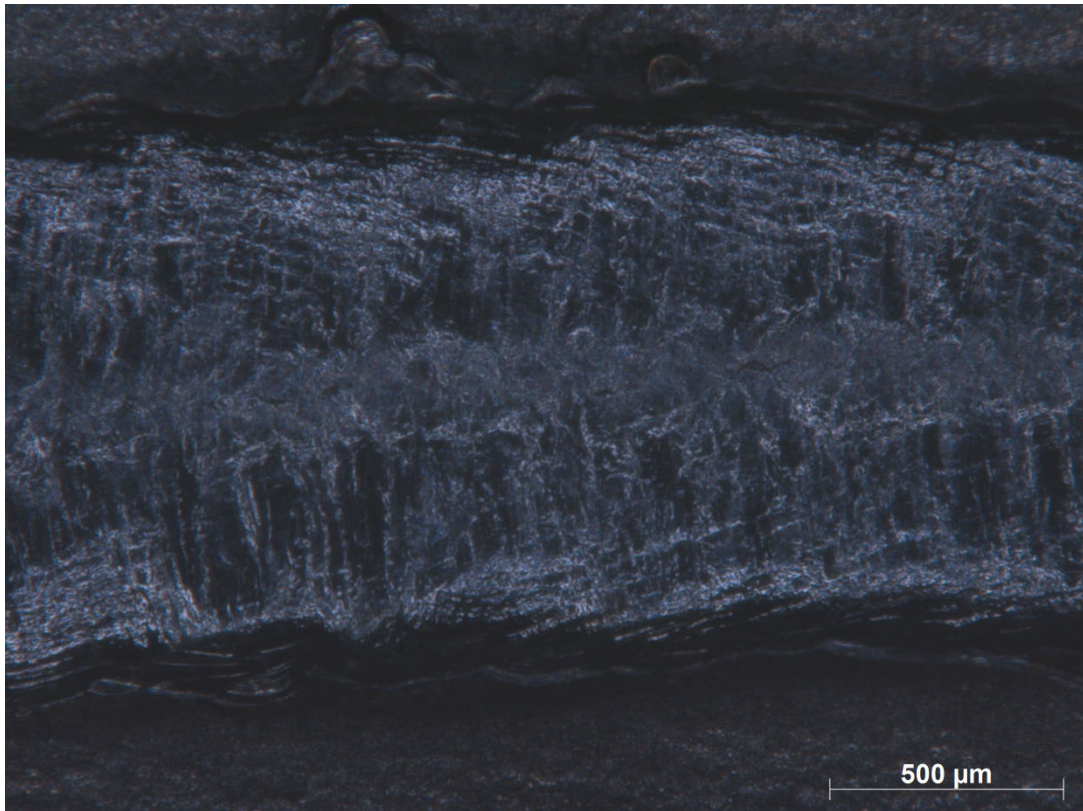
Bend Test 90° - Specimen C
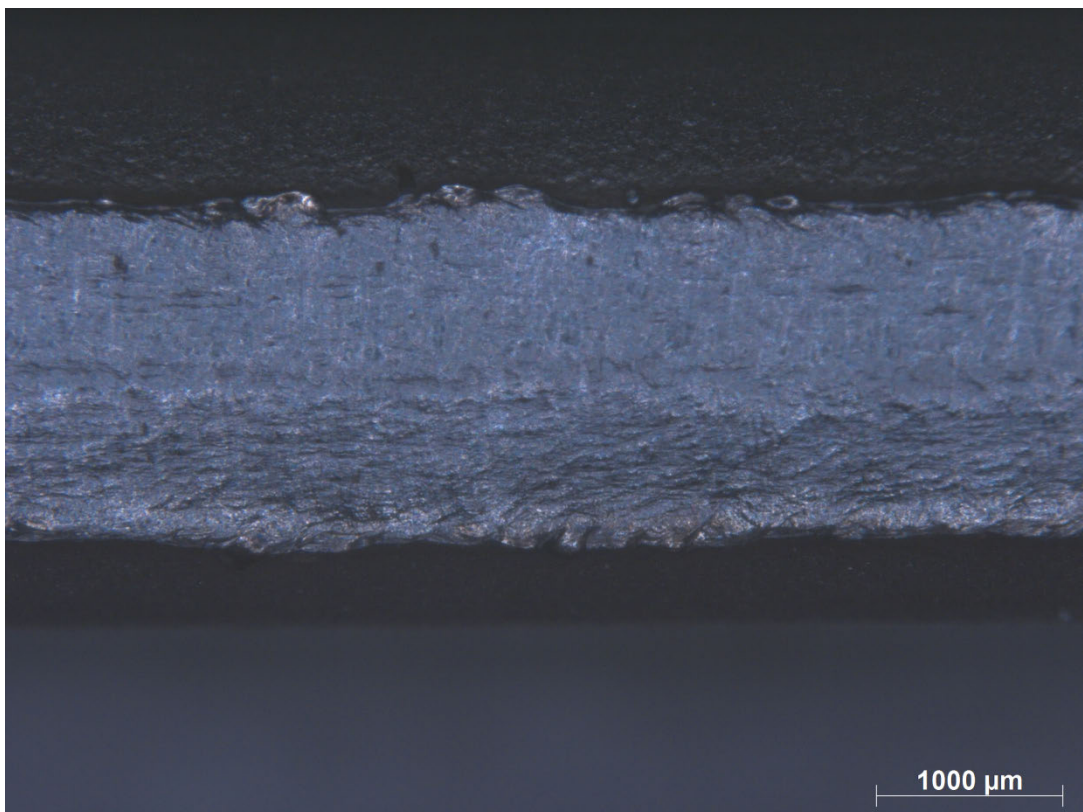
Bend Testing 180° - Specimen C
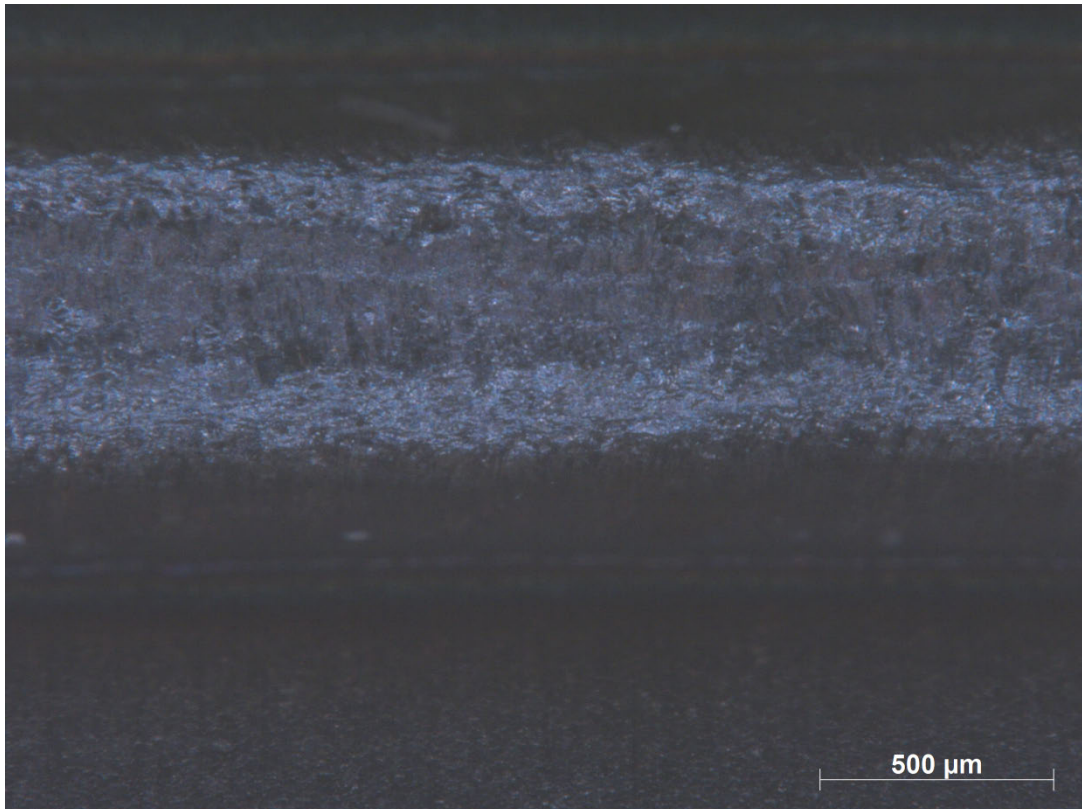
Bend Test 90° - Specimen D
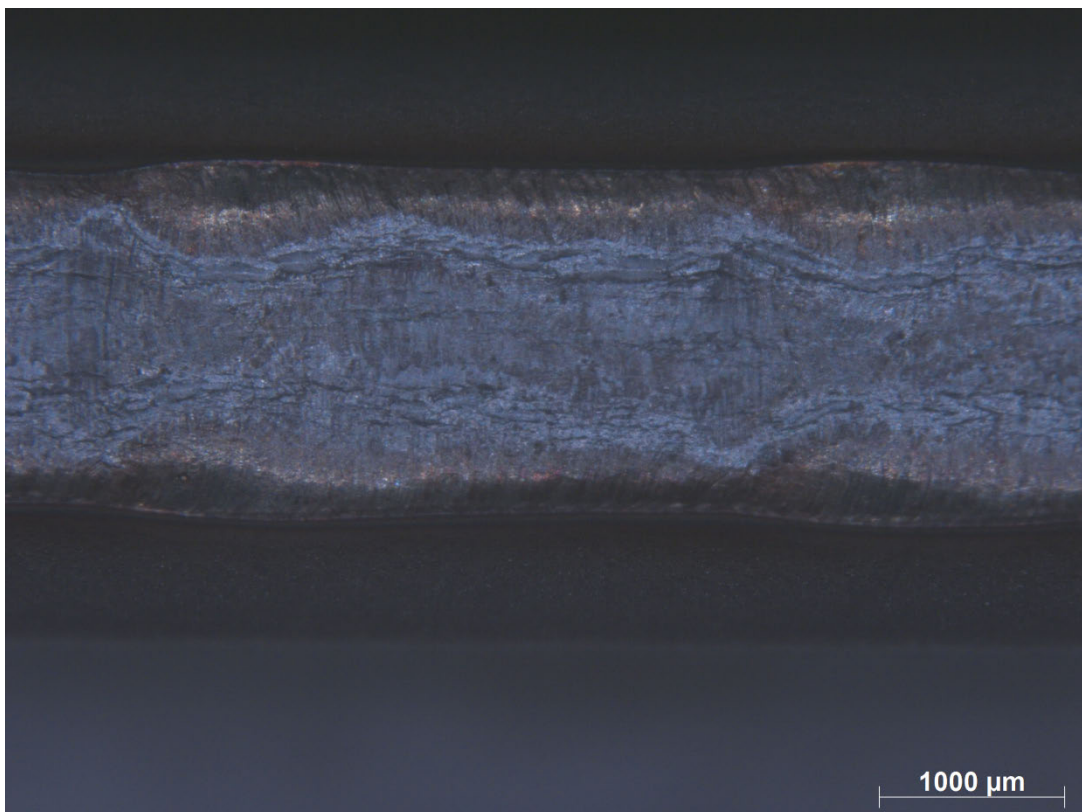
Bend Testing 180° - Specimen D
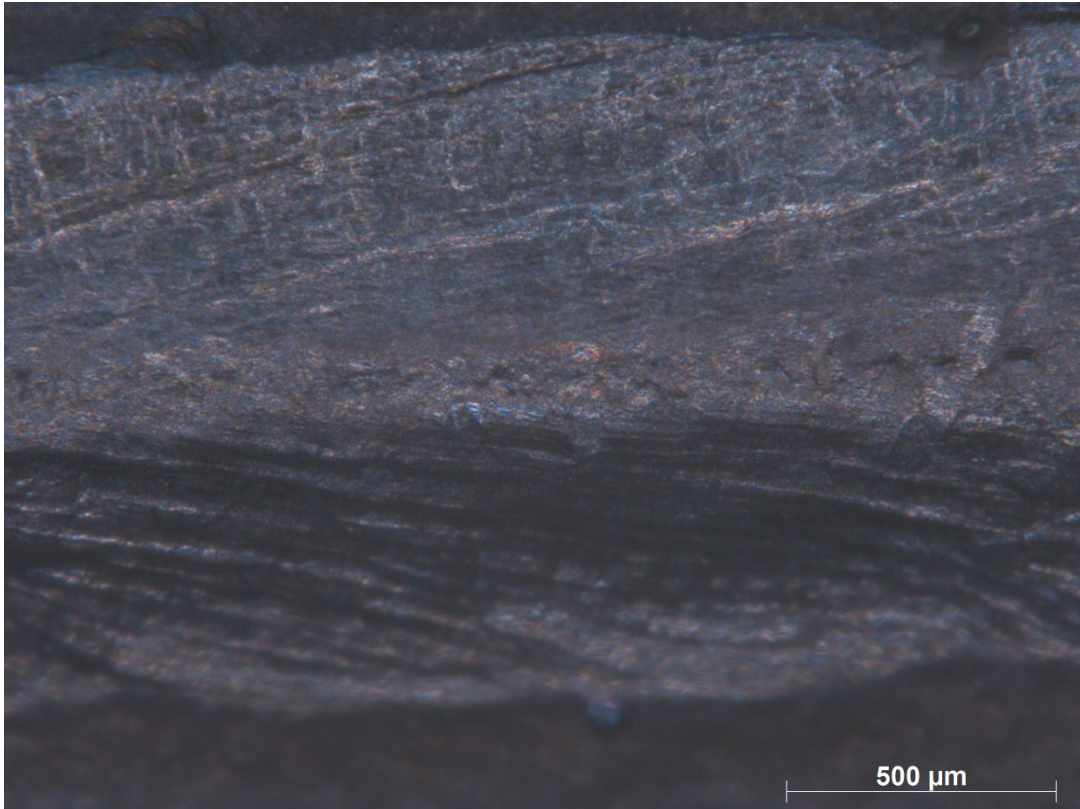
Bend Test 90° - Specimen E
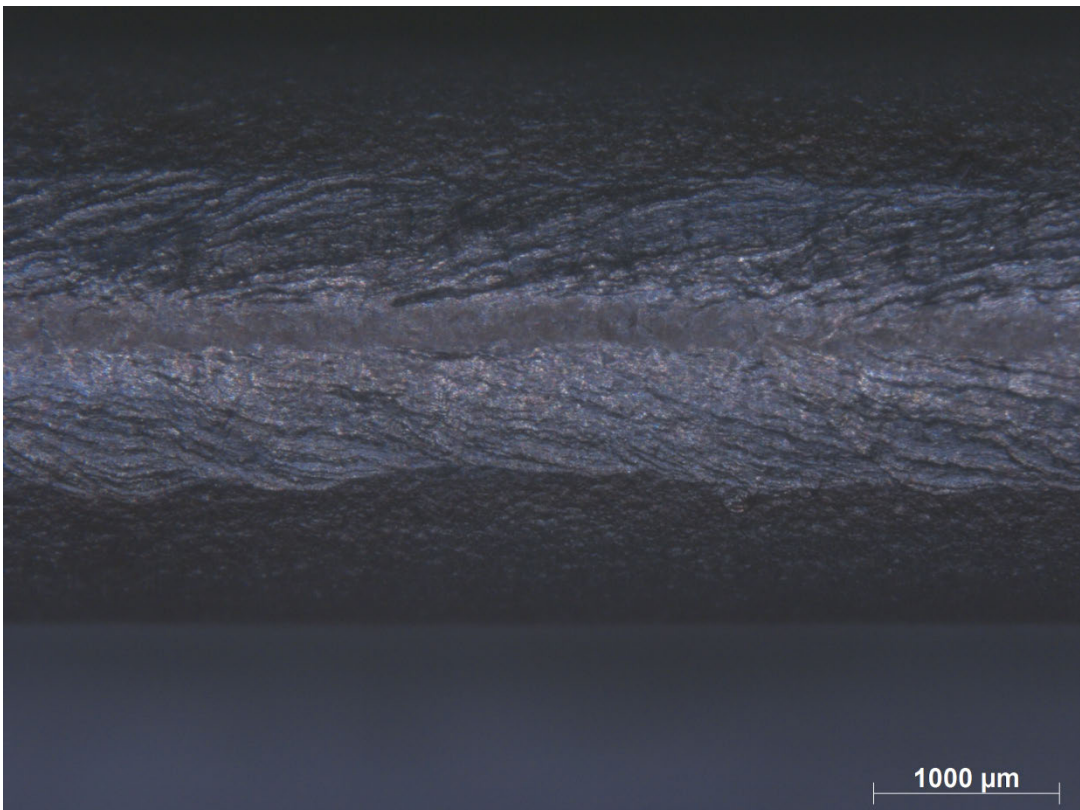
Bend Testing 180° - Specimen E
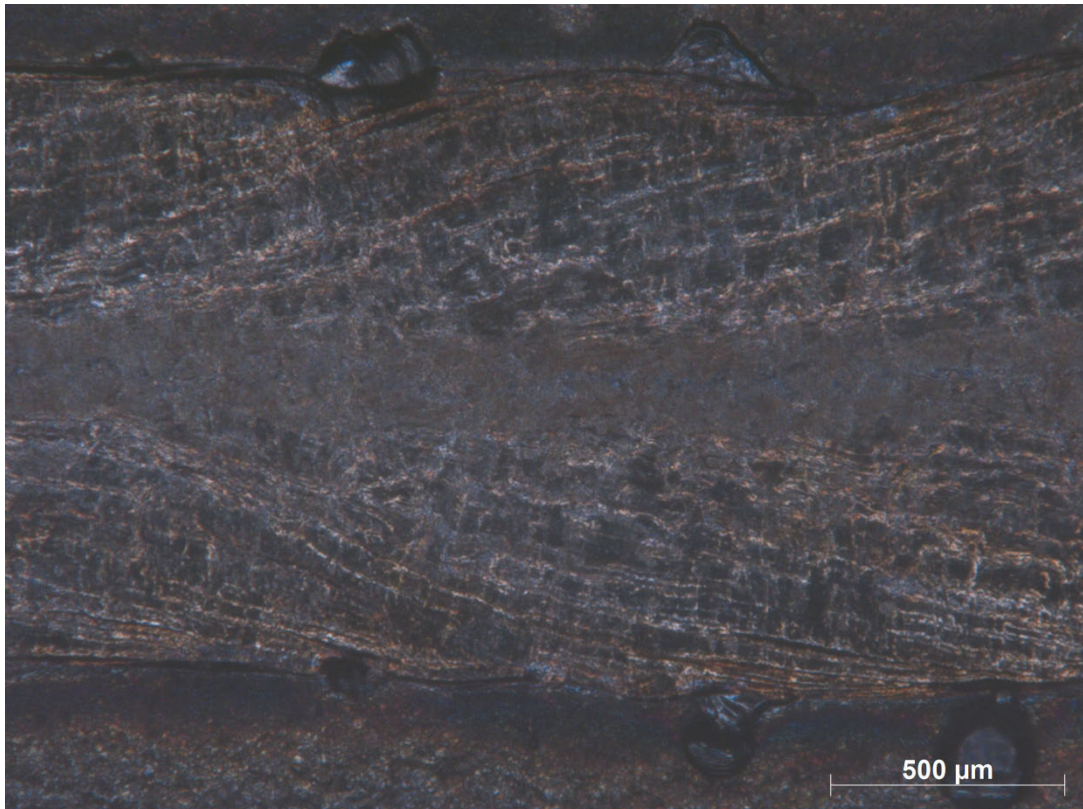
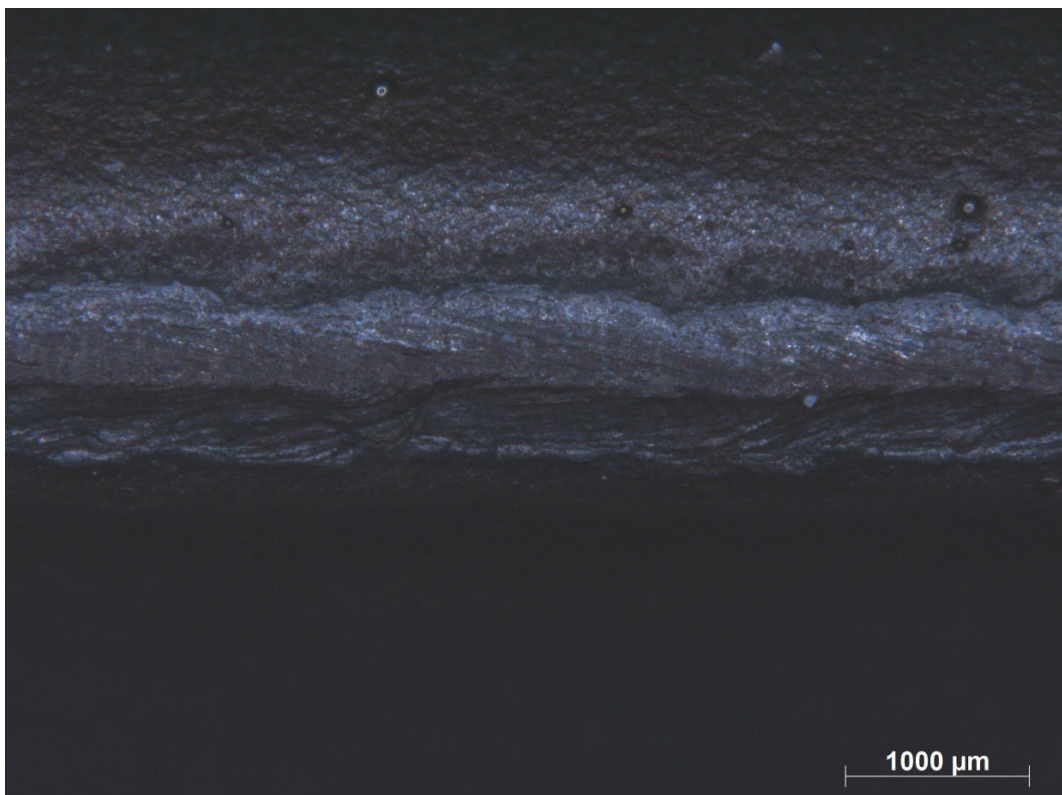**Bend Test 90° - Specimen F**
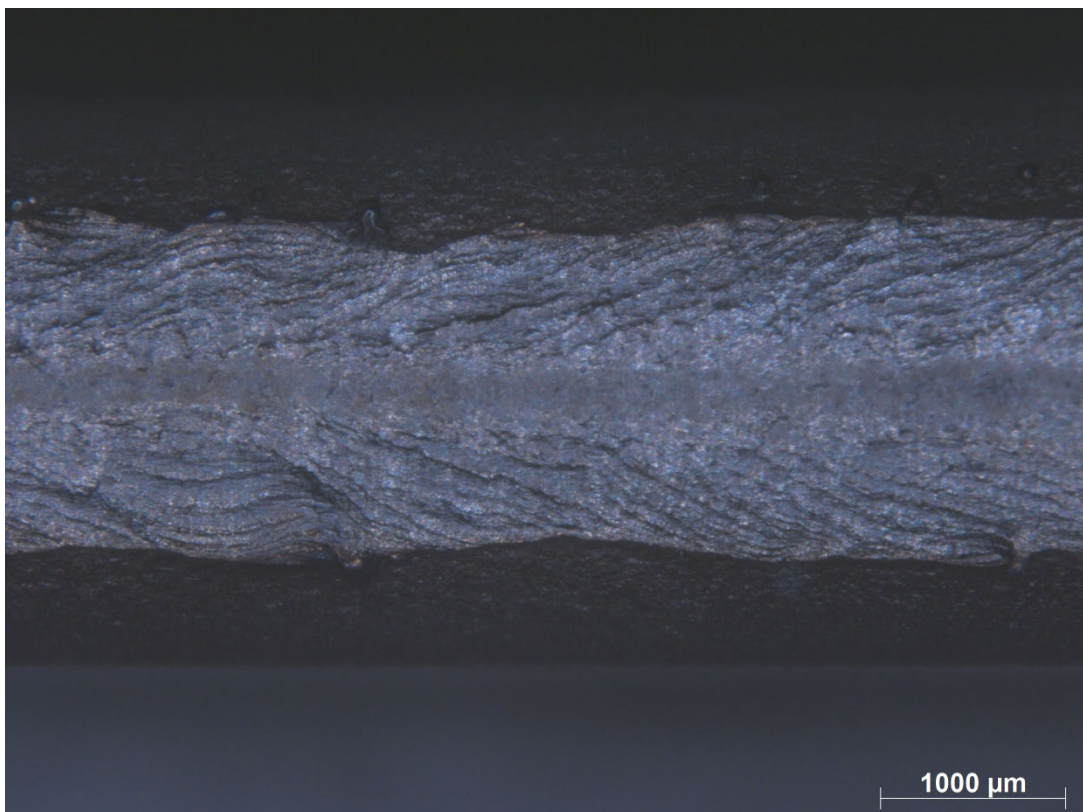
Bend Testing 180° - Specimen F
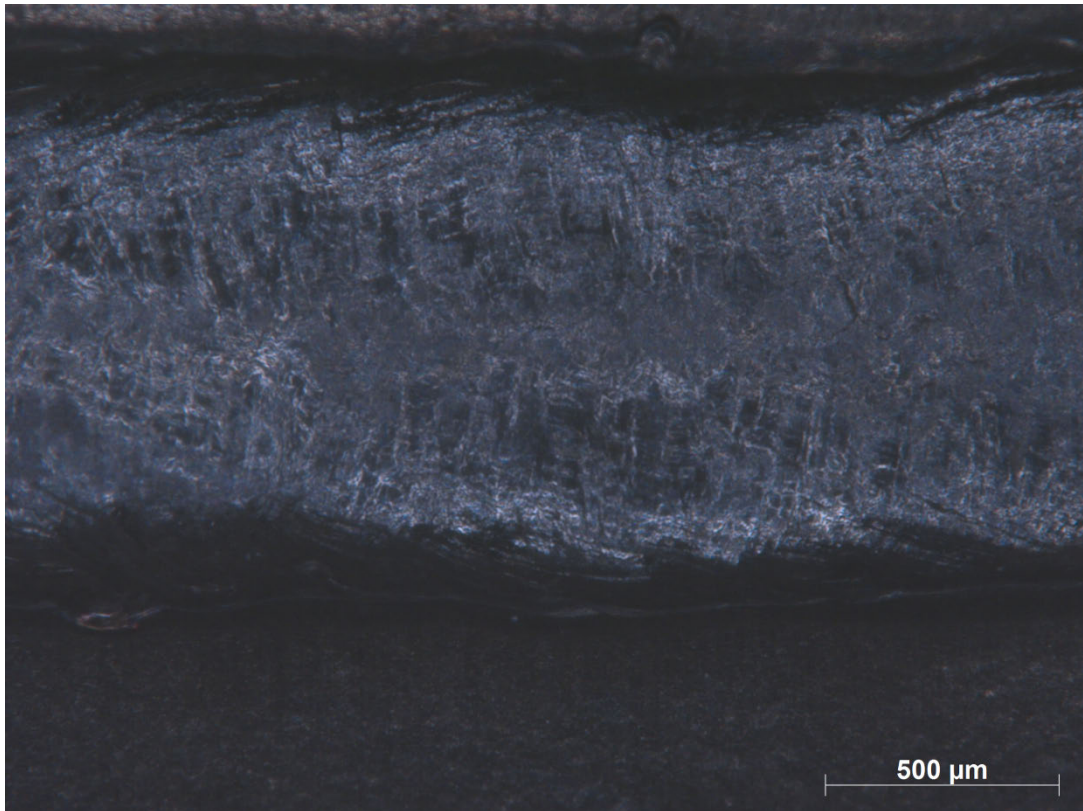
Bend Test 90° - Specimen G
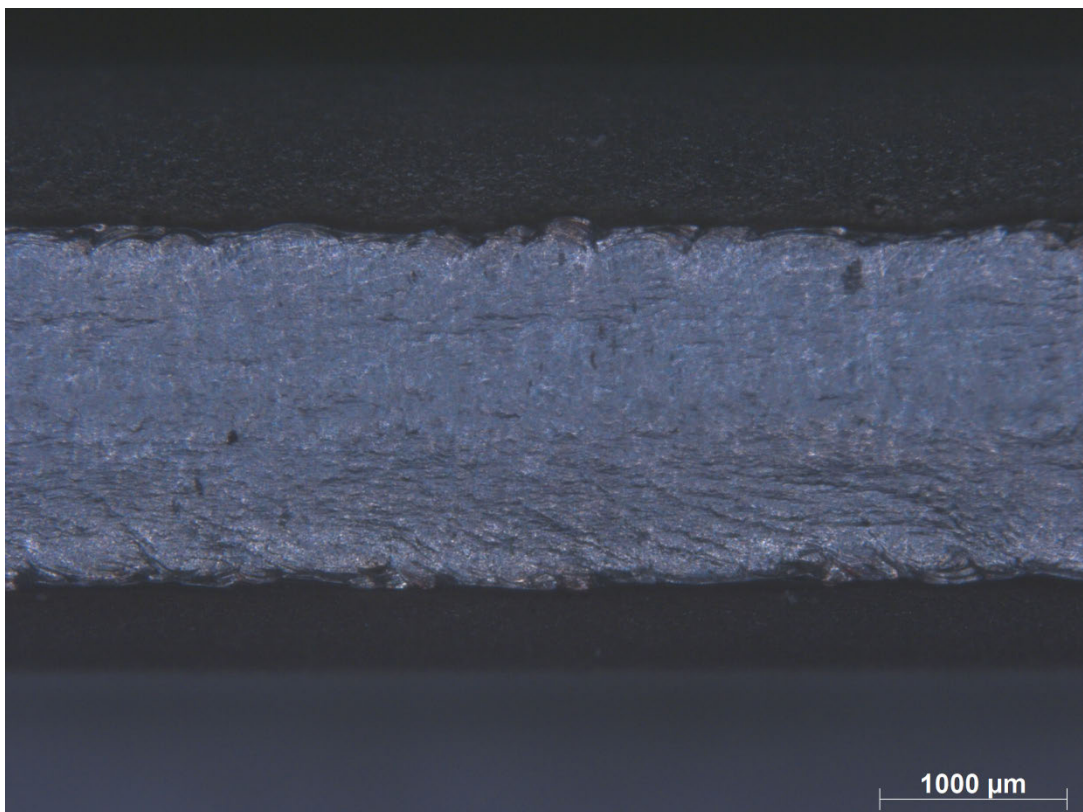
Bend Testing 180° - Specimen G
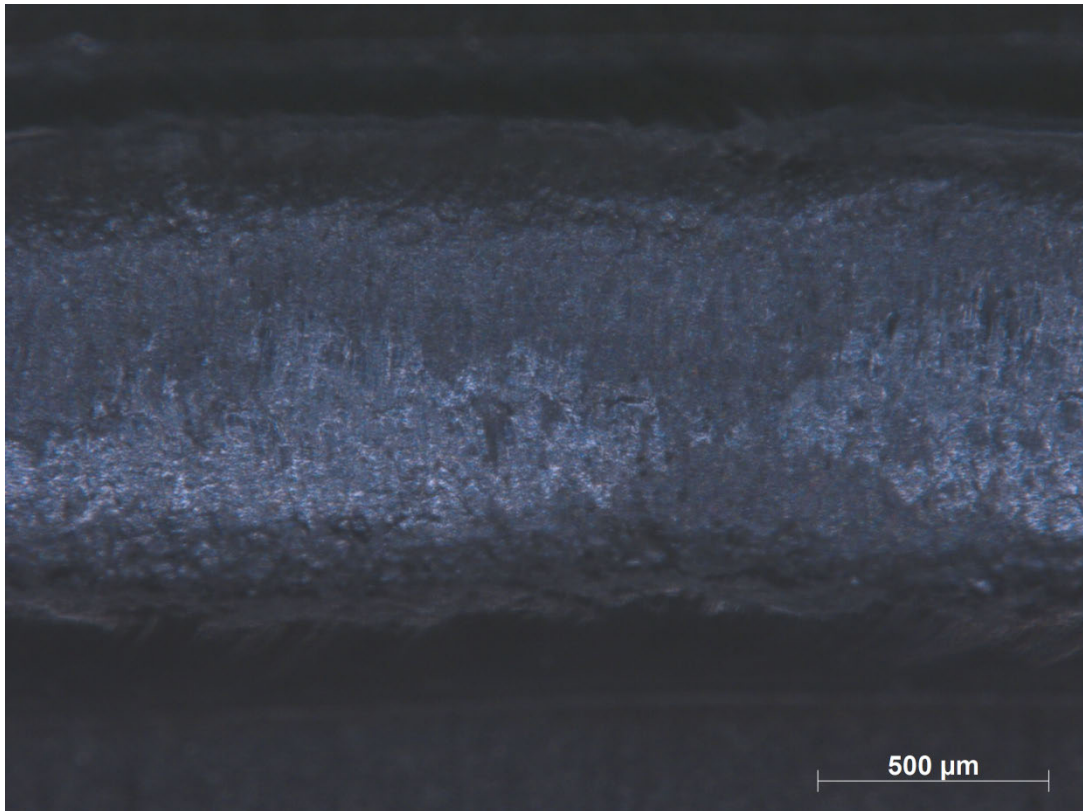
Bend Test 90° - Specimen H
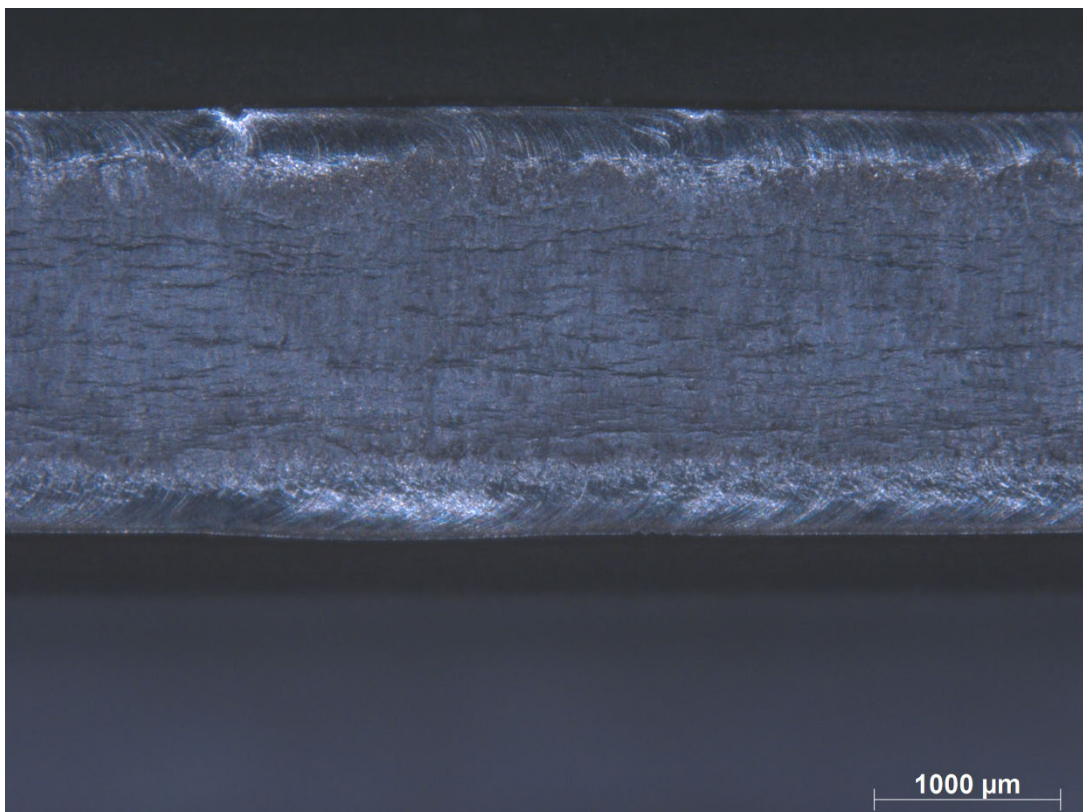
Bend Testing 180° - Specimen H
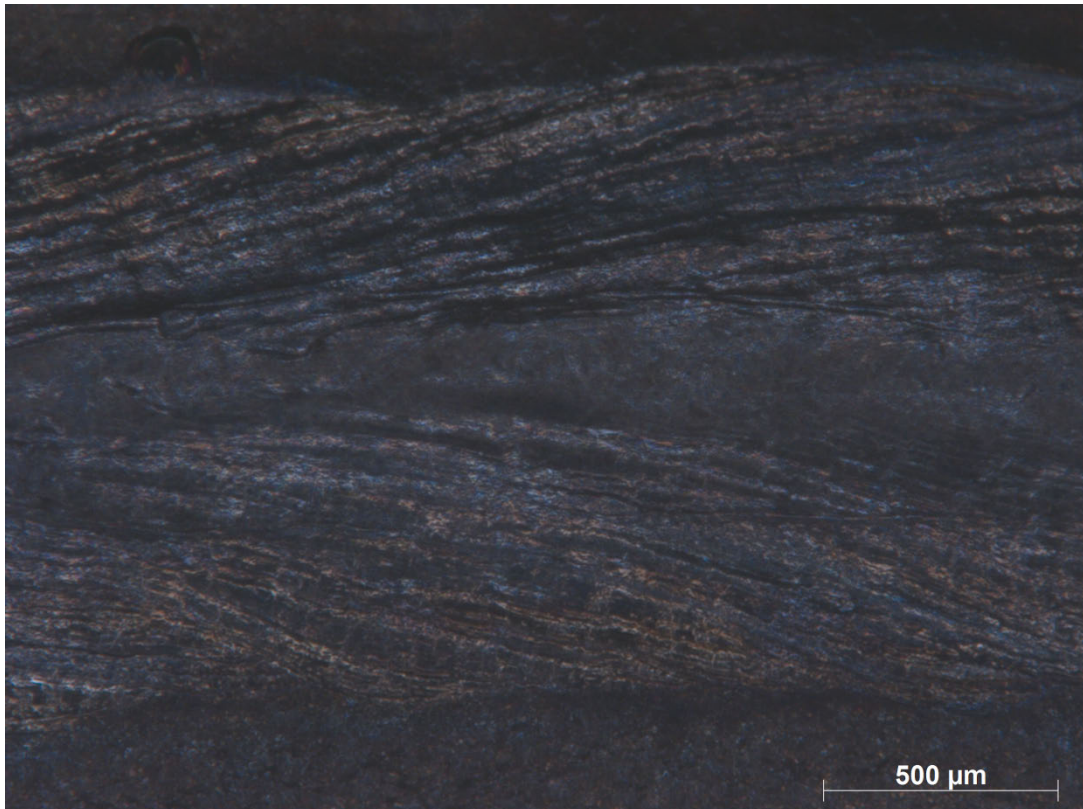
Bend Test 90° - Specimen I
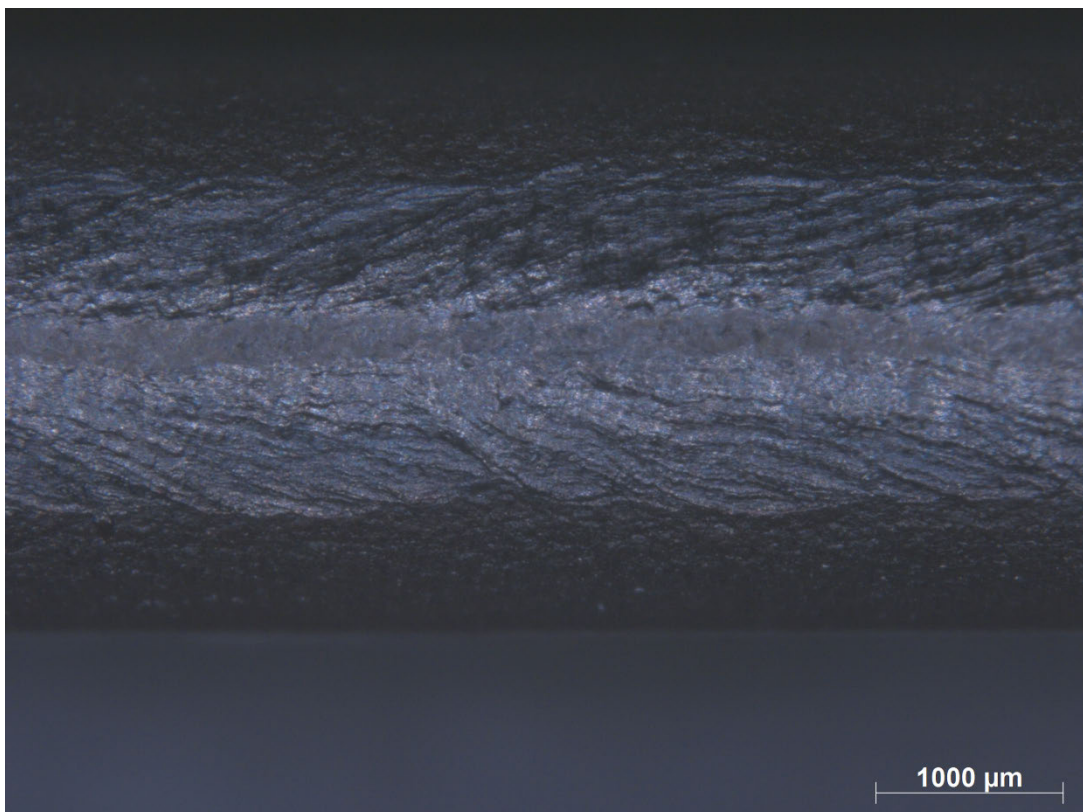
Bend Testing 180° - Specimen I
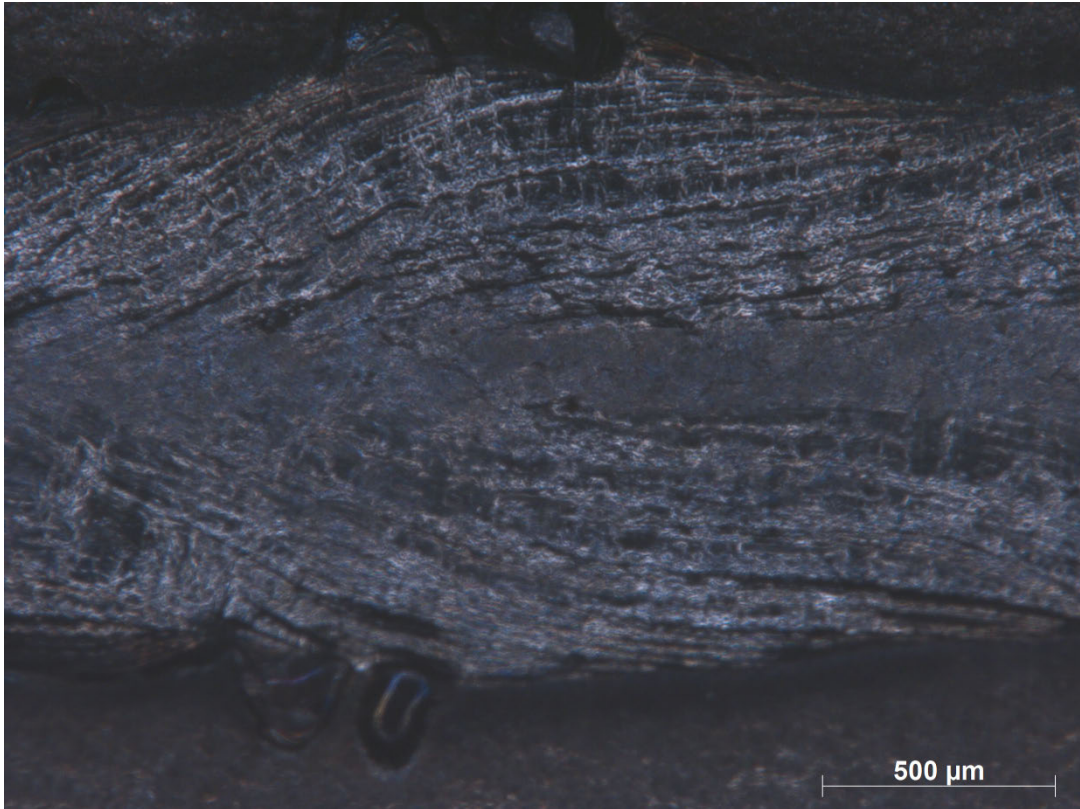
Bend Test 90° - Specimen J
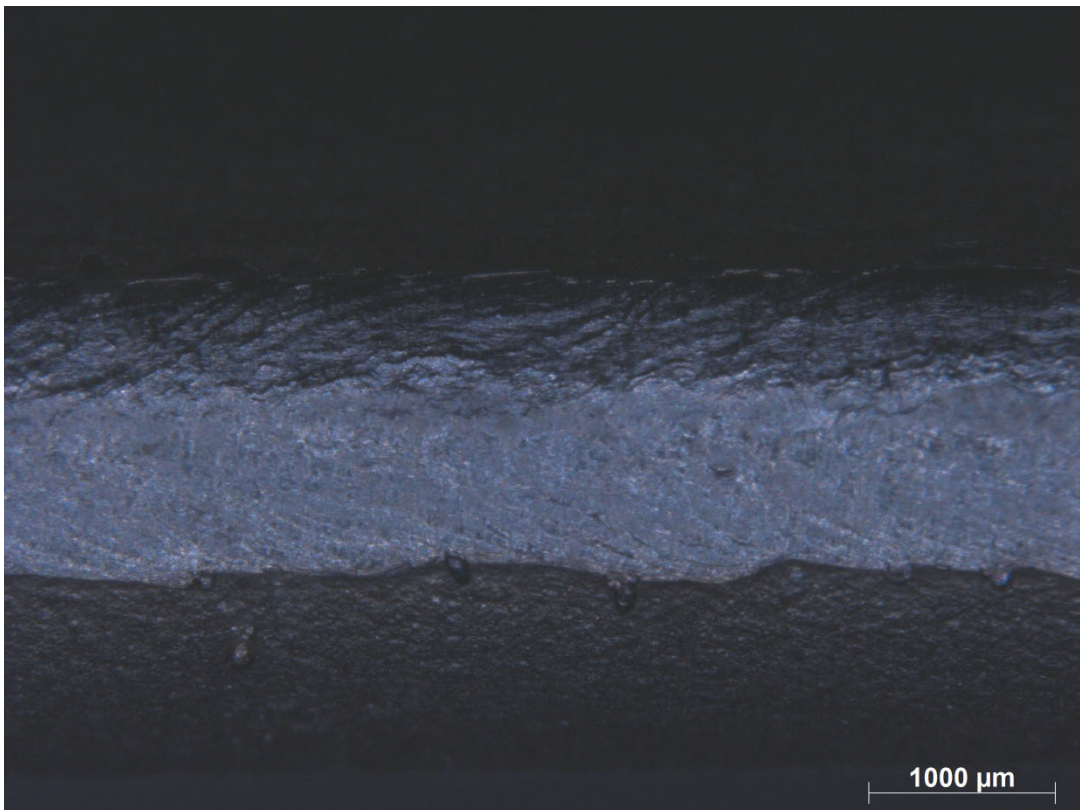
Bend Testing 180° - Specimen J

Bend Test 90° - Specimen K

Bend Testing 180° - Specimen K

Bend Test 90° - Specimen L

Bend Testing – Weld Root
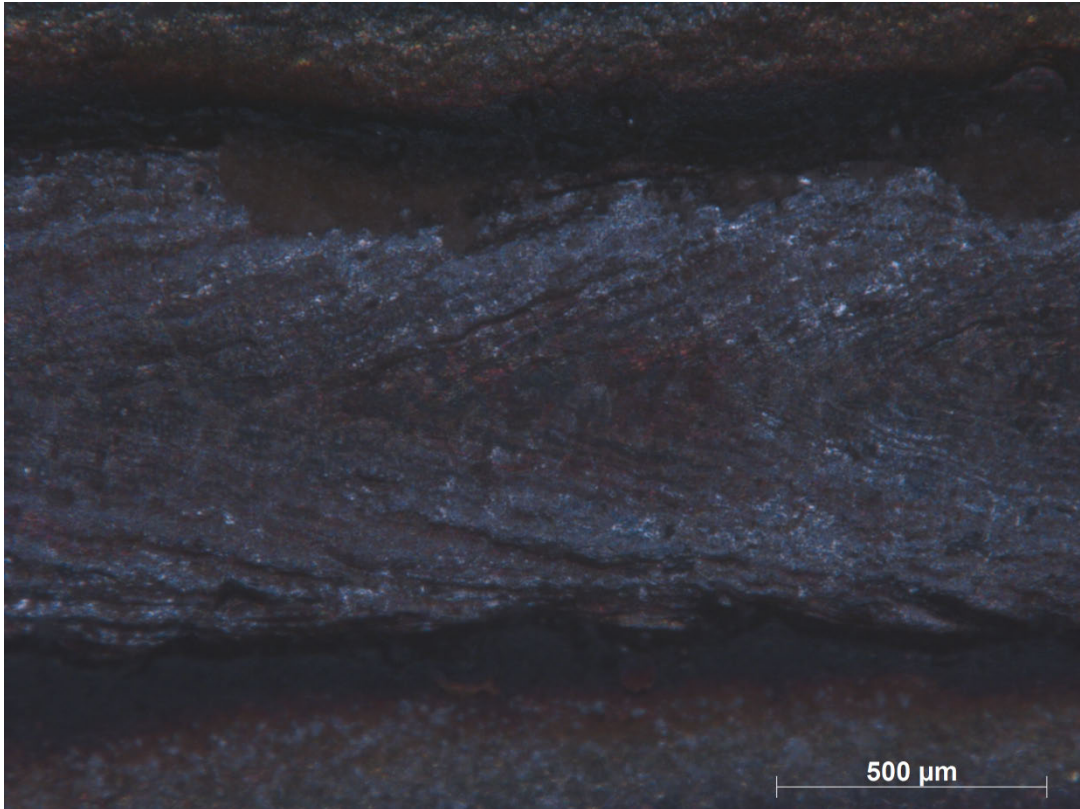

Bend Testing 90° (Weld Root) - Specimen A
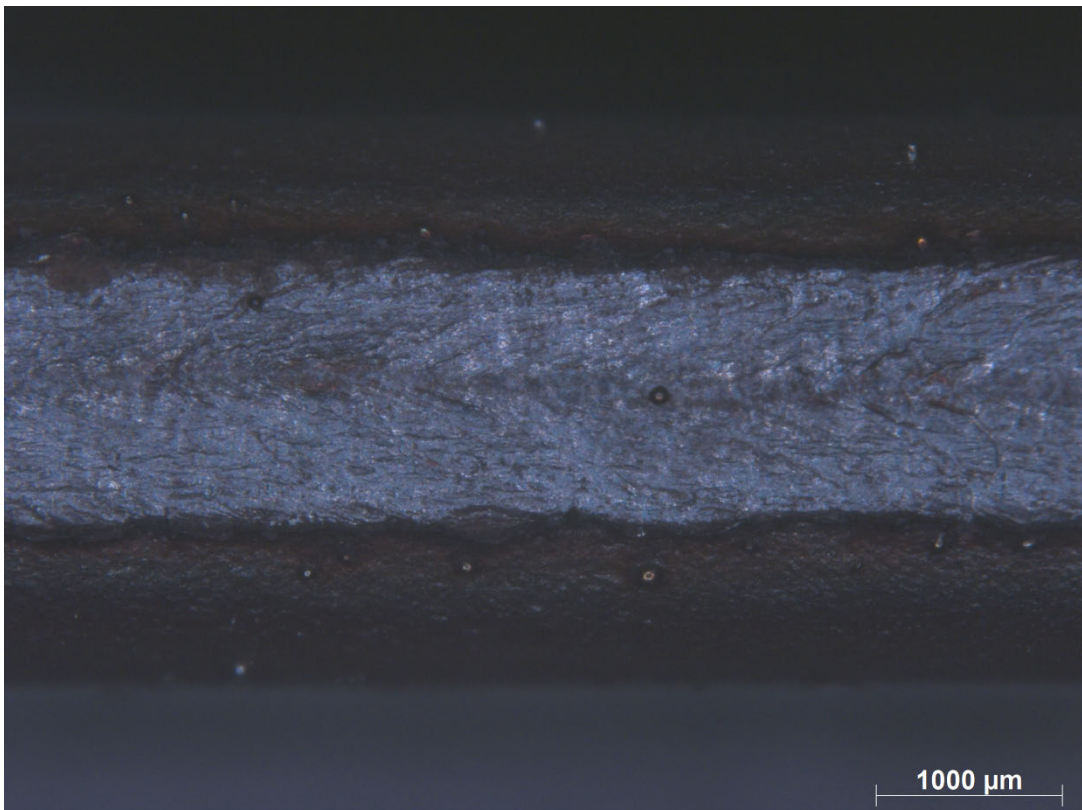

Bend Testing 180° (Weld Root) - Specimen A

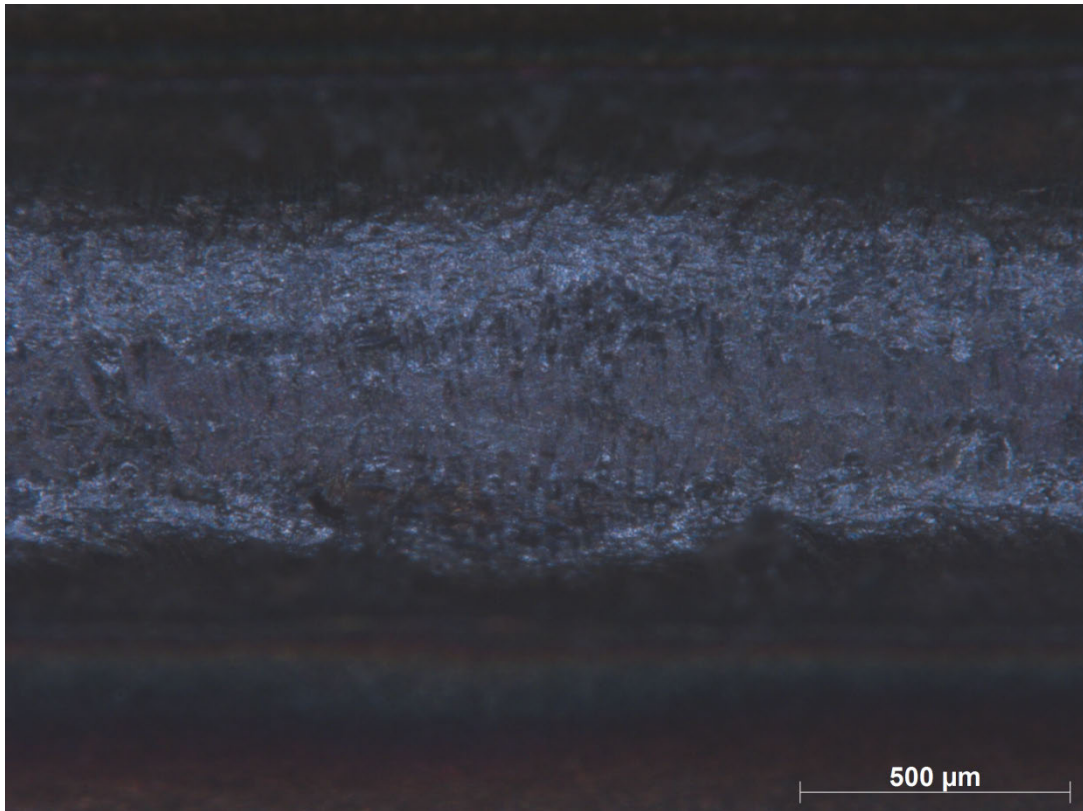**Bend Testing 90° (Weld Root) - Specimen B**
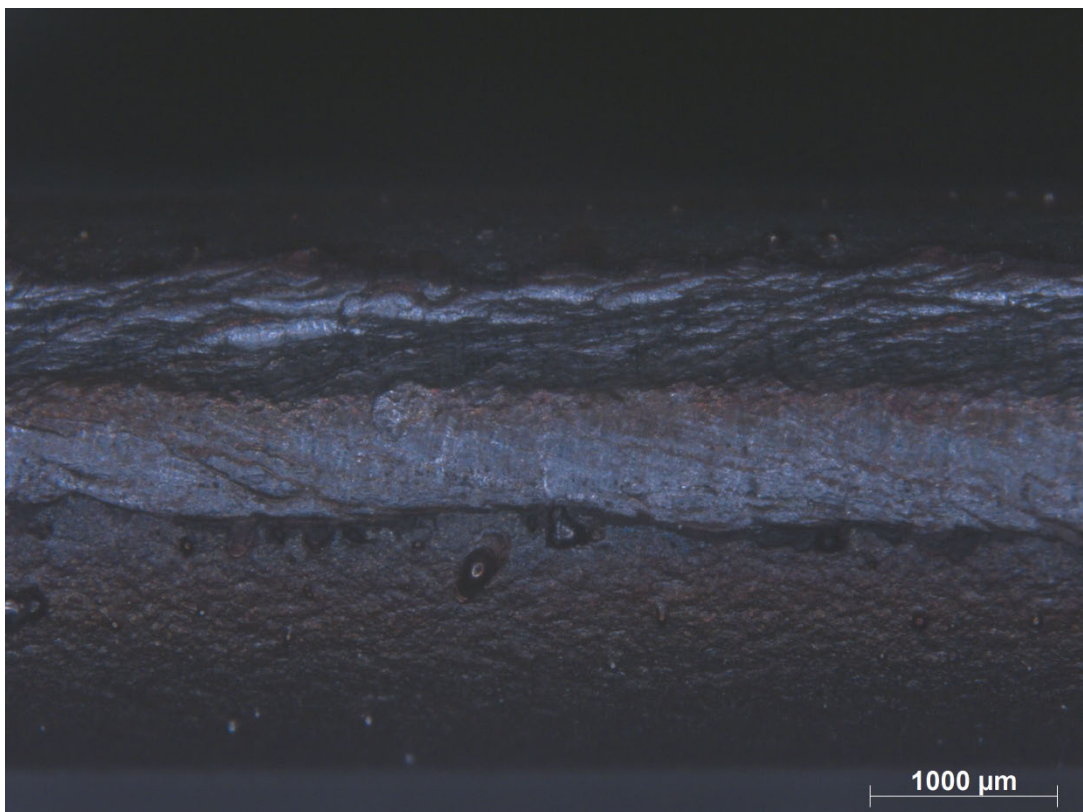
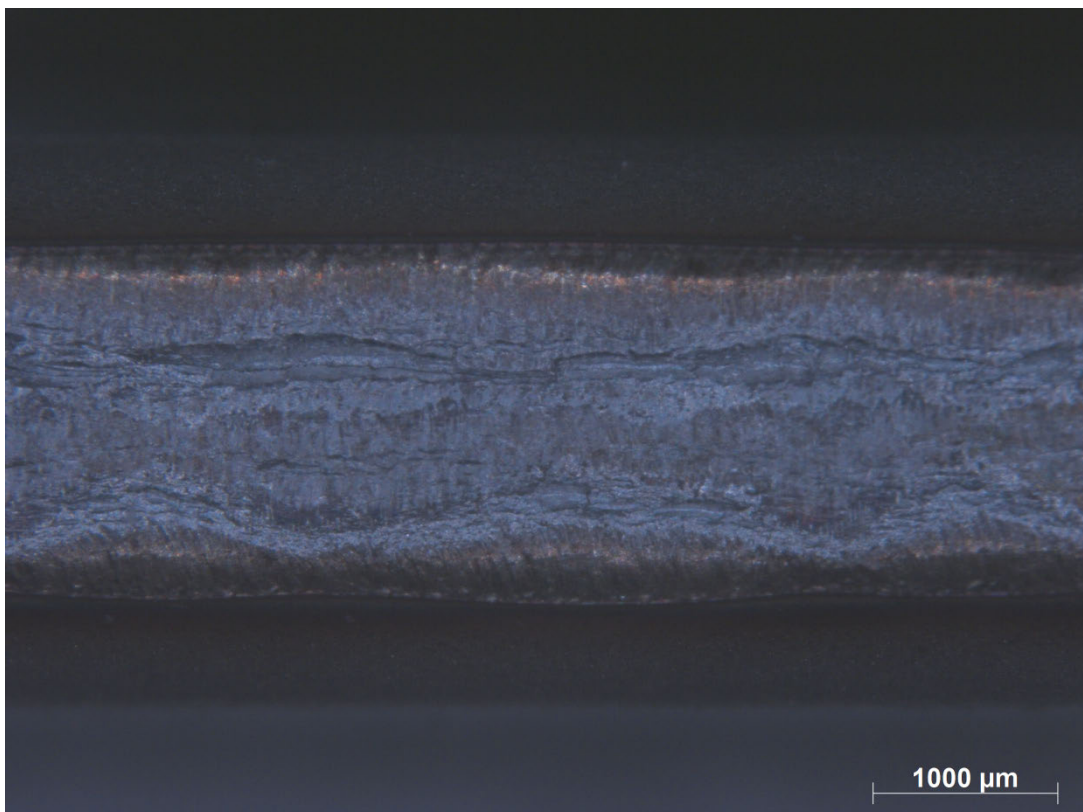**Bend Testing 180° (Weld Root) - Specimen B**
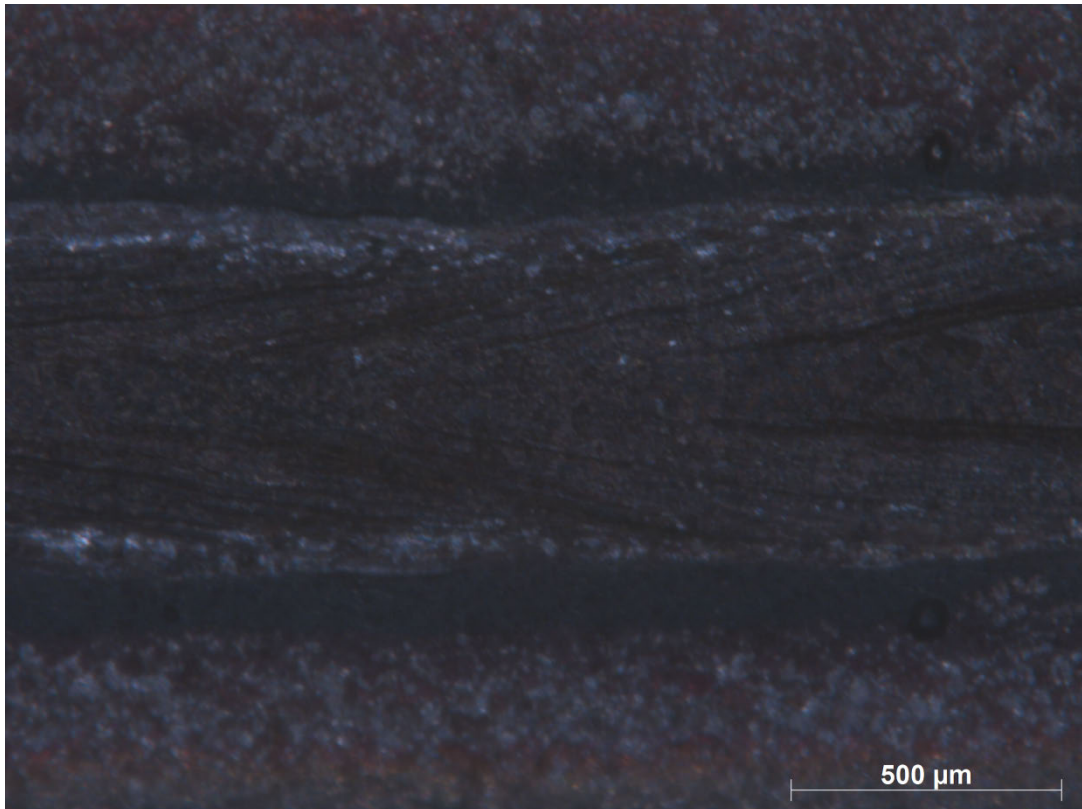
Bend Testing 90° (Weld Root) - Specimen C

Bend Testing 180° (Weld Root) - Specimen C

Bend Testing 90° (Weld Root) - Specimen D

Bend Testing 180° (Weld Root) - Specimen D

Bend Testing 90° (Weld Root) - Specimen E

Bend Testing 180° (Weld Root) - Specimen E
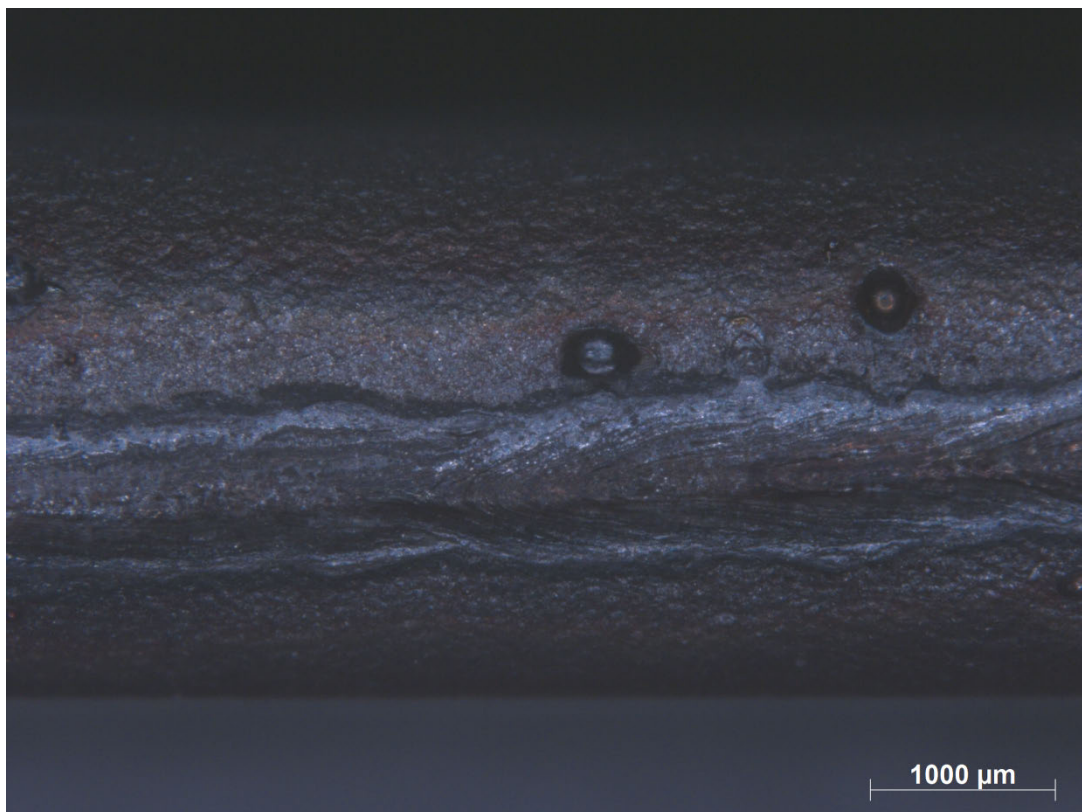
Bend Testing 90° (Weld Root) - Specimen F

Bend Testing 180° (Weld Root) - Specimen F

Bend Testing 90° (Weld Root) - Specimen G

Bend Testing 180° (Weld Root) - Specimen G

59

Bend Testing 90° (Weld Root) - Specimen H
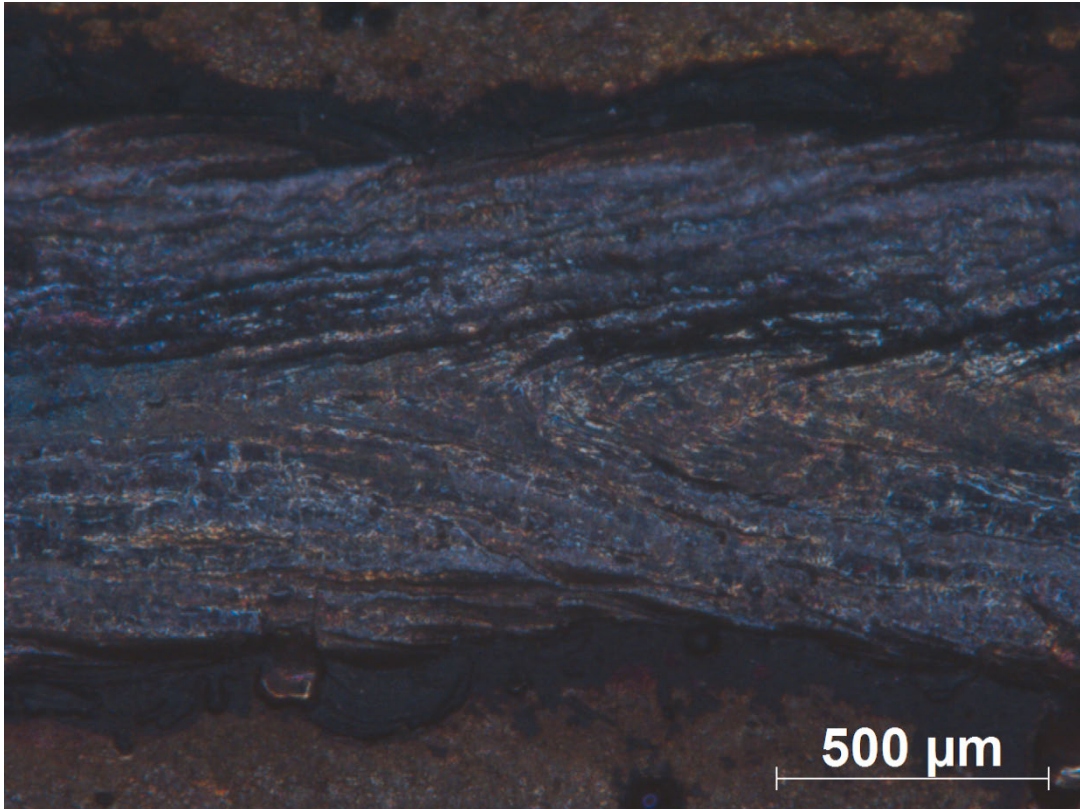

Bend Testing 180° (Weld Root) - Specimen H

Bend Testing 90° (Weld Root) - Specimen I

Bend Testing 180° (Weld Root) - Specimen I
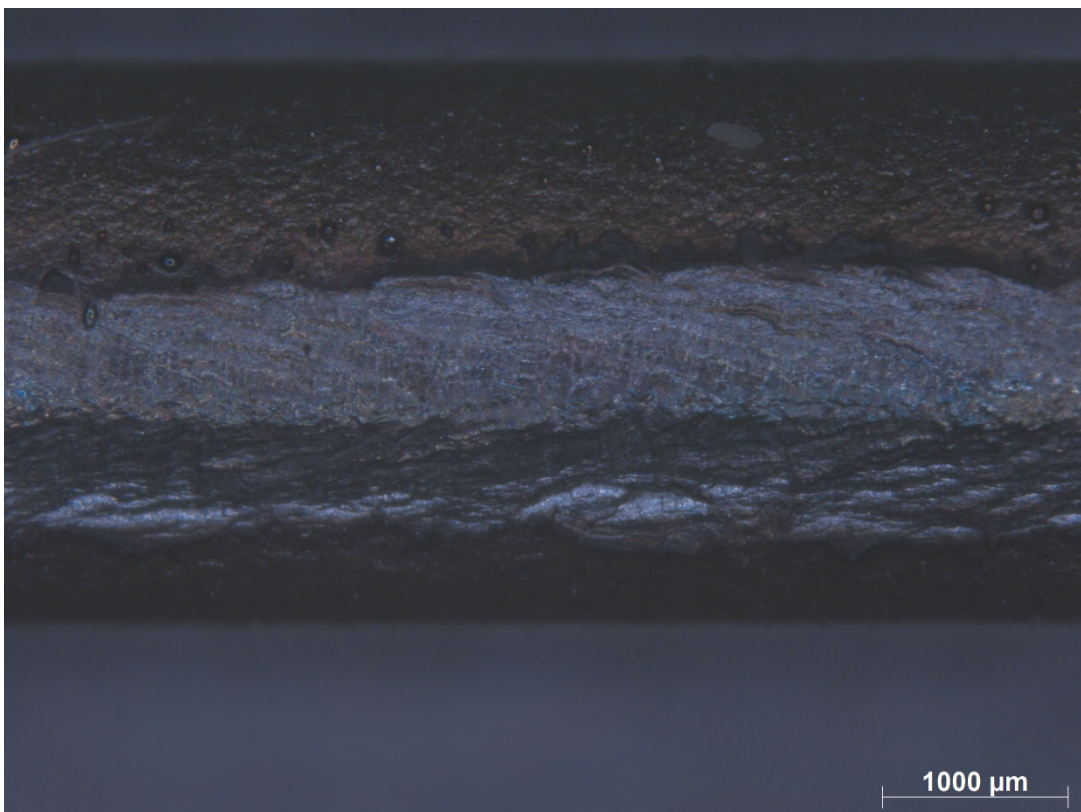
Bend Testing 90° (Weld Root) - Specimen J

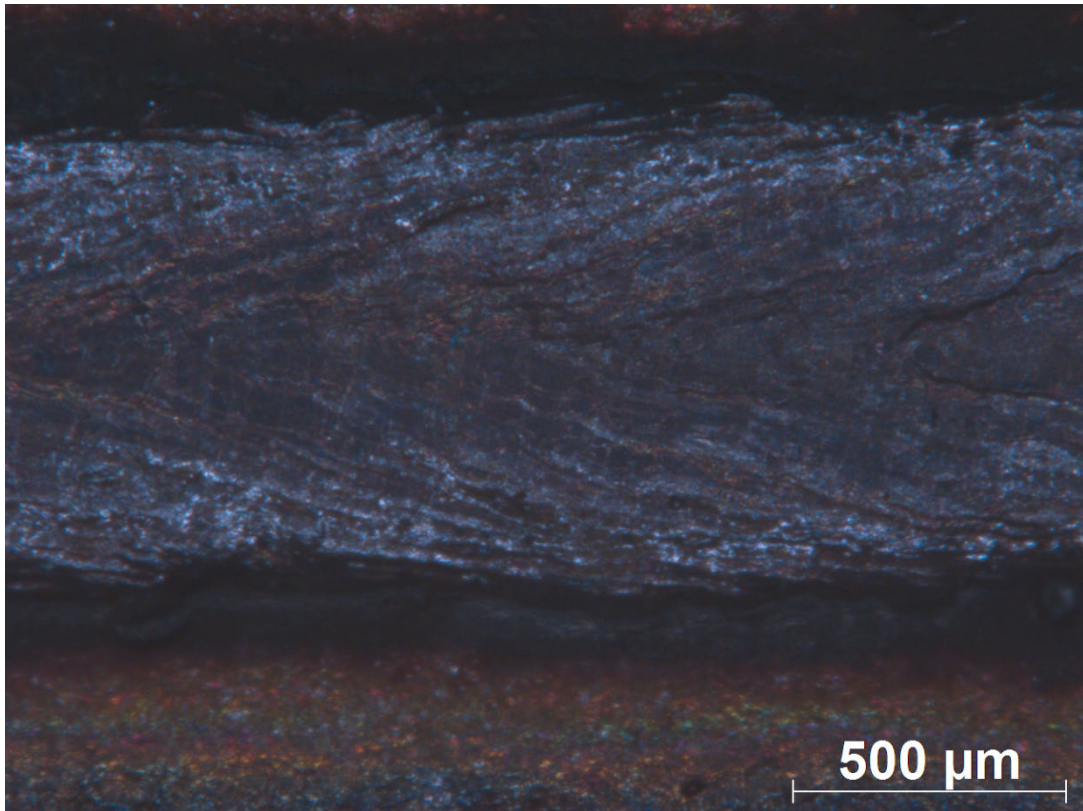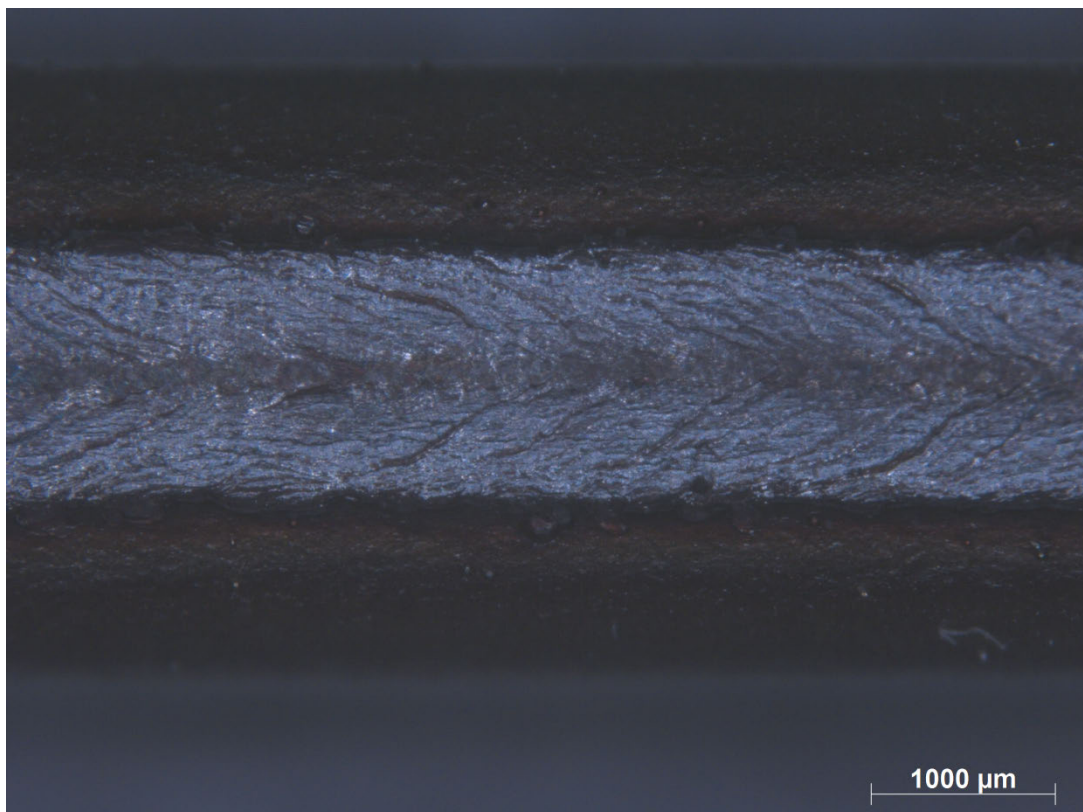**Bend Testing 180° (Weld Root) - Specimen J**

Bend Testing 90° (Weld Root) - Specimen K
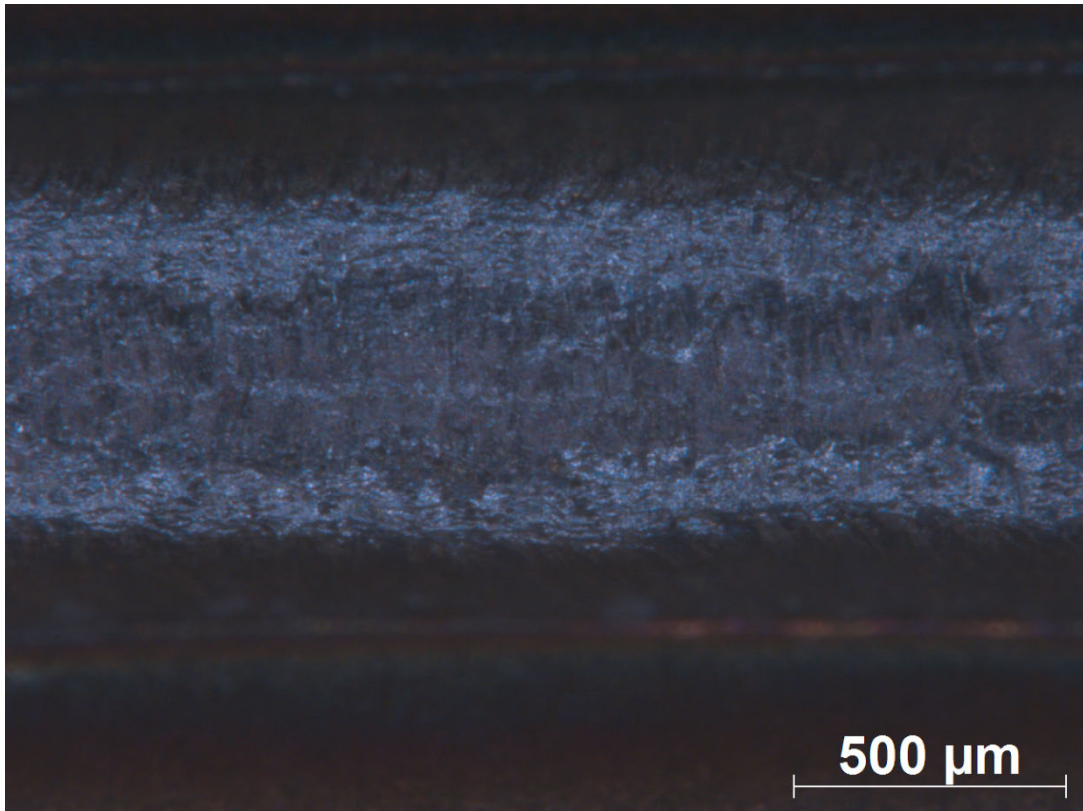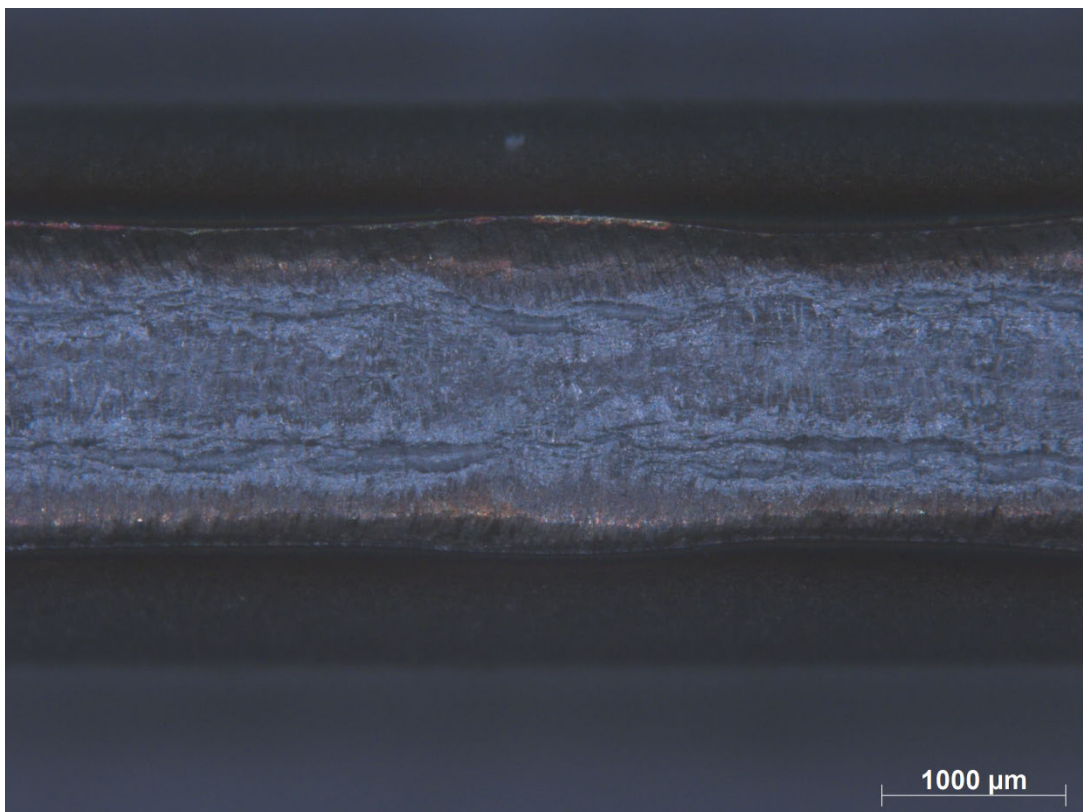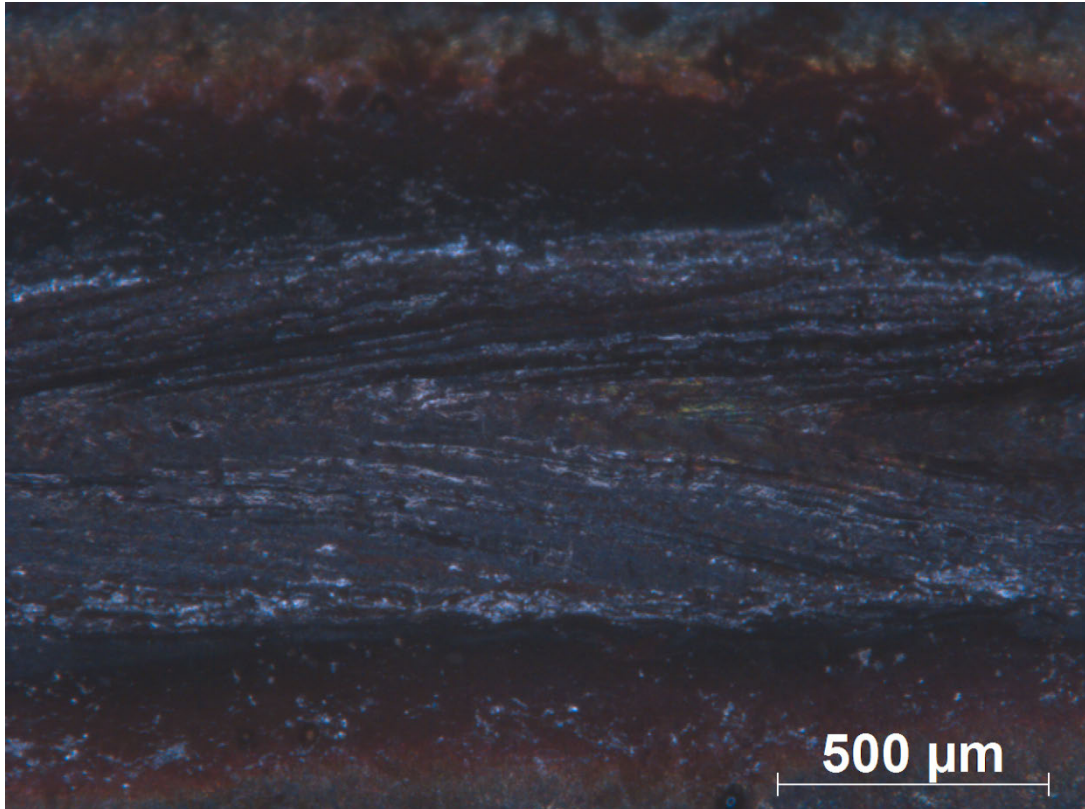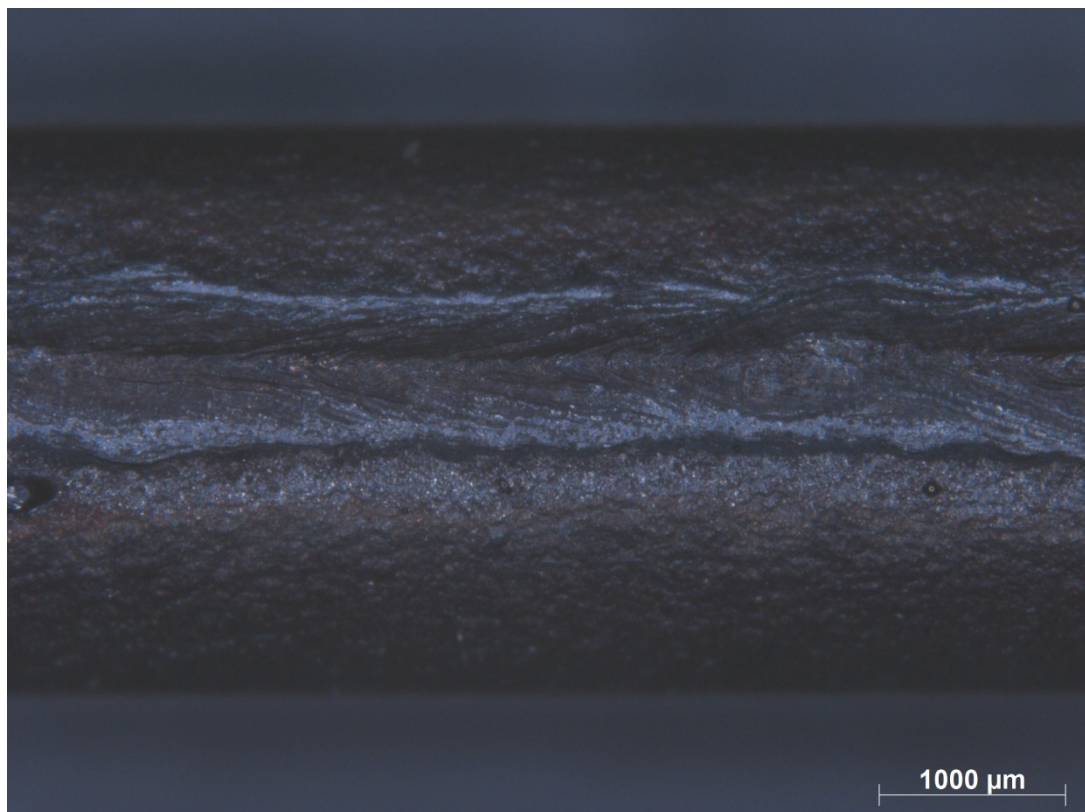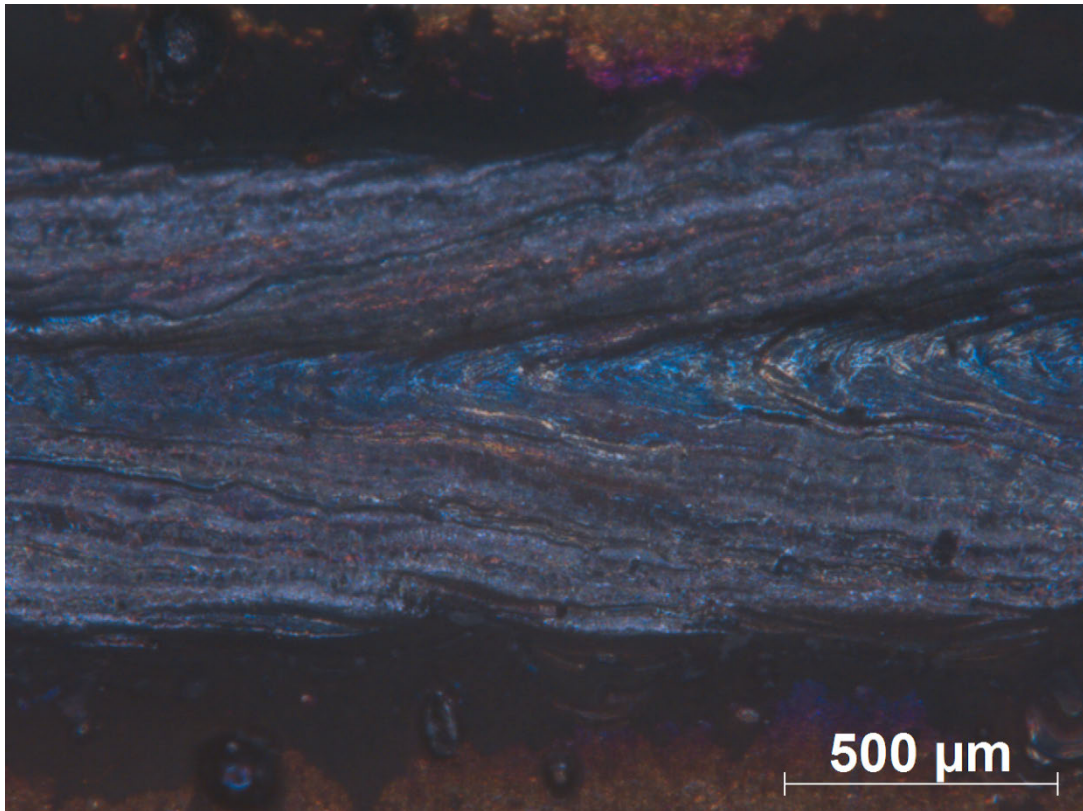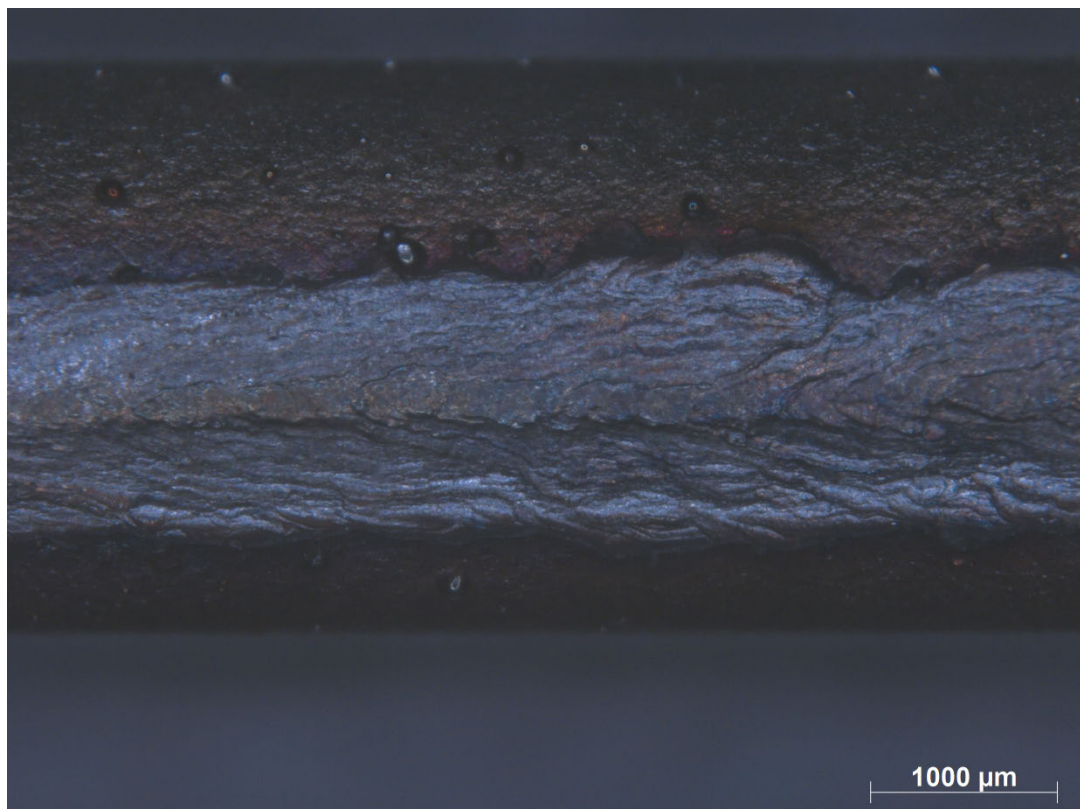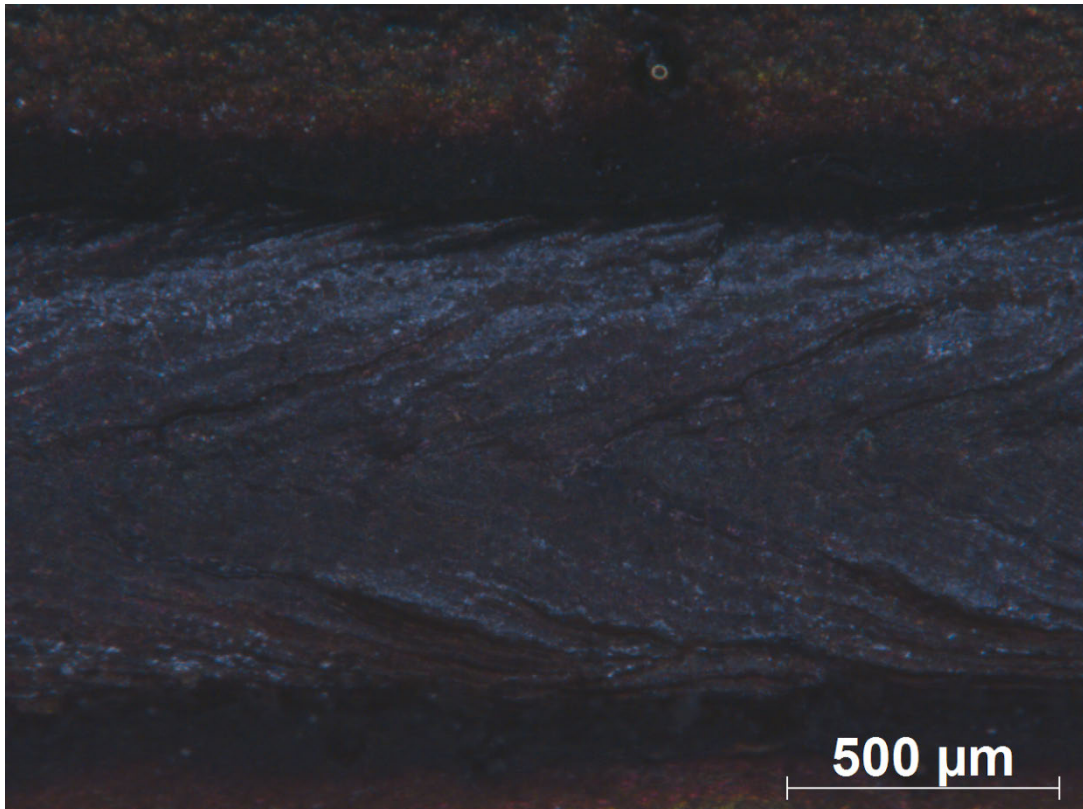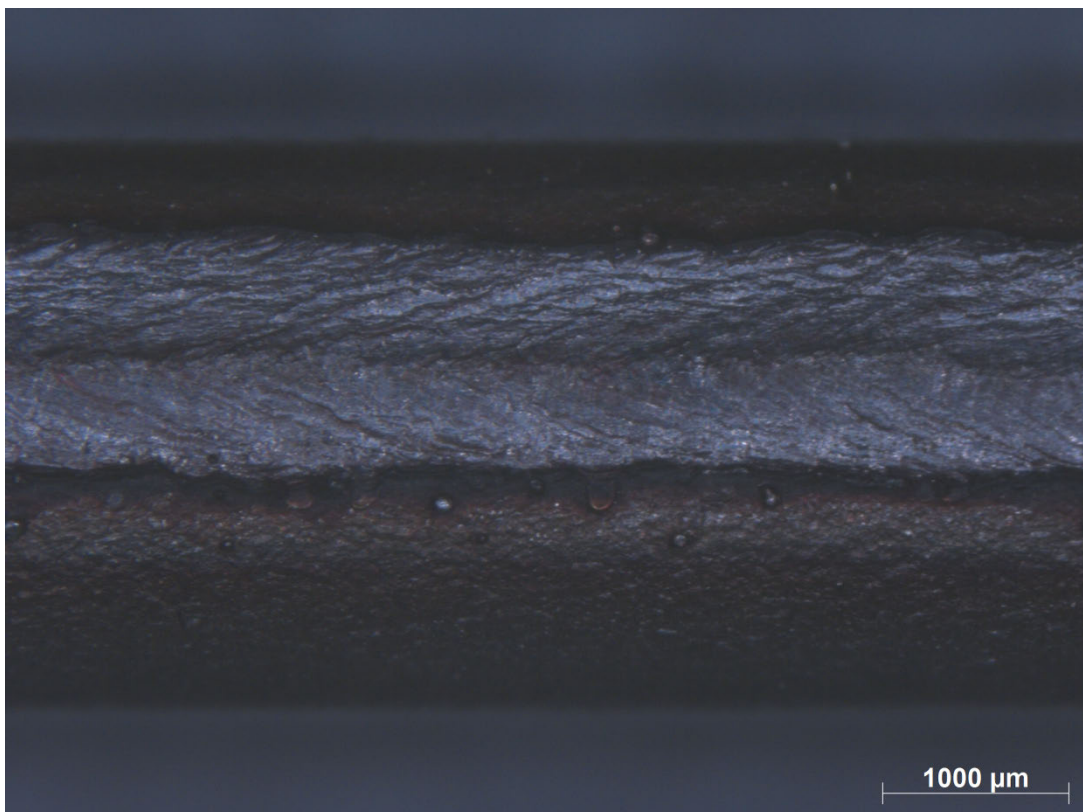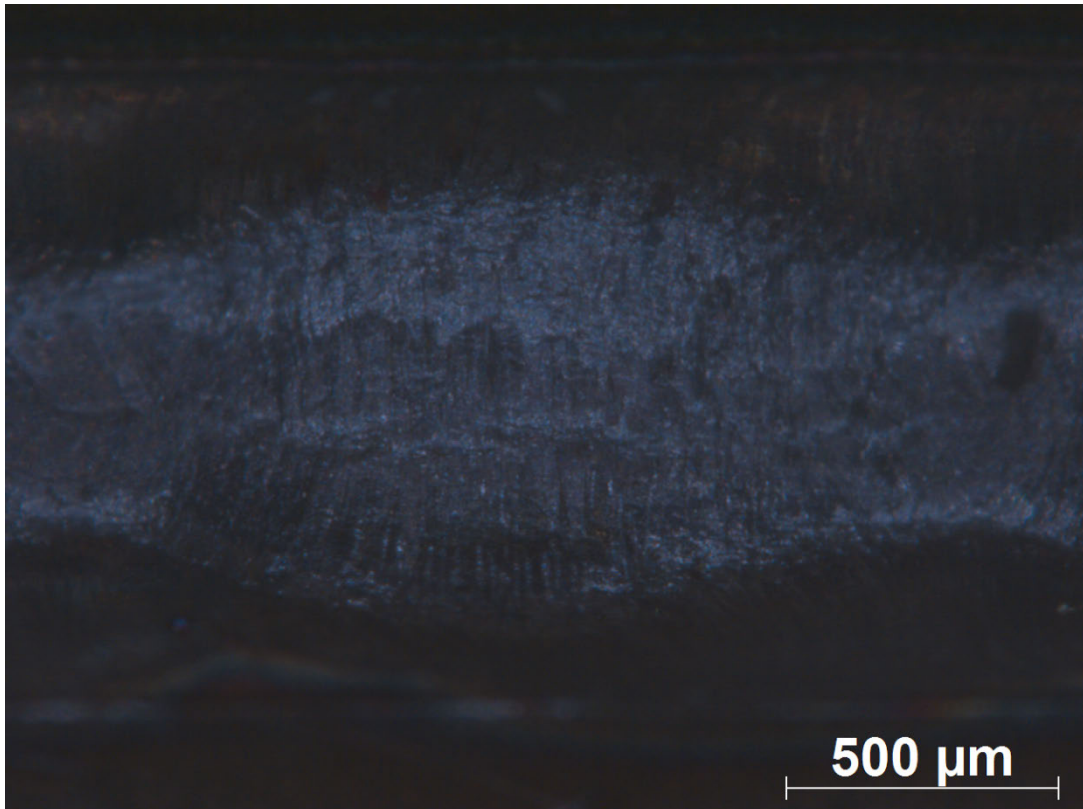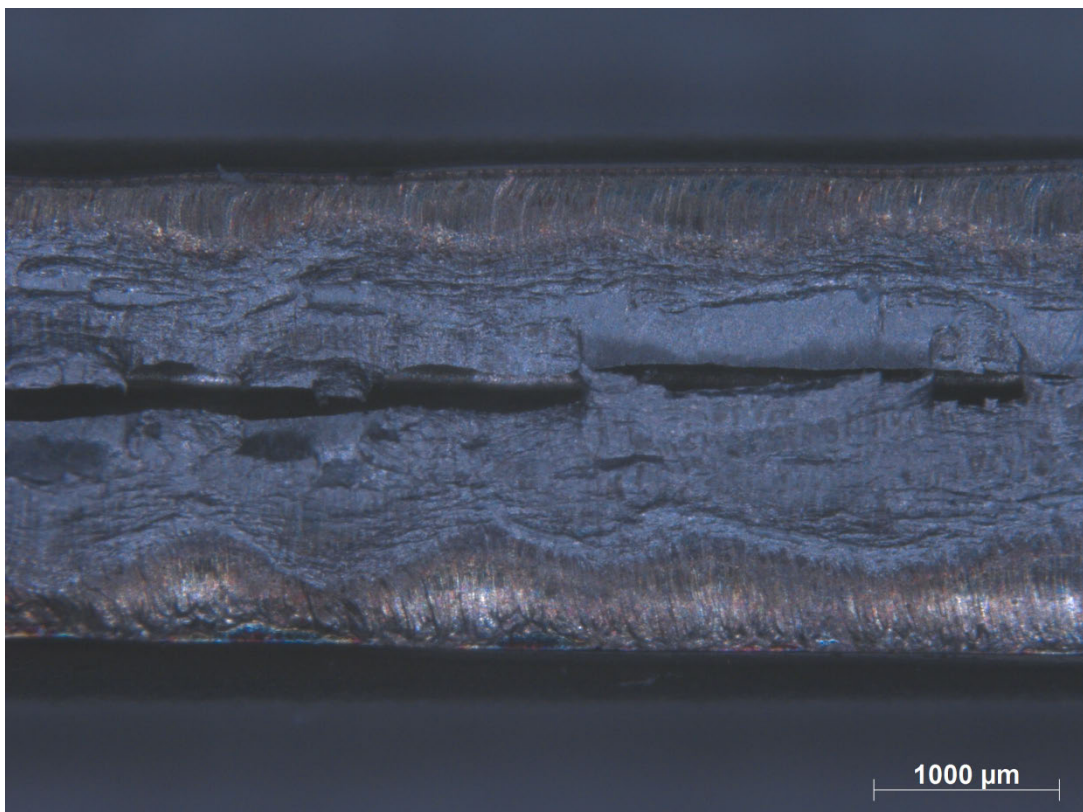

Bend Testing 180° (Weld Root) - Specimen K

63

Bend Testing 90° (Weld Root) - Specimen L

Bend Testing 180° (Weld Root) - Specimen L

Appendix V – MATLAB PROGRAM

```matlab
%Assignment on Heat Conduction in MMK 210 Joining Technology
%Johan Ahlstrom, Materials and Manufacturing Technology

clear;

clf;

%Input parameters
geometry=2;          %1. Geometry 2='thin' 3='thick' plate
mtrl=4;              %2. Material 1=Copper 2=Monel_400 3=Carbon_steel
4=Aust_steel
T0=293;              %3. Preheat temperature K (20/300 C corresponding to
293/573K)
power_in=2e3;        %4.a Power in
eff=0.65;            %4.b Coupling efficiency
q=power_in*eff;      %4. Net power J/s
d=1.5e-3;            %5. Plate thickness m, only relevant for thin plate
z=-0.00;             %6. z-coordinate m, only relevant for thick plate
(negative)
v=0.08333;           %7. Welding speed m/s
%End of input parameters!!!
%%materialname=['Copper      '; 'Monel_400   '; 'Carbon_steel'; 'Aust_steel
'];

%Text string for material name (used for text output and in diagrams)
if mtrl==1
Materialtxt='Copper';
elseif mtrl==2
Materialtxt='Monel 400';
elseif mtrl==3
Materialtxt='Carbon steel';
else
Materialtxt='Austenitic stainless steel';
end

if geometry==2
    disp('Thin plate');
    disp(['Plate thickness (m) = ' num2str(d)]);
else
    disp('Thick plate');
    disp(['Depth (m) = ' num2str(-z)]);
end
disp(['Material: ' Materialtxt]);
disp(['Net power (J/s): ' num2str(q)]);
disp(['Welding speed (m/s): ' num2str(v)]);


%Material data given as [Copper Monel_400 Carbon_steel Aust_steel]
a=[9.6e-5 8.0e-6 9.1e-6 3.8e-6];    %Thermal diffusivity m^2/s
lambda=[384 35.2 41 15];            %Thermal conductivity J/(m*s*K)
Tm=[1336 1573 1800 1723];           %Melting temperature K


%Definition of contour plot levels
Tcurve1=[773 773];        %The command 'contour' requires vector as input
(stod tidigare 673/400!!!!!)
Tcurve2=[1073 1073];
Tcurve3=[1473 1473];
```

65

```matlab
    TcurveTm=[Tm(mtrl) Tm(mtrl)];  %Tm

    %Definition of vectors for geometry definition and time
    ksimin=-0.065;            %ksimax-ksimin=ymax-ymin in combination with
    command
    ksimax=0.01;              % axis('square') will yield figures with equal
    scaling
    ymin=-0.005;              % on both axes which is important for
    interpretation!!!
    ymax=0.005;
    step=2e-5;

    if geometry==2
        tmax=2;              %This might have to be adjusted for certain parameters
        tstep=0.001;
    else
        tmax=2;               %This might have to be adjusted for certain
    parameters
        tstep=0.001;
    end

    x=0.01;                   %Defines the location of the studied point in t-T
    diagram

    ksi=[ksimin:step:ksimax]';  %ksi vector
    y=[ymin:step:ymax];         %y vector
    %y=[ymin:step:ymin/10 ymin/10:step/10:ymax/10 ymax/10:step:ymax];  % finer
    y vector
    [KSI,Y]=meshgrid(ksi,y);    %coordinate matrix
    t=[0:tstep:tmax];           %Time vector

    %Computation of temperature field
    if geometry==2
      T=T0+q/(2*pi*lambda(mtrl)*d)*exp(-v*KSI/(2*a(mtrl))).* ...
        besselk(0,v*sqrt(KSI.^2+Y.^2)/(2*a(mtrl)));
    else
      T=T0+q/(2*pi*lambda(mtrl))*exp(-v*KSI/(2*a(mtrl))).* ...
        exp(-v*sqrt(KSI.^2+Y.^2+z^2)/(2*a(mtrl)))./(sqrt(KSI.^2+Y.^2+z^2)+eps);
    end

    %Search the y coordinates for which the max. T is close to Tm and Tm/2 (in
    Kelvin)
    %The indices are stored in yindexTm and yindexTmhalf respectively
    %[Dev1,yindexTm]=min(abs((max(T')-Tm(mtrl))));
    %[Dev2,yindexTmhalf]=min(abs((max(T')-Tm(mtrl)/2)));
    [Dev1,yindexTm]=min(abs((max(T,[],2)-Tm(mtrl))));
    [Dev2,yindexTmhalf]=min(abs((max(T,[],2)-Tm(mtrl)/2)));
    %Computation of time-temperature curves
    if geometry==2
      Tvect0=T0+q/(2*pi*lambda(mtrl)*d)*exp(v*(v*t-x)/(2*a(mtrl))).*  ...
          besselk(0,v*sqrt((x-v*t).^2)/(2*a(mtrl)));
      Tvect1=T0+q/(2*pi*lambda(mtrl)*d)*exp(v*(v*t-x)/(2*a(mtrl))).*  ...
          besselk(0,v*sqrt((x-v*t).^2+y(yindexTm)^2)/(2*a(mtrl)));
      Tvect2=T0+q/(2*pi*lambda(mtrl)*d)*exp(v*(v*t-x)/(2*a(mtrl))).*  ...
          besselk(0,v*sqrt((x-v*t).^2+y(yindexTmhalf)^2)/(2*a(mtrl)));
    else
      Tvect0=T0+q/(2*pi*lambda(mtrl))*exp(v*(v*t-x)/(2*a(mtrl))).*  ...
          exp(-v*sqrt((x-v*t).^2+z^2)/(2*a(mtrl)))./(sqrt((x-
    v*t).^2+z^2)+eps);
      Tvect1=T0+q/(2*pi*lambda(mtrl))*exp(v*(v*t-x)/(2*a(mtrl))).*  ...
          exp(-v*sqrt((x-v*t).^2+y(yindexTm)^2+z^2)/(2*a(mtrl))) ...
          ./sqrt((x-v*t).^2+y(yindexTm)^2+z^2);
```

```matlab
    Tvect2=T0+q/(2*pi*lambda(mtrl))*exp(v*(v*t-x)/(2*a(mtrl))).*  ...
        exp(-v*sqrt((x-v*t).^2+y(yindexTmhalf)^2+z^2)/(2*a(mtrl))) ...
        ./sqrt((x-v*t).^2+y(yindexTmhalf)^2+z^2);
end


%Computation of Delta-t_800-500C in the melt line.
%This temperature interval is mainly relevant for C steel, but it is
%still useful for all materials for comparison of cooling rates.
[Tm_approx,tindexTmax]=max(Tvect1);
[Dev3,tindexprel]=min(abs(Tvect1(tindexTmax:length(Tvect1))-1073));
tindexT800=tindexprel+tindexTmax-1;
%Tvect0(tindexT800)
[Dev4,tindexprel]=min(abs(Tvect1(tindexTmax:length(Tvect1))-773));
tindexT500=tindexprel+tindexTmax-1;
%Tvect0(tindexT500)
Deltat8to5=(tindexT500-tindexT800)*tstep;


%Quality check and printout of result
[Tmax,yindexTmax]=max(max(T'));
if Tmax<Tm(mtrl)
    disp('Successful run, but the temperatures do not reach T_m at this
depth');
else
    if (Dev1 > 100)      %Dev 1 anger avvikelsen mellan vektorn och verklig
Tm
        disp('Invalid run, repeat with smaller step');
    elseif (Dev3+Dev4) > 25    %Dev 3 och 4 anger vektorns temperaturapprox
        disp('Invalid run, repeat with smaller tstep');
    else
    disp(['Delta-t_800-500C (s) = ' num2str(Deltat8to5)]);
    disp('Successful run! ');
    disp(' ');
    end
end



%%%%%%%%Plotting

%Isotherms
figure(1)
clf
hold on
set(0,'DefaultAxesLineStyleOrder',{'-','--','-.',':'});
if Tmax<Tm(mtrl)
    disp('Lower T isotherms plotted instead');
    disp(' ');
    [Ct,Ht]=contour(ksi,y,T-273);
    clabel(Ct,Ht);
else
    [C,H(1)]=contour(ksi,y,T,Tcurve1);
    [C,H(2)]=contour(ksi,y,T,Tcurve2);
    if (mtrl==1)
      [C,H(3)]=contour(ksi,y,T,TcurveTm);
      legend(H,'500 C','800 C','1063 C (T_m)');
    else
      [C,H(3)]=contour(ksi,y,T,Tcurve3);
      [C,H(4)]=contour(ksi,y,T,TcurveTm);
      legend(H,'500 C','800 C','1200 C',[num2str(Tm(mtrl)-273) ' C
(T_m)']);
    end
end
axis('square');
```

67

```matlab
axis([ksimin ksimax ymin ymax]);
title(['Isotherms for ' Materialtxt ', T_0=' num2str(T0-273) 'C, electrode
in (0,0)']);
xlabel('\xi (m)');
ylabel('y (m)');
%pause

% To print this graph, activate one of the following rows by deleting the
"%"-sign
% For the report, either the copy figure option in the graph window, or the
% tiff-format is recommended. Write "help print" in the Matlab command
window to
% get more information

%print isoterm
%print -dtiff isoterm

%Temperature vs Time
   figure(2)
   clf
   hold on
   plot(t,Tvect0-273,'-',t,Tvect1-273,'-.',t,Tvect2-273,'--');
   axis([0 tmax 0 1600]);
   title(['Temperature - time curves for ' Materialtxt ', T_0='  ...
          num2str(T0-273) 'C at x=0.1m']);
   xlabel('time (s)');
   ylabel('temperature (C)');
   yh=num2str(abs(y(yindexTmhalf)));
   dist=['Distance from centre line ' yh 'm '];
   legend('In the centre line','At the melt pool border',dist);
%pause

% To print this graph, activate one of the following rows by deleting the
"%"-sign

%print tidtemp
%print -dtiff tidtemp


figure(3)
clf
%map=0.9-0.9.*colormap('gray');  % These two lines can be commented if you
%colormap(map);                  % are printing to a color printer, not
otherwise!!!
mesh(ksi,y,T-273)
axis([ksimin ksimax ymin ymax 0 1600])
caxis([0 1600])
colorbar
xlabel('\xi (m)');
ylabel('y (m)');
zlabel('Temperature (C)');
```